The Ins and Outs of Cholera Toxin Retro-translocation

by

Paul Christopher Moore

A dissertation submitted in partial fulfillment
of the requirements for the degree of
Doctor of Philosophy
(Cellular and Molecular Biology)
in The University of Michigan
2012

Doctoral Committee:

Associate Professor Billy Tsai, Chair
Professor Peter Arvan
Professor Robert S. Fuller
Associate Professor Amy Chang
Associate Professor Kristen J. Verhey

ACKNOWLEDGEMENTS

First and foremost, I would like to express my sincerest gratitude to Billy Tsai. I really am amazed at how much I have grown as a scientist in my time under his tutelage. His (almost scary) enthusiasm in the lab is only paralleled by his desire to help his students mature as independent researchers. Looking back to when I started in the lab, I am humbled not only by how much I've improved at the bench but also by how much more clearly I see as a scientist. Even then, Bill's keen insight and natural talents in the lab still astonish me. I'm very fortunate to have had some of that scientific prowess rub off on me, and I know that my time in the Tsai lab has prepared me for what lies ahead.

To my committee, thank you for your invaluable input over the years. I'm not exactly saying I relished the thought of having committee meetings, but they weren't nearly as frightening as people made them out to be. In fact, sometimes they were as much fun as they were educational (and they were always very educational).

As for the Tsai lab itself, I must thank all the members past and present. Although the faces have changed over the years, the positive attitude of the lab has stayed the same. There aren't any other people in the world that I would rather share the agony and ecstasy of bench research with. Best of luck to all of you in your endeavors.

TABLE OF CONTENTS

LIST OF FIGURES

LIST OF ABBREVIATIONS

A1AT	α-1 antitrypsin
AT	Anthrax toxin
ATP	Adenosine triphosphate
BFA	Brefeldin A
cAMP	Cyclic adenosine monophosphate
CFTR	Cystic Fibrosis Transductance Regulator
CE	Cytosolic extract
CT	Cholera toxin
CTA	Cholera toxin A subunit
CTA1	Cholera toxin A1 peptide
CTB	Cholera toxin B subunit
DSP	Dithiobis succinimidyl propionate
DT	Diphtheria toxin
DTT	Dithiothreitol
DUB	Deubiquitinase
Ero1	ER oxidoreductase 1
EF	Anthrax edema factor
ER	Endoplasmic reticulum
ERAD	ER-associated degradation
Endo H	Endoglycosidase H
FBS	Fetal bovine serum
GTP	Guanosine triphosphate
HA	Hemagglutinin
HCN	50 mM HEPES 7.5, 2 mM CaCl2,150 mM NaCl
Hsp	Heat shock protein
IP	Immunoprecipitation
LF	Anthrax lethal factor
MAD	Mitochondria-associated degradation
Mal-PEG	Maleimide polyethylene glycol 5000
NEM	N-ethylmaleimide
NTP	Nucleotide triphosphate
P1/P2	Pellet fraction 1/ pellet fraction 2
PA	Anthrax protective antigen
PDI	Protein disulfide isomerase
PMQC	Plasma membrane quality control
PNGase F	Peptide-N-glycosidase F
RT	Ricin toxin
siRNA	small interfering RNA

SRP	Signal recognition particle
S1/S2	Supernatant fraction 1/ Supernatant fraction 2
ST	Shiga toxin
TCRα	T-cell receptor alpha
UPR	Unfolded protein response
UPS	Ubiquitin proteasome system
VCP	Valosin-containing protein (p97)

CHAPTER 1

Introduction

The eukaryotic cell is a highly complex and tightly organized entity that must constantly respond to changes in both internal and external environments. When native or exogenous proteins are deemed unnecessary or harmful to cellular homeostasis they are recognized by quality control systems and marked for degradation. Some viruses and toxins have evolved to hijack these destructive pathways to traverse the cell and attain their respective goals of replication and cytotoxicity. Interestingly, analyzing how pathogens manipulate these pathways reveals unique insight into how the cellular machinery normally operates.

1-1. Protein folding and ER-associated degradation

Depending on cell type and other environmental factors, it is estimated that as much as a third of newly synthesized proteins do not properly fold (*1*). Left unaddressed, protein misfolding can result in loss or gain of function aggregates that have dire effects at both cellular and organismal levels. In some cases, such as in α-1 antitrypsin (A1AT) deficiency, both may occur simultaneously. Aggregation of wild type or mutant A1AT leads to gain of function toxicity in liver cells that can result in hepatitis and cirrhosis, among other diseases (*2*). This

aggregation further causes loss of function by preventing the effective secretion of A1AT and its subsequent inhibition of elastase, ultimately resulting in connective tissue damage in the lungs (*3*). In order to remedy such toxic effects it is important to understand the factors that drive both folding and misfolding of proteins and how the cell overcomes the latter.

Protein folding in the cell

Decades of research lead to the general model that actively translated proteins are funneled through diverse energy landscapes to reach their native folding state (*4*). From an overly simplistic view, the primary driving forces would be directed intra-molecular interactions of charged residues and exclusion of hydrophobic residues as they are exposed upon exiting the ribosome. Over the years it has become clear that the cellular energy landscape is significantly more complicated than this. For one, compartments that have a high oxidizing potential, such as in the endoplasmic reticulum (ER), favor the formation of both intra- and intermolecular disulfide bonds that affect the folding states of monomers and oligomers (*5, 6*). Secondly, with a cellular protein concentration estimated to be as high as three hundred mg/mL, proteins encounter intermolecular interactions that influence their folding fate (*7*). Some proteins, such as members of the heat shock protein family (see below), act as molecular chaperones that prevent aggregation due to exposure of hydrophobic patches and thereby improve folding efficiency (*8*). Post-translational modifications contribute yet another facet to the hurdles that must be overcome to achieve a

functional conformation. N-linked glycosylation, for example, not only directly affects folding state but also serves as a beacon for lectins and lectin-like chaperones in the ER and the Golgi (see below) (*9*). Finally, many proteins must endure a drastic change in environment as they are passed through or inserted into lipid bilayers either co- or post-translationally.

Integration of the aforementioned factors is inevitably antagonized by miscues that result in inadequate folding. For example, proteins that are destined for the ER contain signal sequences that allow them to be targeted to the Sec61 translocon by signal recognition particle (SRP) (*10*). Poor recognition of ER signal sequences, such as those found in prion proteins, leads to mislocalization and aggregation of these proteins in the cytosol (*11, 12*). Interestingly, attenuation of translation rate is often enough to alleviate targeting malfunctions and allow for proper localization and folding (*13*). Similarly, abnormally high protein production can lead to a decrease in folding efficiency. In pancreatic β cells insulin production accounts for 50% of total protein production upon glucose stimulation (*14*). ER resident chaperones can be overwhelmed by this sudden influx of secretory proteins, resulting in ER stress and, under extreme conditions, apoptosis and type I diabetes (*15*). External stressors provide further opposition to protein folding. Redox stress, which can be artificially induced by chemicals such as dithiothreitol (DTT) and diamide, interferes with normal disulfide bond formation (*16*). Proper N-glycosylation of ER proteins can be blocked using the drug tunicamycin (*17*). Finally, since many ER chaperones rely on binding to

calcium, disruption of calcium ion stores in the ER leads to protein misfolding and ER stress. This effect can be produced by the drug thapsigargin (*18*).

Regardless of how and where proteins misfold, the cell must respond in order to maintain normal operations and, under more serious conditions, avert widespread cellular stress and an inclination towards apoptosis. Initially, the cell attempts to use a variety of quality control pathways to refold proteins into their native, functional conformations. However, if this approach fails proteins are redirected to degradation machinery in order to dispose of problematic proteins and recycle their amino acids. In general, the cell degrades proteins by delivering them either to the lysosome or to the cytosolic 26S proteasome. The main pathways involved in this process have evolved at specific sub-cellular locations including the plasma membrane (plasma membrane quality control, or PMQC), the mitochondria (mitochondrial-associated degradation, or MAD) and the ER (ER-associated degradation, or ERAD) (*19-24*). While there is some overlap in their components, each pathway employs a unique array of machinery and strategies to recognize and remedy protein misfolding. The following section will focus on the elements of ERAD as it is the most well characterized pathway and the most relevant to the body of this thesis.

The many faces of ERAD

When components of the T-cell receptor complex were shown to be degraded in a lysosome-independent manner it set off a cascade of research that resulted in the discovery that both soluble and transmembrane proteins can be

expelled from the ER and degraded in the cytosol (*25*). It is now evident that there are several unique branches of ERAD displaying the ability to target proteins with folding "lesions" in the ER lumen, membrane and the cytosol (*26*). Nonetheless, all ERAD paths share four basic steps: substrate recognition, retro-translocation, ubiquitination and degradation (Figure 1-1).

Three major types of chaperones coordinately process misfolded proteins and determine their ultimate fate. The most well documented family of protein chaperones, the heat shock protein (Hsp) family, plays a crucial role in misfolded protein recognition in both the cytosol and the ER lumen. The ATPases Hsp70 and Hsp90 best represent the family in the cytosol. Appropriately, their respective homologs, BiP and GRP94, are the most important players in the ER (*27*). While Hsp70 and Hsp90 both use hydrophobic domains to recognize the exposed hydrophobic cores of misfolded proteins, they are regulated through different co-chaperones and interact with substrates at different points in their ATPase cycles (*28-31*). Furthermore, it has long been believed that Hsp70 and BiP are more geared towards refolding by improving substrate solubility while Hsp90 and GRP94 operate downstream and favor protein degradation (*32-36*). Conversely, there are distinct cases of the opposite occurring (*37, 38*), as will be discussed in more detail below. Hsp40 homologs, which are found in the ER lumen, membrane and cytosol, not only control the ATPase cycle of Hsp70 but also are implicated in directly chaperoning misfolded proteins (*28*). The aptly named protein disulfide isomerase (PDI) family of chaperones manages the

formation of disulfide bonds in the ER. The eponymous PDI and 19 other known PDI-like family members rely on their catalytic thioredoxin domains to reduce, isomerize and oxidize the disulfide bonds of target proteins (*39*). Moreover, these proteins have been shown to display redox-independent chaperone activity whereby family members sometimes play opposing roles in determining whether to fold or unfold substrates (*40-43*). Lastly, chaperones known as lectins are responsible for interacting with misfolded proteins based on their glycosylation state. As mentioned previously, upon arrival to the ER proteins have glycans added en bloc to asparagine residues found in an Asn-X-Ser/Thr motif (X is any amino acid other than proline), a process referred to as N-linked glycosylation (*9*). If a protein becomes misfolded in the ER its N-glycans become exposed to lectins, which bind to the sugar moieties, and glycanases, which trim the N-glycans. The lectins calnexin and calreticulin regulate a cycle that recognizes newly misfolded proteins and attempts to refold them. If these substrates remain unfolded for an extensive period of time their N-glycans are irreversibly trimmed, allowing them to be targeted by other lectins such as EDEM and ERManI, removed from the calnexin/calreticulin cycle, and marked for degradation (*44-46*). This balance between various lectins and glycanases is the primary factor driving the decision between refolding and degradation (*47, 48*). As such, an imbalance between chaperone-mediated refolding and N-glycan trimming can lead to erroneous degradation of ER proteins and promote a disease-state. It was recently discovered that a process called ERAD tuning uses autophagy to deliver

unnecessary chaperones to the lysosome and thereby preserve appropriate folding/degradation equilibrium (*49*).

Complex, substrate-dependent cooperation between all types of ERAD chaperones dictates whether a protein can be refolded or will be relegated for destruction (*50-53*). Predictably, many lumenal and transmembrane chaperones facilitate degradation by acting as conduits between misfolded proteins and the retro-translocation machinery (*54-56*). Remarkably, it is unclear which proteins actually constitute the retro-translocation pore, or retro-translocon. Initial studies in yeast indicated that Sec61, the forward translocon, mediated the removal of a membrane protein for proteolysis (*57-59*). While this model of using the same pore for entrance to and exit from the ER was logical, it was not long before other putative retro-translocon components appeared on the scene. Much recent work has centered on the Derlin family of transmembrane proteins. From yeast to mammals, these proteins act not only as membrane chaperones but also have the ability to form hetero-oligomers that could potentially form pores in the membrane (*60, 61*). Additionally, they have been shown to interact physically and functionally with Sec61 in elimination of misfolded proteins from the ER (*62, 63*). Another class of proteins with the potential to assist in formation of a retro-translocon is composed of transmembrane E3 ligases. These ligases, which include Hrd1 and gp78, are similar to the Derlins in that they can chaperone ERAD substrates and can be found in complex with the other alleged retro-translocon constituents (*64-66*). Where they differ, however, is in their ability to

ubiquitinate target proteins. E2 ubiquitin-conjugating enzymes in the cytosol transfer ubiquitin moieties to over 500 different E3 ligases (*67*). These ligases, which participate in various quality control and housekeeping pathways throughout the cell, confer substrate specificity (*68*). With regards to ERAD, the vast majority of known E3 ligases are integral membrane proteins that transfer ubiquitin chains to substrates being actively retro-translocated through the ER membrane (*69*). This poly-ubiquitination signal is what ultimately guides misfolded proteins into the ubiquitin-proteasome system (UPS) where they will reach the end of their journey.

Before ubiquitinated ERAD substrates can be degraded they must first be extracted from the ER membrane. While the poly-ubiquitin chain itself prevents backwards movement through the retro-translocon, the AAA-ATPase p97/VCP is believed to be the sole factor that actively ratchets proteins into the cytosol. Although p97 performs a wide variety of functions in the cell, it is recruited for ERAD by directly associating with retro-translocon components like the Derlins, Hrd-1 and gp78 (*22, 70-74*). Moreover, the wide range of partner proteins p97 utilizes determines its specificity. In this case, p97 complexes with Ufd1 and Npl4 to recognize ubiquitinated substrates and p97 itself forms dual hexameric rings that sequentially hydrolyze ATP to pull proteins out of the membrane (*75-78*). Chaperones then bind the dislocated proteins to maintain their solubility while being targeted to the 26S proteasome. The proteasome is actually a collection of numerous activities organized in two subunits: the 19S cap and the 20S core

(*68*). The 19S cap contains components that bind ubiquitin and deubiquitinases (DUBs) that cleave and release free ubiquitin into the cytosol (*79, 80*). Deubiquitinated substrates can then move into the pore of the 20S core where they are degraded by three distinct proteolytic activities (*81*). At last, the resulting peptides are released from the proteasome and continue to be degraded by cytosolic proteases. It should be noted that developing work on cytosolic DUBs has revealed another layer of regulation for the UPS. For one, some DUBs are believed to regulate the timing of substrate delivery to the proteasome by directly trimming substrate poly-ubiquitination, thereby retarding degradation (*82*). On the other hand, there is evidence that several DUBs actually control the ubiquitination states of ERAD/UPS machinery. For example, there is mounting evidence that Usp13 may modulate the activity of p97 while Yod1 and Atx3 appear to regulate an unknown trans-acting factor (*83, 84*). In both cases, deubiquitination of ERAD machinery promotes substrate retro-translocation.

In the event that the standard levels of ERAD components are insufficient, the cell relies on autophagy and the unfolded protein response (UPR) to alleviate stress from unfolded proteins (*85*). Autophagy, a process in which proteins and organelles are delivered to lysosomes for degradation, is beyond the scope of this thesis. The UPR is activated in response to elevated levels of misfolded proteins in the ER. The most well characterized and conserved (from yeast to mammals) UPR pathway goes through BiP and Ire1. Unfolded proteins not only titrate BiP away from Ire1 but also directly interact with Ire1 to promote its

dimerization and activation (*86-89*). Ire1 splices mRNA for the transcription factor Xbp1, permitting it to upregulate ER stress response genes. Mammalian cells have evolved pathways through ATF6 and PERK that operate in a similar manner to Ire1 (*90*). Ultimately, the goal of the UPR is to compensate for ER stress by upregulating translation of ER chaperones (BiP, Derlins) and degradation machinery (E3 ligases) while attenuating overall protein translation. However, under chronic duress these UPR pathways will eventually contribute to activation of apoptotic factors and cell death (*91-94*).

ERAD and disease

As mentioned before, folding malfunctions on a cellular level can ultimately lead to severe complications for an organism as a whole. With regards to ERAD alone, there are over 60 known human diseases including Huntington's, Parkinson's, diabetes and various cancers (*95*). These diseases can be categorized as mutations affecting ERAD machinery or affecting substrate folding. In the first case, mutations in ERAD machinery itself prevent degradation of misfolded proteins and promote toxic aggregation. Similarly, proteins that have a high propensity to aggregate can overwhelm the destructive pathways and thereby lead to accumulation of misfolded proteins. As expected, both routes are strongly tied to prolonged UPR induction and apoptosis (*96*). On the other hand, mutations in substrates account for the vast majority of ERAD diseases. Although these mutations can lead to stress from aggregation, most promote folding lesions, chaperone recognition, and premature degradation. In any case, the

rising number of ERAD-linked diseases has encouraged further research and has led to a rapid increase in our knowledge of the field.

While studies on T-cell receptor originally opened the door to ERAD, it was work on the cystic fibrosis transmembrane conductance regulator (CFTR) that established the first link between ERAD and human disease (*97, 98*). Wild-type CFTR is composed of 1,480 amino acids that form a multi-domain, transmembrane protein involved in chloride transport. It is co-translationally inserted into the ER membrane and then directed along secretory pathways to the plasma membrane (*99-103*). Although not an issue in all cell types (*104*), CFTR commonly misfolds due to its complex domain structure and, consequently, as much as 80% of newly synthesized CFTR is degraded (*98*). Mutations that further affect the stability of CFTR or its chloride transport function result in cystic fibrosis, a disease characterized by digestive and nutrient disorders, delayed growth, severe constipation and mucus build-up in the lungs. The overall consequence is a drastic reduction in life expectancy (currently about 35 years) (*105*). The most common and well-studied mutation in CFTR is ΔF508. While this deletion does not grossly reduce chloride transport efficiency, it causes improper folding and completely ablates cellular levels of CFTR (*103, 106-108*). The eventual discovery that ΔF508 is degraded prior to Golgi arrival in a lysosome-independent manner just happened to coincide with the birth of the ERAD field (*97, 98, 109, 110*).

From the very start, research on CFTR defined not only ERAD but also triggered paradigm shifts in our understanding of chaperones and protein degradation. As mentioned above, Hsp70 and Hsp90 are typically placed into restorative and degradative roles, respectively. However, these chaperones experience a role reversal when dealing with CFTR. For one, Hsp90 has been shown to stabilize both wild type and mutant CFTR (*111, 112*). This anomaly spurred the revelation that emphasis on different stages of the Hsp90 ATPase cycle determines substrate fate (*113, 114*). As for Hsp70, it was demonstrated that ΔF508 engages Hsp70-Hsp40 complexes more tightly than wild type and requires Hsp70 for degradation (*115*). This lent credence to the idea that, regardless of the chaperone, prolonged binding grants more time to deliver substrates to the retro-translocon and the UPS. CFTR research also shed some light on how chaperones interact temporally and spatially with substrates. Hsp70, calnexin and calreticulin can each interact with CFTR during and after insertion depending on where folding lesions appear in relation to the membrane (*116-119*). Likewise, it was observed that ubiquitination of CFTR occurs both co- and post-translationally (*120*). Whether CFTR poly-ubiquitination is mediated by cytoplasmic (CHIP) or transmembrane (RMA1, gp78) E3 ligases depends on where and when lesions are presented (*121, 122*). Furthermore, cross talk between E3 ligases and chaperones controls substrate fate. RMA1, for example, must interact with an Hsp40 to receive CFTR from Hsp70. Disruption of this hand off actually leads to improved folding efficiency (*123*).

By studying the mechanisms of ERAD-related diseases we garner a great deal of information about how ERAD pathways normally operate. As validated by CFTR, coordination between chaperones, co-chaperones and ligases are specific not only to substrates but also to types of lesions. In the end, therapies for cystic fibrosis and other ERAD diseases will require targeting of these complex interfaces. The discovery that foreign pathogens can utilize cellular machinery to move through the cell has only broadened the opportunities to pick apart the mechanisms of protein folding and degradation.

1-2. How toxins co-opt cellular machinery

Foreign pathogens, such as toxins and viruses, are designed to survive extracellular environments before reaching their target cells or organisms. Protein toxins, the subject of this segment, also remain folded to prevent premature activation at their source (bacteria and plants). Upon delivery to a host cell, the covalent and non-covalent interactions that maintain toxin integrity also create a barrier to pathogen entry into the host cell. Toxins have evolved to utilize host machinery and changes in environment to drive disassembly, entry and toxicity. While the details of toxin disassembly may vary greatly, most of these pathogens have common strategies for fulfilling their objectives. In general, there are four aspects to toxin disassembly.

First, majority of toxins choose to disassemble at a handful of different locations in the cell. As the endosome/lysosome and ER are the most frequently exploited, they will be the only sites represented in this discussion. Second,

toxins rely on a repertoire of host factors to undergo disassembly. The usual avenues include a selection of membrane receptors, proteases, pH change, disulfide bond reduction and chaperone-mediated conformational changes. Naturally, the next important facet of this process is the actual physical change incurred by the toxin resulting from exposure to the cellular machinery. This is a concerted, stepwise process that can involve domain rearrangement, subunit release, and even complete unfolding and refolding of the toxin. Finally, disassembly must serve a distinct purpose for propagating toxicity. Since most toxins must eventually access the cytoplasm, the most significant barriers they encounter are biological membranes. Disassembly must confer some advantage to the toxin that allows it to bypass cellular membranes and deliver catalytic subunits into the cytoplasm. Ultimately, successful intoxication requires collaboration of all four features. As will be made evident, toxins that share a common point of entry tend to be more similar in overall entry strategy. For this reason, the remainder of this section will be divided to focus on toxins that hijack endosomal or ER pathways.

Toxins that escape the endosome

As with all the examples presented here, toxins that pass through the endo/lysosome undergo proteolytic priming and receptor-mediated endocytosis to enter the cell. These toxins are unique, however, in that receptor binding typically initiates a conformational change. Once inside the cell they rely on endosomal acidification to drive further disassembly of the toxin and, most

importantly, formation of a pore in the endosomal membrane. It is this pore-forming ability that permits translocation of toxic subunits into the cytoplasm. The two toxins that best represent this model are anthrax toxin and diphtheria toxin.

Anthrax toxin (AT), the toxic agent that leads to widespread vascular leakage and shock, is composed of three basic subunits: edema factor (EF), lethal factor (LF) and protective antigen (PA) (*124*). EF acts as a calcium/calmodulin-activated adenylate cyclase, LF as a zinc-dependent protease, and PA as a pore through which either EF or LF is transported. PA is characterized by four domains: Domain 1 harbors a furin-cleavage site (*125*), domain 2 contains a disordered 2β2-2β3 loop that serves as the membrane-spanning pore segment (*126*), domain 3 is responsible for PA oligomerization (*127*), and domain 4 mediates binding to the host receptors ANTXR1/ANTXR2 (*128*). PA proteolysis, possibly executed on the host cell's surface by furin family proteases (*125*), cleaves the native PA into two subunits: an N-terminal 20-kDa fragment (PA_{20}) and a C-terminal 63-kDa peptide (PA_{63}) (Figure 1-2a). Although these two subunits remain associated with each other non-covalently, PA_{20} is eventually released from PA_{63} upon cell entry. Not only does PA_{20} removal allow PA_{63} to oligomerize, forming a heptameric ring structure called the prepore (Figure 1-2a) (*129*), its release is also required for PA_{63} to engage EF or LF for translocation (*130*).

As its name suggests, the heptameric PA_{63} prepore must undergo additional conformational changes to form the final pore. This conversion

involves the concerted actions of receptor binding and low pH. Receptor binding to domain 4 of PA_{63} alters the prepore conformation and lowers the threshold for prepore-to-pore conversion by one pH unit (*131*). Based on similarities to the staphylococcal α-hemolysin pore, it is postulated that low endosomal pH then induces a dramatic conformational change in the PA_{63} prepore, driving insertion of the 2β2-2β3 loops into the endosomal membrane (Figure 1-2a) (*124*). This transformation creates a mushroom-shaped pore, with the β–loop structures representing the stem of the mushroom. Low pH also triggers EF and LF N-terminal domain unfolding (Figure 1-2a), enabling their translocation across the PA_{63} pore along a voltage gradient (*124, 132*). The central role that low pH plays in enabling AT to breach the endosomal membrane is consistent with an early study demonstrating that perturbing cellular pH blocks intoxication (*133*).

To complete translocation, the cytosolic COPI coatomer complex pulls LF (and possibly EF) into the cytosol (Figure 1-2a) (*134*). As EF and LF are unfolded prior to translocation, these toxic subunits must refold in the cytosol to restore their catalytic activities. How this is achieved is unclear. Nonetheless, the current findings depict a disassembly scenario in which proteolysis and receptor engagement prime AT for subsequent low-pH-induced conformation changes. These changes in turn propel AT's toxic subunits across the endosomal membrane and into the cytosol.

A different combination of triggers disassembles diphtheria toxin (DT), a member of the A-B toxin family that causes severe upper respiratory illness. DT

is synthesized as a single 58-kDa polypeptide chain where the A subunit is the catalytic portion and the B subunit is the receptor-binding and channel component of the toxin. Upon entry into host cells, it disassembles and crosses the endosomal membrane to reach the cytosol and then ADP-ribosylates elongation factor 2 to block protein synthesis, leading to cell death (*135*). In addition to receptor and pH-mediated changes, DT disassembly involves two new triggers: disulfide bond reduction and chaperone mediated unfolding.

Disassembly of DT is initiated by furin-mediated proteolysis either at the cell surface or after endocytosis (Figure 1-2b) (*136*). Proteolysis generates two toxin subunits that are linked by a disulfide bond, the catalytic DTA (*137*) and DTB. DTB is further separated into an N-terminal DTT that transforms into a transmembrane domain and a C-terminal DTR that mediates receptor binding (*138*). Receptor-mediated endocytosis, via DTR, targets the toxin to acidic endosomes (Figure 1-2b). Here, DTT protonation acts as the crucial trigger, evoking a striking conformational change that enables DTT α-helices to insert into the endosomal membrane (*139*) and form a putative channel for DTA translocation (*140*). Membrane-inserted DTT may also function as a transmembrane chaperone, interacting with partially unfolded DTA to prevent its refolding or aggregation during translocation (Figure 1-2b) (*141*). This finding is consistent with data implicating DTA unfolding as a prerequisite for translocation (*142*).

As is the case for AT, the COPI coat has been implicated in extracting DTA into the cytosol. Hsp90 likely assists in refolding DTA to generate the catalytically active form (Figure 1-2b) (*143*). Although there is evidence that the disulfide bond linking DTA and DTB must remain intact during translocation (*144*), reduction of this bond is required to release DTA into the cytosol. The cytosolic thioredoxin reductase may be responsible for this reaction (*143*). Remarkably, the same essential sequence of reactions in DT disassembly is also observed in the disassembly of botulinum neurotoxin (BoNT), the causative agent of botulism (*145*).

Toxins that traverse the ER membrane

Whereas toxins that exploit the endosomal pathway rely on receptor binding and pH change to form a pore and translocate toxic subunits, toxins that travel to the ER use a drastically different strategy. As discussed in the previous section, the ER employs a vast array of chaperones to maintain proper protein folding states. Terminally misfolded proteins are recognized for ERAD and expelled into the cytoplasm through pre-existing pores in the ER membrane (i.e., retro-translocons). By mimicking a misfolded state, toxins that are targeted to the ER can hijack ERAD machinery in order to transfer their toxic subunits to the cytosol. Accordingly, disulfide bond reduction and chaperone-mediated unfolding play a significantly more prominent role in disassembly of these toxins. Cholera, shiga and ricin toxins, all of which are A-B toxins, best exemplify this strategy.

Cholera toxin (CT) produced by *Vibrio cholerae* is an archetypal toxin of ER disassembly. It is the virulence factor that induces a signaling cascade in intestinal epithelial cells, leading to secretory diarrhea. Structurally, CT is composed of two subunits: the catalytic CTA and the receptor-binding CTB (Figure 1-3) (*146*). After proteolytic cleavage, which likely occurs on the target cell surface (*147*), CTA is separated into two domains linked by a disulfide bond. CTA1 is enzymatic while CTA2 is inserted into a pentameric ring formed by CTB subunits. Once CTA1 reaches the cytosol it is activated by ARF family members and ADP-ribosylates $G_{\alpha S}$, leading to constitutive activation of adenylate cyclase, increased cAMP production, and massive chloride secretion (*148, 149*). Before this can happen, however, CT must be disassembled in the host cell. To intoxicate intestinal epithelial cells, CTB binds to ganglioside GM1 on the plasma membrane, undergoes endocytosis, and traffics to the ER (*150*). After ER arrival, CTB targets the toxin to the ER membrane retro-translocation complex composed of Derlin-1 and Hrd1 (Figure1-3) (*60*). CTA is then reduced by an unidentified reductase, separating CTA1 from CTA2. This reduction is important not only for retro-translocation of CTA1, but also for stimulating the enzymatic activity of the toxin (*151*). Next, PDI bound to Derlin-1 and Hrd1 unfolds CTA (*43, 152*). This unfolding reaction is redox driven; reduced PDI binds and unfolds CTA1, whereas oxidized PDI releases the unfolded toxin. This reaction is putatively catalyzed by the ER resident oxidase Ero1α (*153*). The released toxin then passes through a retro-translocon formed by Derlin-1 and Hrd1 or by Sec61

(*66, 154*). Upon reaching the cytosolic surface of the ER membrane, Hrd1-catalyzed ubiquitination mediates CTA1 release into the cytosol (Figure 1-3) (*64*). As CTA1 is ubiquitinated neither on its two lysines nor at its N-terminus (*155*), it is possible that CTA1 is ubiquitinated on non-lysines to promote its retro-translocation (*156*). Alternatively, ubiquitination of other cellular factors may influence CTA1 release. Regardless, CTA1 rapidly refolds in the cytosol (*155*), enabling it to evade proteasomal degradation. It remains unclear whether or not cytosolic ATPases such as p97 (*157, 158*) or Hsp90 (*159*) help pull CTA1 into the cytosol.

Shiga toxin (ST), the causative agent for dysentery and hemorrhagic colitis, also uses proteases, reductases and chaperones for ER disassembly. ST is composed of a catalytic STA and a pentameric, receptor-binding STB subunit. STA functions as an N-glycosidase that removes a single adenine nucleotide from the 28S rRNA, thereby blocking protein synthesis and leading to cell death (*160*). STB binds to the glycolipid receptor globotriaosylceramide Gb3 (*161*) and directs endocytosis of the toxin. Upon cell entry, STA is cleaved by furin in the endosome, generating STA1 and STA2 domains that remain linked by a disulfide bond (*162*). These domains play analogous structural roles to CTA1 and CTA2. After proteolytic cleavage, ST is directed to ER where the STA1-STA2 disulfide linker is reduced by PDI proteins (*163*). As with CTA1, this reaction enables STA1 to be released from the rest of the toxin and enhances its catalytic activity (*162*). Interaction of STA1 with ER-resident chaperones such as ERdj3, BiP and

GRP94 (*164*) unfolds and delivers the toxin for retro-translocation, possibly through the Sec61 channel (*165*). The ability of STA1 to refold, a trait akin to that of CTA1, explains how it circumvents degradation in the cytosol.

In addition to the two aforementioned bacterial toxins, the plant toxin ricin (RT) is also disassembled in the ER. Originally synthesized as a single polypeptide, ricin is cleaved to generate catalytic RTA and receptor-binding RTB subunits that are held together by a disulfide bond in a 1:1 ratio (*166*). Like STA1, RTA acts as an N-glycosidase that halts protein synthesis; RTB binds to β1-4 linked galactosides present on glycolipids and glycoproteins, presenting ricin with a variety of pathways with which to reach the ER. In the ER, the disulfide bond is reduced, releasing and activating RTA (*167, 168*). Indirect evidence suggests that RTA unfolding is required for retro-translocation; EDEM, which is involved in processing glycosylated ERAD substrates in the calnexin-calreticulin cycle, has also been implicated in facilitating RTA retro-translocation (*169*). Once in the cytosol, ricin appears to refold with the help of ribosomes (*170*) and Hsp70 (*171*).

As demonstrated above, toxins that exploit the endosomal pathway and those that pass through the ER employ radically divergent strategies. The most obvious contrast in these approaches lies in dependence on cellular machinery. Anthrax and diphtheria, for example, are reliant on pH change but retain the autonomous ability to form membrane-spanning pores. Cholera, shiga and ricin toxins, on the other hand, each have a propensity to unfold but are heavily dependent on endogenous machinery to attain their goals. Interestingly, the

dissimilarities in the physical structures of the ER toxins are reflected in the different ERAD chaperones that each hijacks.

Using cholera toxin to study ERAD

Just like the link between cystic fibrosis and ERAD, studying the manner in which ER-directed toxins interact with ERAD machinery serves a dual purpose; unraveling the mechanism of toxin delivery not only reveals details about the disease state but also provides unique insight into how ERAD pathways normally operate. Superficially, ERAD substrates can be categorized based on several criteria including glycosylation, ubiquitination and whether a protein is soluble or contains transmembrane segments. Comparing and contrasting how the cell manages the many permutations of endogenous and exogenous substrates enables us to decipher the complex cross talk between components of the ERAD machinery.

Cholera toxin, for example, acts as a soluble, non-glycosylated, non-ubiquitinated ERAD substrate. In this respect, it is devoid of the established signals that direct misfolded proteins for retro-translocation and degradation, yet CT successfully hijacks chaperones used by endogenous, canonical substrates. This bizarre overlap only emphasizes the fact that the mechanisms of ERAD are still poorly characterized. CT also serves as a powerful biochemical tool for studying ERAD. For one, the toxin can be added at will to cells and avoids proteasomal degradation. As such, toxin levels can be analyzed without adjusting for rates of synthesis and degradation. Also, intoxication circumvents

complications with protein over-expression and knockdown. Most importantly, simple cellular fractionation can identify ER arrival and retro-translocation of the toxin. Cells can be permeabilized with digitonin to separate the cytosol from the ER. Generation of CTA1 in the ER signals successful toxin trafficking and the amount of CTA1 in the cytosol indicates the efficiency of retro-translocation. By correlating retro-translocation efficiency with manipulation of ERAD components it is simple to unravel the temporal and spatial arrangements of the pathway.

The main objective of this dissertation is to highlight the ERAD constituents that drive cholera toxin retro-translocation on both the ER and cytosolic sides of the membrane. More specifically, this work mechanistically details how toxin is targeted for retro-translocation in the ER and how it is then extracted from the ER membrane into the cytosol. Ascertaining the method of CT intoxication will undoubtedly clarify the mechanisms of ERAD. Ultimately, by unraveling the ERAD web we can evolve our knowledge of disease and our ability to prevent it.

1-3. Figures

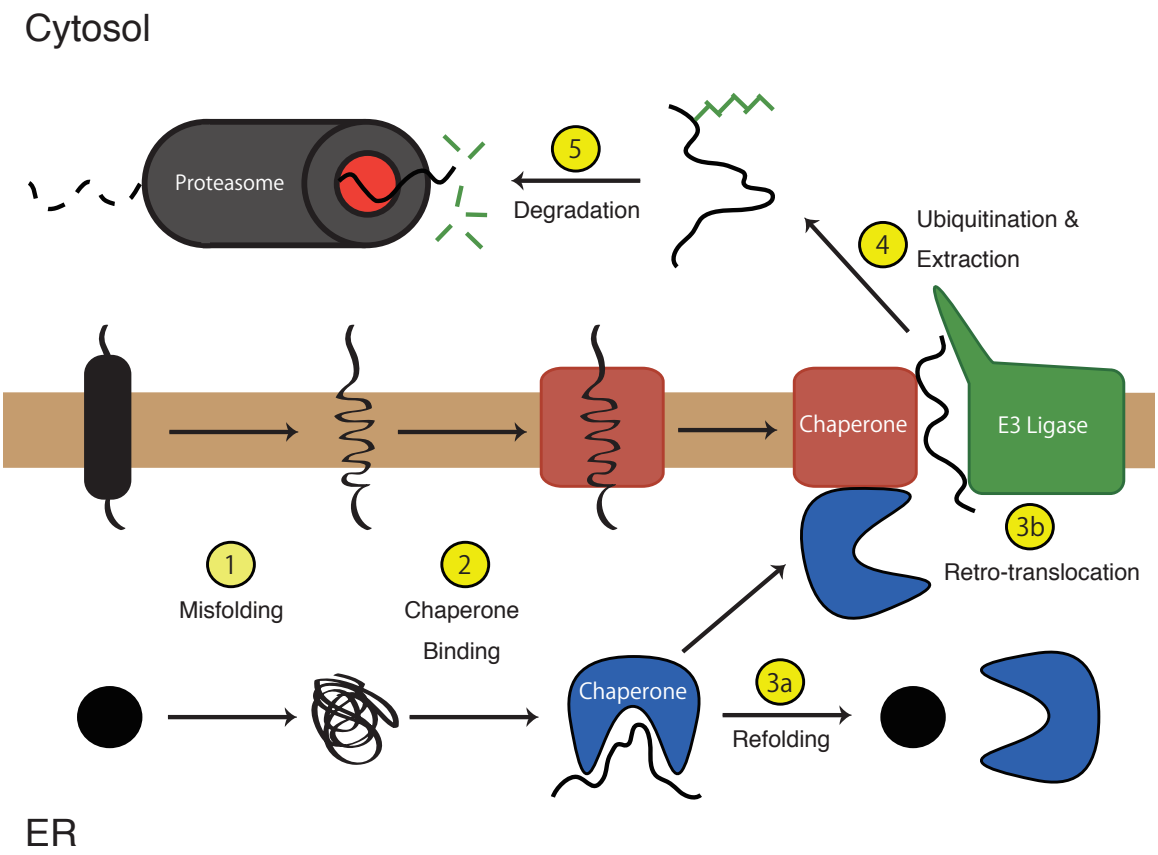

Figure 1-1. Stages of ER-associated degradation

Translational errors or environmental stress induce misfolding of soluble and membrane-associated ER proteins (step 1). Lumenal and membrane chaperones prevent aggregation of misfolded proteins (step 2) and attempt to return them to a folded state (step 3a); proteins that are incapable of refolding are instead targeted for ERAD. Terminally misfolded proteins are released from their chaperones and retro-translocated through a pore in the membrane that is putatively composed of membrane chaperones, E3 ligases, and/or Sec61 (step 3b). Upon reaching the cytosol, ERAD substrates are poly-ubiquitinated by E3 ligases and extracted from the membrane (step 4). Poly-ubiquitination recruits the 26S proteasome which deubiquitinates ERAD substrates and degrades them (step 5).

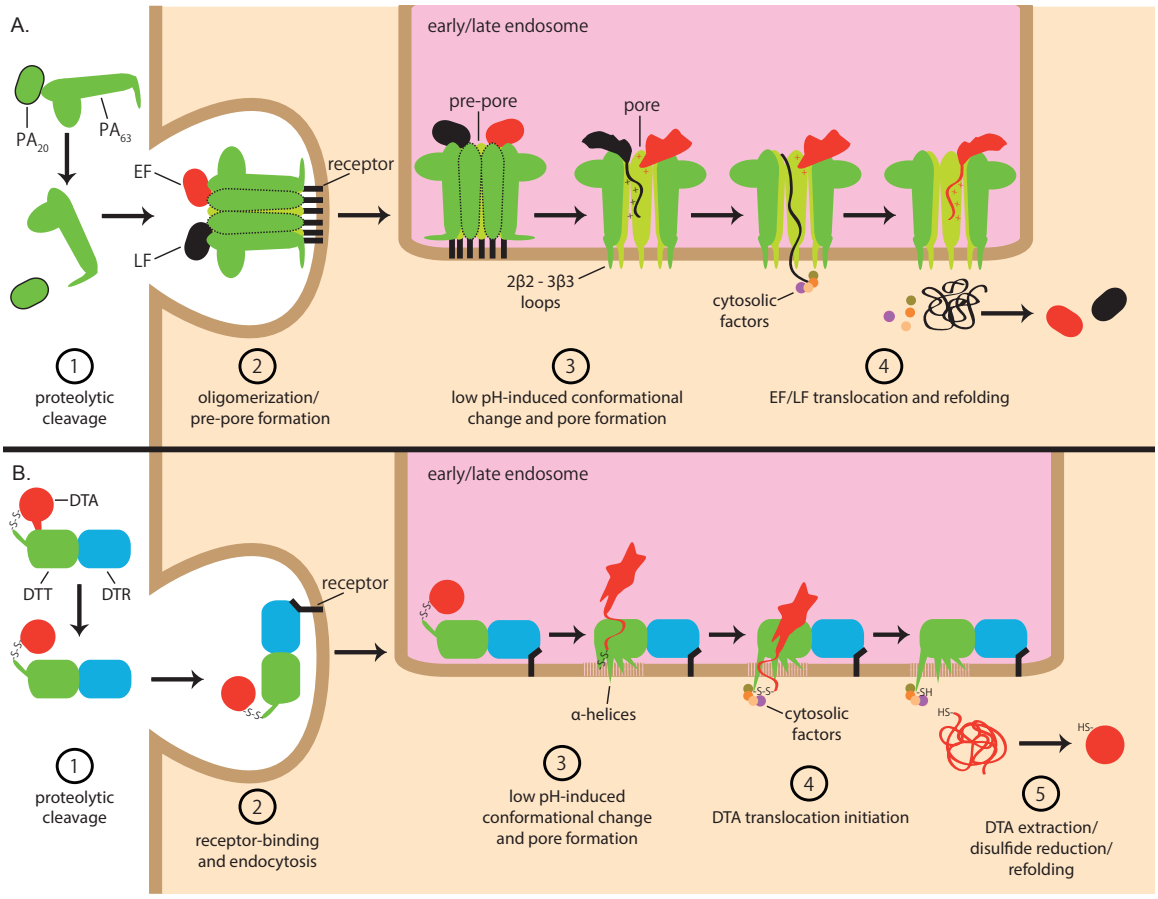

Figure 1-2. Pore-forming toxins enter cells through the endosome

(A) Proteolysis (step 1), receptor binding, and oligomerization (step 2) prime AT for subsequent low-pH-induced conformational changes (step 3). These changes then eject AT's toxic subunit EF or LF across the endosomal membrane through a pore formed by the PA_{63} subunit of AT (step 4). (B) Proteolysis (step 1), receptor-mediated endocytosis (step 2), low-pH-induced conformational change (step 3), chaperone-guided membrane translocation (step 4), disulfide bond reduction, and chaperone-dependent refolding (step 5) transfer DT's toxic DTA subunit across the endosomal membrane via the DTT subunit.

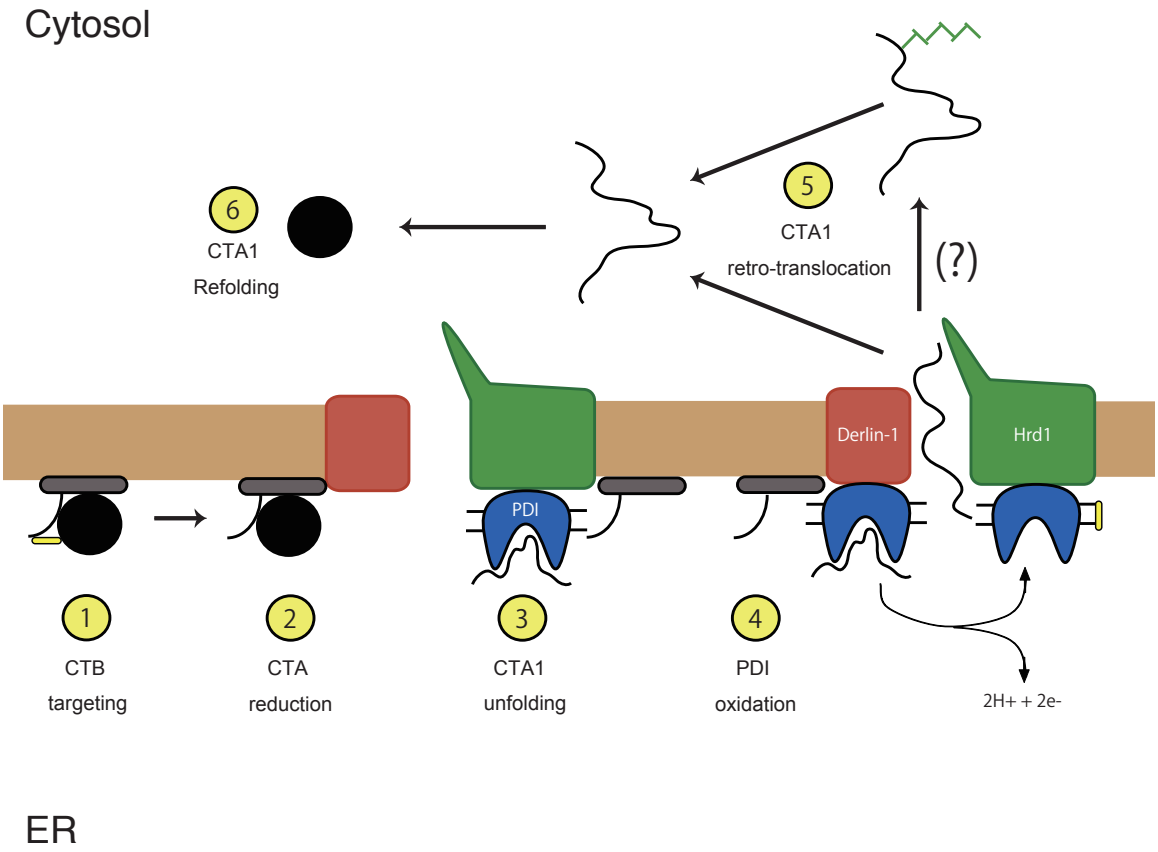

Figure 1-3. Cholera toxin hijacks ERAD to reach the cytosol

In the ER, CT is first targeted to the Derlin-1/Hrd1 membrane complex (step 1). The toxin is then reduced by an unknown reductase (step 2), generating CTA1. PDI bound to Derlin-1/Hrd1 then unfolds CTA1 (step 3). Oxidation of PDI releases unfolded CTA1 (step 4) for retro-translocation across a channel putatively composed of Derlin-1/Hrd1. Whether the toxin undergoes E3-mediated ubiquitination is unclear. A ubiquitin-dependent reaction, potentially involving cytosolic chaperones, pulls the toxin into the cytosol (step 5) where it automatically refolds (step 6).

1-4. References

1. U. Schubert *et al.*, Rapid degradation of a large fraction of newly synthesized proteins by proteasomes. *Nature* **404**, 770 (Apr 13, 2000).
2. ADAM Medical Encyclopedia. (A.D.A.M., Inc., 2010), vol. 2012.
3. D. H. Perlmutter, Pathogenesis of chronic liver injury and hepatocellular carcinoma in alpha-1-antitrypsin deficiency. *Pediatric research* **60**, 233 (Aug, 2006).
4. K. A. Dill, S. B. Ozkan, M. S. Shell, T. R. Weikl, The protein folding problem. *Annual review of biophysics* **37**, 289 (2008).
5. C. Hwang, A. J. Sinskey, H. F. Lodish, Oxidized redox state of glutathione in the endoplasmic reticulum. *Science* **257**, 1496 (Sep 11, 1992).
6. J. L. Brodsky, W. R. Skach, Protein folding and quality control in the endoplasmic reticulum: Recent lessons from yeast and mammalian cell systems. *Current opinion in cell biology* **23**, 464 (Aug, 2011).
7. R. J. Ellis, Macromolecular crowding: obvious but underappreciated. *Trends in biochemical sciences* **26**, 597 (Oct, 2001).
8. C. M. Dobson, Protein folding and misfolding. *Nature* **426**, 884 (Dec 18, 2003).
9. M. Aebi, R. Bernasconi, S. Clerc, M. Molinari, N-glycan structures: recognition and processing in the ER. *Trends in biochemical sciences* **35**, 74 (Feb, 2010).
10. I. Saraogi, S. O. Shan, Molecular mechanism of co-translational protein targeting by the signal recognition particle. *Traffic* **12**, 535 (May, 2011).
11. N. S. Rane, O. Chakrabarti, L. Feigenbaum, R. S. Hegde, Signal sequence insufficiency contributes to neurodegeneration caused by transmembrane prion protein. *The Journal of cell biology* **188**, 515 (Feb 22, 2010).
12. K. L. Shaffer, A. Sharma, E. L. Snapp, R. S. Hegde, Regulation of protein compartmentalization expands the diversity of protein function. *Developmental cell* **9**, 545 (Oct, 2005).
13. C. Kimchi-Sarfaty *et al.*, A "silent" polymorphism in the MDR1 gene changes substrate specificity. *Science* **315**, 525 (Jan 26, 2007).
14. F. C. Schuit, P. A. In't Veld, D. G. Pipeleers, Glucose stimulates proinsulin biosynthesis by a dose-dependent recruitment of pancreatic beta cells. *Proceedings of the National Academy of Sciences of the United States of America* **85**, 3865 (Jun, 1988).
15. S. G. Fonseca, F. Urano, M. Burcin, J. Gromada, Stress hypERactivation in the beta-cell. *Islets* **2**, 1 (Jan-Feb, 2010).
16. J. S. Cox, C. E. Shamu, P. Walter, Transcriptional induction of genes encoding endoplasmic reticulum resident proteins requires a transmembrane protein kinase. *Cell* **73**, 1197 (Jun 18, 1993).
17. A. Varki, M. E. Etzler, R. D. Cummings, J. D. Esko, in *Essentials of Glycobiology,* A. Varki *et al.*, Eds. (Cold Spring Harbor (NY), 2009).

18. I. G. Ganley, P. M. Wong, N. Gammoh, X. Jiang, Distinct autophagosomal-lysosomal fusion mechanism revealed by thapsigargin-induced autophagy arrest. *Molecular cell* **42**, 731 (Jun 24, 2011).
19. T. Okiyoneda, P. M. Apaja, G. L. Lukacs, Protein quality control at the plasma membrane. *Current opinion in cell biology* **23**, 483 (Aug, 2011).
20. T. Okiyoneda *et al.*, Peripheral protein quality control removes unfolded CFTR from the plasma membrane. *Science* **329**, 805 (Aug 13, 2010).
21. M. Chatenay-Lapointe, G. S. Shadel, Stressed-out mitochondria get MAD. *Cell metabolism* **12**, 559 (Dec 1, 2010).
22. E. B. Taylor, J. Rutter, Mitochondrial quality control by the ubiquitin-proteasome system. *Biochemical Society transactions* **39**, 1509 (Oct, 2011).
23. J. M. Heo *et al.*, A stress-responsive system for mitochondrial protein degradation. *Molecular cell* **40**, 465 (Nov 12, 2010).
24. S. Xu, G. Peng, Y. Wang, S. Fang, M. Karbowski, The AAA-ATPase p97 is essential for outer mitochondrial membrane protein turnover. *Molecular biology of the cell* **22**, 291 (Feb 1, 2011).
25. J. Lippincott-Schwartz, J. S. Bonifacino, L. C. Yuan, R. D. Klausner, Degradation from the endoplasmic reticulum: disposing of newly synthesized proteins. *Cell* **54**, 209 (Jul 15, 1988).
26. J. L. Brodsky, The protective and destructive roles played by molecular chaperones during ERAD (endoplasmic-reticulum-associated degradation). *The Biochemical journal* **404**, 353 (Jun 15, 2007).
27. T. M. Buck, C. M. Wright, J. L. Brodsky, The activities and function of molecular chaperones in the endoplasmic reticulum. *Seminars in cell & developmental biology* **18**, 751 (Dec, 2007).
28. E. A. Craig, P. Huang, R. Aron, A. Andrew, The diverse roles of J-proteins, the obligate Hsp70 co-chaperone. *Reviews of physiology, biochemistry and pharmacology* **156**, 1 (2006).
29. L. Shaner, K. A. Morano, All in the family: atypical Hsp70 chaperones are conserved modulators of Hsp70 activity. *Cell stress & chaperones* **12**, 1 (Spring, 2007).
30. K. A. Krukenberg, T. O. Street, L. A. Lavery, D. A. Agard, Conformational dynamics of the molecular chaperone Hsp90. *Quarterly reviews of biophysics* **44**, 229 (May, 2011).
31. D. R. Southworth, D. A. Agard, Client-loading conformation of the Hsp90 molecular chaperone revealed in the cryo-EM structure of the human Hsp90:Hop complex. *Molecular cell* **42**, 771 (Jun 24, 2011).
32. J. Melnick, J. L. Dul, Y. Argon, Sequential interaction of the chaperones BiP and GRP94 with immunoglobulin chains in the endoplasmic reticulum. *Nature* **370**, 373 (Aug 4, 1994).
33. I. G. Haas, M. Wabl, Immunoglobulin heavy chain binding protein. *Nature* **306**, 387 (Nov 24-30, 1983).

34. S. I. Nishikawa, S. W. Fewell, Y. Kato, J. L. Brodsky, T. Endo, Molecular chaperones in the yeast endoplasmic reticulum maintain the solubility of proteins for retrotranslocation and degradation. *The Journal of cell biology* **153**, 1061 (May 28, 2001).
35. T. Imamura *et al.*, Involvement of heat shock protein 90 in the degradation of mutant insulin receptors by the proteasome. *The Journal of biological chemistry* **273**, 11183 (May 1, 1998).
36. V. Gusarova, A. J. Caplan, J. L. Brodsky, E. A. Fisher, Apoprotein B degradation is promoted by the molecular chaperones hsp90 and hsp70. *The Journal of biological chemistry* **276**, 24891 (Jul 6, 2001).
37. R. R. Ramos, A. J. Swanson, J. Bass, Calreticulin and Hsp90 stabilize the human insulin receptor and promote its mobility in the endoplasmic reticulum. *Proceedings of the National Academy of Sciences of the United States of America* **104**, 10470 (Jun 19, 2007).
38. A. Bertolotti, Y. Zhang, L. M. Hendershot, H. P. Harding, D. Ron, Dynamic interaction of BiP and ER stress transducers in the unfolded-protein response. *Nature cell biology* **2**, 326 (Jun, 2000).
39. F. Hatahet, L. W. Ruddock, Protein disulfide isomerase: a critical evaluation of its function in disulfide bond formation. *Antioxidants & redox signaling* **11**, 2807 (Nov, 2009).
40. C. Appenzeller-Herzog, L. Ellgaard, The human PDI family: versatility packed into a single fold. *Biochimica et biophysica acta* **1783**, 535 (Apr, 2008).
41. G. Rajpal, I. Schuiki, M. Liu, A. Volchuk, P. Arvan, Action of protein disulfide isomerase on proinsulin exit from endoplasmic reticulum of pancreatic beta-cells. *The Journal of biological chemistry* **287**, 43 (Jan 2, 2012).
42. M. L. Forster, J. J. Mahn, B. Tsai, Generating an unfoldase from thioredoxin-like domains. *The Journal of biological chemistry* **284**, 13045 (May 8, 2009).
43. M. L. Forster *et al.*, Protein disulfide isomerase-like proteins play opposing roles during retrotranslocation. *The Journal of cell biology* **173**, 853 (Jun 19, 2006).
44. Y. Oda, N. Hosokawa, I. Wada, K. Nagata, EDEM as an acceptor of terminally misfolded glycoproteins released from calnexin. *Science* **299**, 1394 (Feb 28, 2003).
45. E. M. Quan *et al.*, Defining the glycan destruction signal for endoplasmic reticulum-associated degradation. *Molecular cell* **32**, 870 (Dec 26, 2008).
46. C. Hirsch, R. Gauss, S. C. Horn, O. Neuber, T. Sommer, The ubiquitylation machinery of the endoplasmic reticulum. *Nature* **458**, 453 (Mar 26, 2009).
47. N. Hosokawa *et al.*, Enhancement of endoplasmic reticulum (ER) degradation of misfolded Null Hong Kong alpha1-antitrypsin by human ER

mannosidase I. *The Journal of biological chemistry* **278**, 26287 (Jul 11, 2003).
48. S. W. Mast *et al.*, Human EDEM2, a novel homolog of family 47 glycosidases, is involved in ER-associated degradation of glycoproteins. *Glycobiology* **15**, 421 (Apr, 2005).
49. R. Bernasconi *et al.*, Role of the SEL1L:LC3-I Complex as an ERAD Tuning Receptor in the Mammalian ER. *Molecular cell*, (May 23, 2012).
50. M. Sakoh-Nakatogawa, S. Nishikawa, T. Endo, Roles of protein-disulfide isomerase-mediated disulfide bond formation of yeast Mnl1p in endoplasmic reticulum-associated degradation. *The Journal of biological chemistry* **284**, 11815 (May 1, 2009).
51. R. Gauss, K. Kanehara, P. Carvalho, D. T. Ng, M. Aebi, A complex of Pdi1p and the mannosidase Htm1p initiates clearance of unfolded glycoproteins from the endoplasmic reticulum. *Molecular cell* **42**, 782 (Jun 24, 2011).
52. M. Hagiwara *et al.*, Structural basis of an ERAD pathway mediated by the ER-resident protein disulfide reductase ERdj5. *Molecular cell* **41**, 432 (Feb 18, 2011).
53. S. Pollock *et al.*, Specific interaction of ERp57 and calnexin determined by NMR spectroscopy and an ER two-hybrid system. *The EMBO journal* **23**, 1020 (Mar 10, 2004).
54. P. Moore, K. M. Bernardi, B. Tsai, The Ero1alpha-PDI redox cycle regulates retro-translocation of cholera toxin. *Molecular biology of the cell* **21**, 1305 (Apr 1, 2010).
55. N. Hosokawa *et al.*, Human XTP3-B forms an endoplasmic reticulum quality control scaffold with the HRD1-SEL1L ubiquitin ligase complex and BiP. *The Journal of biological chemistry* **283**, 20914 (Jul 25, 2008).
56. C. M. Cabral, Y. Liu, K. W. Moremen, R. N. Sifers, Organizational diversity among distinct glycoprotein endoplasmic reticulum-associated degradation programs. *Molecular biology of the cell* **13**, 2639 (Aug, 2002).
57. M. Pilon, R. Schekman, K. Romisch, Sec61p mediates export of a misfolded secretory protein from the endoplasmic reticulum to the cytosol for degradation. *The EMBO journal* **16**, 4540 (Aug 1, 1997).
58. R. K. Plemper, S. Bohmler, J. Bordallo, T. Sommer, D. H. Wolf, Mutant analysis links the translocon and BiP to retrograde protein transport for ER degradation. *Nature* **388**, 891 (Aug 28, 1997).
59. D. C. Scott, R. Schekman, Role of Sec61p in the ER-associated degradation of short-lived transmembrane proteins. *The Journal of cell biology* **181**, 1095 (Jun 30, 2008).
60. K. M. Bernardi, M. L. Forster, W. I. Lencer, B. Tsai, Derlin-1 facilitates the retro-translocation of cholera toxin. *Molecular biology of the cell* **19**, 877 (Mar, 2008).

61. S. G. Crawshaw, B. C. Cross, C. M. Wilson, S. High, The oligomeric state of Derlin-1 is modulated by endoplasmic reticulum stress. *Molecular membrane biology* **24**, 113 (Mar-Apr, 2007).
62. J. Wahlman *et al.*, Real-time fluorescence detection of ERAD substrate retrotranslocation in a mammalian in vitro system. *Cell* **129**, 943 (Jun 1, 2007).
63. M. Willer, G. M. Forte, C. J. Stirling, Sec61p is required for ERAD-L: genetic dissection of the translocation and ERAD-L functions of Sec61P using novel derivatives of CPY. *The Journal of biological chemistry* **283**, 33883 (Dec 5, 2008).
64. K. M. Bernardi *et al.*, The E3 ubiquitin ligases Hrd1 and gp78 bind to and promote cholera toxin retro-translocation. *Molecular biology of the cell* **21**, 140 (Jan 1, 2010).
65. R. M. Garza, B. K. Sato, R. Y. Hampton, In vitro analysis of Hrd1p-mediated retrotranslocation of its multispanning membrane substrate 3-hydroxy-3-methylglutaryl (HMG)-CoA reductase. *The Journal of biological chemistry* **284**, 14710 (May 29, 2009).
66. P. Carvalho, A. M. Stanley, T. A. Rapoport, Retrotranslocation of a misfolded luminal ER protein by the ubiquitin-ligase Hrd1p. *Cell* **143**, 579 (Nov 12, 2010).
67. Y. C. Tsai, A. M. Weissman, Ubiquitylation in ERAD: reversing to go forward? *PLoS biology* **9**, e1001038 (Mar, 2011).
68. D. Finley, Recognition and processing of ubiquitin-protein conjugates by the proteasome. *Annual review of biochemistry* **78**, 477 (2009).
69. Y. Imai, M. Soda, R. Takahashi, Parkin suppresses unfolded protein stress-induced cell death through its E3 ubiquitin-protein ligase activity. *The Journal of biological chemistry* **275**, 35661 (Nov 17, 2000).
70. K. Bagola, M. Mehnert, E. Jarosch, T. Sommer, Protein dislocation from the ER. *Biochimica et biophysica acta* **1808**, 925 (Mar, 2011).
71. B. N. Lilley, H. L. Ploegh, A membrane protein required for dislocation of misfolded proteins from the ER. *Nature* **429**, 834 (Jun 24, 2004).
72. Y. Ye *et al.*, Recruitment of the p97 ATPase and ubiquitin ligases to the site of retrotranslocation at the endoplasmic reticulum membrane. *Proceedings of the National Academy of Sciences of the United States of America* **102**, 14132 (Oct 4, 2005).
73. N. W. Bays, R. G. Gardner, L. P. Seelig, C. A. Joazeiro, R. Y. Hampton, Hrd1p/Der3p is a membrane-anchored ubiquitin ligase required for ER-associated degradation. *Nature cell biology* **3**, 24 (Jan, 2001).
74. X. Zhong *et al.*, AAA ATPase p97/valosin-containing protein interacts with gp78, a ubiquitin ligase for endoplasmic reticulum-associated degradation. *The Journal of biological chemistry* **279**, 45676 (Oct 29, 2004).
75. Y. Ye, H. H. Meyer, T. A. Rapoport, The AAA ATPase Cdc48/p97 and its partners transport proteins from the ER into the cytosol. *Nature* **414**, 652 (Dec 6, 2001).

76. E. Jarosch *et al.*, Protein dislocation from the ER requires polyubiquitination and the AAA-ATPase Cdc48. *Nature cell biology* **4**, 134 (Feb, 2002).
77. E. Rabinovich, A. Kerem, K. U. Frohlich, N. Diamant, S. Bar-Nun, AAA-ATPase p97/Cdc48p, a cytosolic chaperone required for endoplasmic reticulum-associated protein degradation. *Molecular and cellular biology* **22**, 626 (Jan, 2002).
78. Y. Ye, Y. Shibata, C. Yun, D. Ron, T. A. Rapoport, A membrane protein complex mediates retro-translocation from the ER lumen into the cytosol. *Nature* **429**, 841 (Jun 24, 2004).
79. K. Husnjak *et al.*, Proteasome subunit Rpn13 is a novel ubiquitin receptor. *Nature* **453**, 481 (May 22, 2008).
80. P. Schreiner *et al.*, Ubiquitin docking at the proteasome through a novel pleckstrin-homology domain interaction. *Nature* **453**, 548 (May 22, 2008).
81. A. F. Kisselev, T. N. Akopian, K. M. Woo, A. L. Goldberg, The sizes of peptides generated from protein by mammalian 26 and 20 S proteasomes. Implications for understanding the degradative mechanism and antigen presentation. *The Journal of biological chemistry* **274**, 3363 (Feb 5, 1999).
82. Y. Liu, Y. Ye, Roles of p97-associated deubiquitinases in protein quality control at the endoplasmic reticulum. *Current protein & peptide science*, (Jul 18, 2012).
83. M. E. Sowa, E. J. Bennett, S. P. Gygi, J. W. Harper, Defining the human deubiquitinating enzyme interaction landscape. *Cell* **138**, 389 (Jul 23, 2009).
84. K. M. Bernardi, B. Tsai, *(Unpublished Data)*.
85. K. B. Kruse, J. L. Brodsky, A. A. McCracken, Autophagy: an ER protein quality control process. *Autophagy* **2**, 135 (Apr-Jun, 2006).
86. C. W. Lai, D. E. Aronson, E. L. Snapp, BiP availability distinguishes states of homeostasis and stress in the endoplasmic reticulum of living cells. *Molecular biology of the cell* **21**, 1909 (Jun 15, 2010).
87. J. J. Credle, J. S. Finer-Moore, F. R. Papa, R. M. Stroud, P. Walter, On the mechanism of sensing unfolded protein in the endoplasmic reticulum. *Proceedings of the National Academy of Sciences of the United States of America* **102**, 18773 (Dec 27, 2005).
88. D. Pincus *et al.*, BiP binding to the ER-stress sensor Ire1 tunes the homeostatic behavior of the unfolded protein response. *PLoS biology* **8**, e1000415 (2010).
89. B. M. Gardner, P. Walter, Unfolded proteins are Ire1-activating ligands that directly induce the unfolded protein response. *Science* **333**, 1891 (Sep 30, 2011).
90. T. Okada, H. Yoshida, R. Akazawa, M. Negishi, K. Mori, Distinct roles of activating transcription factor 6 (ATF6) and double-stranded RNA-activated protein kinase-like endoplasmic reticulum kinase (PERK) in

transcription during the mammalian unfolded protein response. *The Biochemical journal* **366**, 585 (Sep 1, 2002).
91. S. J. Marciniak *et al.*, CHOP induces death by promoting protein synthesis and oxidation in the stressed endoplasmic reticulum. *Genes & development* **18**, 3066 (Dec 15, 2004).
92. J. H. Lin *et al.*, IRE1 signaling affects cell fate during the unfolded protein response. *Science* **318**, 944 (Nov 9, 2007).
93. D. T. Rutkowski, R. J. Kaufman, That which does not kill me makes me stronger: adapting to chronic ER stress. *Trends in biochemical sciences* **32**, 469 (Oct, 2007).
94. K. Zhang, R. J. Kaufman, From endoplasmic-reticulum stress to the inflammatory response. *Nature* **454**, 455 (Jul 24, 2008).
95. C. J. Guerriero, J. L. Brodsky, The delicate balance between secreted protein folding and endoplasmic reticulum-associated degradation in human physiology. *Physiological reviews* **92**, 537 (Apr, 2012).
96. L. Zhao, S. L. Ackerman, Endoplasmic reticulum stress in health and disease. *Current opinion in cell biology* **18**, 444 (Aug, 2006).
97. G. L. Lukacs *et al.*, Conformational maturation of CFTR but not its mutant counterpart (delta F508) occurs in the endoplasmic reticulum and requires ATP. *The EMBO journal* **13**, 6076 (Dec 15, 1994).
98. C. L. Ward, R. R. Kopito, Intracellular turnover of cystic fibrosis transmembrane conductance regulator. Inefficient processing and rapid degradation of wild-type and mutant proteins. *The Journal of biological chemistry* **269**, 25710 (Oct 14, 1994).
99. D. C. Gadsby, P. Vergani, L. Csanady, The ABC protein turned chloride channel whose failure causes cystic fibrosis. *Nature* **440**, 477 (Mar 23, 2006).
100. K. Du, M. Sharma, G. L. Lukacs, The DeltaF508 cystic fibrosis mutation impairs domain-domain interactions and arrests post-translational folding of CFTR. *Nature structural & molecular biology* **12**, 17 (Jan, 2005).
101. B. Kleizen, T. van Vlijmen, H. R. de Jonge, I. Braakman, Folding of CFTR is predominantly cotranslational. *Molecular cell* **20**, 277 (Oct 28, 2005).
102. K. Du, G. L. Lukacs, Cooperative assembly and misfolding of CFTR domains in vivo. *Molecular biology of the cell* **20**, 1903 (Apr, 2009).
103. P. H. Thibodeau *et al.*, The cystic fibrosis-causing mutation deltaF508 affects multiple steps in cystic fibrosis transmembrane conductance regulator biogenesis. *The Journal of biological chemistry* **285**, 35825 (Nov 12, 2010).
104. K. Varga *et al.*, Efficient intracellular processing of the endogenous cystic fibrosis transmembrane conductance regulator in epithelial cell lines. *The Journal of biological chemistry* **279**, 22578 (May 21, 2004).
105. ADAM Medical Encyclopedia. (A.D.A.M., Inc., 2010), vol. 2012.

106. W. Dalemans *et al.*, Altered chloride ion channel kinetics associated with the delta F508 cystic fibrosis mutation. *Nature* **354**, 526 (Dec 19-26, 1991).
107. C. M. Haws *et al.*, Delta F508-CFTR channels: kinetics, activation by forskolin, and potentiation by xanthines. *The American journal of physiology* **270**, C1544 (May, 1996).
108. S. H. Cheng *et al.*, Defective intracellular transport and processing of CFTR is the molecular basis of most cystic fibrosis. *Cell* **63**, 827 (Nov 16, 1990).
109. T. J. Jensen *et al.*, Multiple proteolytic systems, including the proteasome, contribute to CFTR processing. *Cell* **83**, 129 (Oct 6, 1995).
110. C. L. Ward, S. Omura, R. R. Kopito, Degradation of CFTR by the ubiquitin-proteasome pathway. *Cell* **83**, 121 (Oct 6, 1995).
111. M. A. Loo *et al.*, Perturbation of Hsp90 interaction with nascent CFTR prevents its maturation and accelerates its degradation by the proteasome. *The EMBO journal* **17**, 6879 (Dec 1, 1998).
112. R. T. Youker, P. Walsh, T. Beilharz, T. Lithgow, J. L. Brodsky, Distinct roles for the Hsp40 and Hsp90 molecular chaperones during cystic fibrosis transmembrane conductance regulator degradation in yeast. *Molecular biology of the cell* **15**, 4787 (Nov, 2004).
113. X. Wang *et al.*, Hsp90 cochaperone Aha1 downregulation rescues misfolding of CFTR in cystic fibrosis. *Cell* **127**, 803 (Nov 17, 2006).
114. A. V. Koulov *et al.*, Biological and structural basis for Aha1 regulation of Hsp90 ATPase activity in maintaining proteostasis in the human disease cystic fibrosis. *Molecular biology of the cell* **21**, 871 (Mar 15, 2010).
115. G. C. Meacham *et al.*, The Hdj-2/Hsc70 chaperone pair facilitates early steps in CFTR biogenesis. *The EMBO journal* **18**, 1492 (Mar 15, 1999).
116. C. M. Farinha, M. D. Amaral, Most F508del-CFTR is targeted to degradation at an early folding checkpoint and independently of calnexin. *Molecular and cellular biology* **25**, 5242 (Jun, 2005).
117. K. Harada *et al.*, Calreticulin negatively regulates the cell surface expression of cystic fibrosis transmembrane conductance regulator. *The Journal of biological chemistry* **281**, 12841 (May 5, 2006).
118. M. F. Rosser, D. E. Grove, L. Chen, D. M. Cyr, Assembly and misassembly of cystic fibrosis transmembrane conductance regulator: folding defects caused by deletion of F508 occur before and after the calnexin-dependent association of membrane spanning domain (MSD) 1 and MSD2. *Molecular biology of the cell* **19**, 4570 (Nov, 2008).
119. C. M. Farinha, P. Nogueira, F. Mendes, D. Penque, M. D. Amaral, The human DnaJ homologue (Hdj)-1/heat-shock protein (Hsp) 40 co-chaperone is required for the in vivo stabilization of the cystic fibrosis transmembrane conductance regulator by Hsp70. *The Biochemical journal* **366**, 797 (Sep 15, 2002).

120. S. Sato, C. L. Ward, R. R. Kopito, Cotranslational ubiquitination of cystic fibrosis transmembrane conductance regulator in vitro. *The Journal of biological chemistry* **273**, 7189 (Mar 27, 1998).
121. G. C. Meacham, C. Patterson, W. Zhang, J. M. Younger, D. M. Cyr, The Hsc70 co-chaperone CHIP targets immature CFTR for proteasomal degradation. *Nature cell biology* **3**, 100 (Jan, 2001).
122. D. Morito *et al.*, Gp78 cooperates with RMA1 in endoplasmic reticulum-associated degradation of CFTRDeltaF508. *Molecular biology of the cell* **19**, 1328 (Apr, 2008).
123. D. E. Grove, C. Y. Fan, H. Y. Ren, D. M. Cyr, The endoplasmic reticulum-associated Hsp40 DNAJB12 and Hsc70 cooperate to facilitate RMA1 E3-dependent degradation of nascent CFTRDeltaF508. *Molecular biology of the cell* **22**, 301 (Feb 1, 2011).
124. R. J. Collier, Membrane translocation by anthrax toxin. *Molecular aspects of medicine* **30**, 413 (Dec, 2009).
125. K. R. Klimpel, S. S. Molloy, G. Thomas, S. H. Leppla, Anthrax toxin protective antigen is activated by a cell surface protease with the sequence specificity and catalytic properties of furin. *Proceedings of the National Academy of Sciences of the United States of America* **89**, 10277 (Nov 1, 1992).
126. B. A. Krantz *et al.*, A phenylalanine clamp catalyzes protein translocation through the anthrax toxin pore. *Science* **309**, 777 (Jul 29, 2005).
127. J. Mogridge, M. Mourez, R. J. Collier, Involvement of domain 3 in oligomerization by the protective antigen moiety of anthrax toxin. *Journal of bacteriology* **183**, 2111 (Mar, 2001).
128. Y. Singh, K. R. Klimpel, C. P. Quinn, V. K. Chaudhary, S. H. Leppla, The carboxyl-terminal end of protective antigen is required for receptor binding and anthrax toxin activity. *The Journal of biological chemistry* **266**, 15493 (Aug 15, 1991).
129. J. C. Milne, D. Furlong, P. C. Hanna, J. S. Wall, R. J. Collier, Anthrax protective antigen forms oligomers during intoxication of mammalian cells. *The Journal of biological chemistry* **269**, 20607 (Aug 12, 1994).
130. J. Mogridge, K. Cunningham, D. B. Lacy, M. Mourez, R. J. Collier, The lethal and edema factors of anthrax toxin bind only to oligomeric forms of the protective antigen. *Proceedings of the National Academy of Sciences of the United States of America* **99**, 7045 (May 14, 2002).
131. D. B. Lacy, D. J. Wigelsworth, R. A. Melnyk, S. C. Harrison, R. J. Collier, Structure of heptameric protective antigen bound to an anthrax toxin receptor: a role for receptor in pH-dependent pore formation. *Proceedings of the National Academy of Sciences of the United States of America* **101**, 13147 (Sep 7, 2004).
132. B. A. Krantz, A. D. Trivedi, K. Cunningham, K. A. Christensen, R. J. Collier, Acid-induced unfolding of the amino-terminal domains of the lethal

and edema factors of anthrax toxin. *Journal of molecular biology* **344**, 739 (Nov 26, 2004).
133. A. M. Friedlander, Macrophages are sensitive to anthrax lethal toxin through an acid-dependent process. *The Journal of biological chemistry* **261**, 7123 (Jun 5, 1986).
134. A. G. Tamayo, A. Bharti, C. Trujillo, R. Harrison, J. R. Murphy, COPI coatomer complex proteins facilitate the translocation of anthrax lethal factor across vesicular membranes in vitro. *Proceedings of the National Academy of Sciences of the United States of America* **105**, 5254 (Apr 1, 2008).
135. A. M. Pappenheimer, Jr., Diphtheria toxin. *Annual review of biochemistry* **46**, 69 (1977).
136. M. Tsuneoka *et al.*, Evidence for involvement of furin in cleavage and activation of diphtheria toxin. *The Journal of biological chemistry* **268**, 26461 (Dec 15, 1993).
137. D. M. Gill, A. M. Pappenheimer, Jr., Structure-activity relationships in diphtheria toxin. *The Journal of biological chemistry* **246**, 1492 (Mar 10, 1971).
138. K. J. Oh, L. Senzel, R. J. Collier, A. Finkelstein, Translocation of the catalytic domain of diphtheria toxin across planar phospholipid bilayers by its own T domain. *Proceedings of the National Academy of Sciences of the United States of America* **96**, 8467 (Jul 20, 1999).
139. E. London, Diphtheria toxin: membrane interaction and membrane translocation. *Biochimica et biophysica acta* **1113**, 25 (Mar 26, 1992).
140. E. Papini *et al.*, Lipid interaction of diphtheria toxin and mutants with altered fragment B. 1. Liposome aggregation and fusion. *European journal of biochemistry / FEBS* **169**, 629 (Dec 15, 1987).
141. J. Ren *et al.*, Interaction of diphtheria toxin T domain with molten globule-like proteins and its implications for translocation. *Science* **284**, 955 (May 7, 1999).
142. A. Wiedlocha, I. H. Madshus, H. Mach, C. R. Middaugh, S. Olsnes, Tight folding of acidic fibroblast growth factor prevents its translocation to the cytosol with diphtheria toxin as vector. *The EMBO journal* **11**, 4835 (Dec, 1992).
143. R. Ratts *et al.*, The cytosolic entry of diphtheria toxin catalytic domain requires a host cell cytosolic translocation factor complex. *The Journal of cell biology* **160**, 1139 (Mar 31, 2003).
144. S. Ariansen *et al.*, Membrane translocation of diphtheria toxin A-fragment: role of carboxy-terminal region. *Biochemistry* **32**, 83 (Jan 12, 1993).
145. L. L. Simpson, Identification of the major steps in botulinum toxin action. *Annual review of pharmacology and toxicology* **44**, 167 (2004).
146. W. I. Lencer, B. Tsai, The intracellular voyage of cholera toxin: going retro. *Trends in biochemical sciences* **28**, 639 (Dec, 2003).

147. W. I. Lencer *et al.*, Proteolytic activation of cholera toxin and Escherichia coli labile toxin by entry into host epithelial cells. Signal transduction by a protease-resistant toxin variant. *The Journal of biological chemistry* **272**, 15562 (Jun 13, 1997).
148. D. Vanden Broeck, C. Horvath, M. J. De Wolf, Vibrio cholerae: cholera toxin. *The international journal of biochemistry & cell biology* **39**, 1771 (2007).
149. C. J. O'Neal, M. G. Jobling, R. K. Holmes, W. G. Hol, Structural basis for the activation of cholera toxin by human ARF6-GTP. *Science* **309**, 1093 (Aug 12, 2005).
150. Y. Fujinaga *et al.*, Gangliosides that associate with lipid rafts mediate transport of cholera and related toxins from the plasma membrane to endoplasmic reticulm. *Molecular biology of the cell* **14**, 4783 (Dec, 2003).
151. J. J. Mekalanos, R. J. Collier, W. R. Romig, Enzymic activity of cholera toxin. II. Relationships to proteolytic processing, disulfide bond reduction, and subunit composition. *The Journal of biological chemistry* **254**, 5855 (Jul 10, 1979).
152. B. Tsai, C. Rodighiero, W. I. Lencer, T. A. Rapoport, Protein disulfide isomerase acts as a redox-dependent chaperone to unfold cholera toxin. *Cell* **104**, 937 (Mar 23, 2001).
153. B. Tsai, T. A. Rapoport, Unfolded cholera toxin is transferred to the ER membrane and released from protein disulfide isomerase upon oxidation by Ero1. *The Journal of cell biology* **159**, 207 (Oct 28, 2002).
154. A. Schmitz, H. Herrgen, A. Winkeler, V. Herzog, Cholera toxin is exported from microsomes by the Sec61p complex. *The Journal of cell biology* **148**, 1203 (Mar 20, 2000).
155. C. Rodighiero, B. Tsai, T. A. Rapoport, W. I. Lencer, Role of ubiquitination in retro-translocation of cholera toxin and escape of cytosolic degradation. *EMBO reports* **3**, 1222 (Dec, 2002).
156. X. Wang *et al.*, Ubiquitination of serine, threonine, or lysine residues on the cytoplasmic tail can induce ERAD of MHC-I by viral E3 ligase mK3. *The Journal of cell biology* **177**, 613 (May 21, 2007).
157. M. Kothe *et al.*, Role of p97 AAA-ATPase in the retrotranslocation of the cholera toxin A1 chain, a non-ubiquitinated substrate. *The Journal of biological chemistry* **280**, 28127 (Jul 29, 2005).
158. R. J. Abujarour, S. Dalal, P. I. Hanson, R. K. Draper, p97 Is in a complex with cholera toxin and influences the transport of cholera toxin and related toxins to the cytoplasm. *The Journal of biological chemistry* **280**, 15865 (Apr 22, 2005).
159. M. Taylor *et al.*, Hsp90 is required for transfer of the cholera toxin A1 subunit from the endoplasmic reticulum to the cytosol. *The Journal of biological chemistry* **285**, 31261 (Oct 8, 2010).
160. Y. Endo *et al.*, Site of action of a Vero toxin (VT2) from Escherichia coli O157:H7 and of Shiga toxin on eukaryotic ribosomes. RNA N-glycosidase

activity of the toxins. *European journal of biochemistry / FEBS* **171**, 45 (Jan 15, 1988).
161. M. Jacewicz, H. Clausen, E. Nudelman, A. Donohue-Rolfe, G. T. Keusch, Pathogenesis of shigella diarrhea. XI. Isolation of a shigella toxin-binding glycolipid from rabbit jejunum and HeLa cells and its identification as globotriaosylceramide. *The Journal of experimental medicine* **163**, 1391 (Jun 1, 1986).
162. O. Garred, B. van Deurs, K. Sandvig, Furin-induced cleavage and activation of Shiga toxin. *The Journal of biological chemistry* **270**, 10817 (May 5, 1995).
163. L. Johannes, W. Romer, Shiga toxins--from cell biology to biomedical applications. *Nature reviews. Microbiology* **8**, 105 (Feb, 2010).
164. T. Falguieres, L. Johannes, Shiga toxin B-subunit binds to the chaperone BiP and the nucleolar protein B23. *Biology of the cell / under the auspices of the European Cell Biology Organization* **98**, 125 (Feb, 2006).
165. M. Yu, D. B. Haslam, Shiga toxin is transported from the endoplasmic reticulum following interaction with the luminal chaperone HEDJ/ERdj3. *Infection and immunity* **73**, 2524 (Apr, 2005).
166. S. Olsnes, A. Pihl, Different biological properties of the two constituent peptide chains of ricin, a toxic protein inhibiting protein synthesis. *Biochemistry* **12**, 3121 (Jul 31, 1973).
167. R. A. Spooner *et al.*, Protein disulphide-isomerase reduces ricin to its A and B chains in the endoplasmic reticulum. *The Biochemical journal* **383**, 285 (Oct 15, 2004).
168. P. T. Richardson *et al.*, Recombinant proricin binds galactose but does not depurinate 28 S ribosomal RNA. *FEBS letters* **255**, 15 (Sep 11, 1989).
169. M. Slominska-Wojewodzka, T. F. Gregers, S. Walchli, K. Sandvig, EDEM is involved in retrotranslocation of ricin from the endoplasmic reticulum to the cytosol. *Molecular biology of the cell* **17**, 1664 (Apr, 2006).
170. R. H. Argent *et al.*, Ribosome-mediated folding of partially unfolded ricin A-chain. *The Journal of biological chemistry* **275**, 9263 (Mar 31, 2000).
171. R. A. Spooner *et al.*, Cytosolic chaperones influence the fate of a toxin dislocated from the endoplasmic reticulum. *Proceedings of the National Academy of Sciences of the United States of America* **105**, 17408 (Nov 11, 2008).

CHAPTER 2

The Ero1α-PDI Redox Cycle Regulates Cholera Toxin Retro-translocation

2-1. Introduction

As described earlier, cholera toxin (CT) undergoes retrograde trafficking to the ER, hijacks ER-associated degradation (ERAD) machinery, and escapes into the cytosol (See Chapter 1-2). While its mode of cytotoxicity is well documented, our understanding of CT retro-translocation from the ER is comparatively rudimentary. Previous work in the field determined that the CTA subunit undergoes proteolytic cleavage to produce CTA1 and CTA2 subunits linked by a disulfide bond. Reduction of this bond in the ER enables CTA1 to be isolated from the holotoxin so that it can be unfolded and processed for retro-translocation. Our goal is to determine the mechanism by which the toxin is recognized as an ERAD substrate, unfolded, and presented for retro-translocation across the ER membrane.

Using *in vitro* techniques, we initially identified the oxidoreductase protein disulfide isomerase (PDI) as an ERAD chaperone capable of unfolding CTA1 (*1*). Presumably this unfolding event could initiate toxin retro-translocation *in vivo*. Further analysis revealed that the affinity of PDI for CTA1 is redox-dependent. Reduced PDI binds and unfolds CTA1, whereas subsequent oxidation of PDI by Ero1α, an established PDI oxidase (*2-5*), promotes toxin release (*6*). Although we

have since demonstrated that PDI is crucial for retro-translocation of CTA1 in cells (*7*), the role of Ero1α in regulating this reaction remains unexplored.

Additionally, because CTA1 refolds rapidly once it is released from PDI (*8*), we hypothesized that PDI-mediated unfolding of the toxin must be physically coupled to the retro-translocon. This would permit the released toxin to cross the ER membrane without refolding. We previously found that Derlin-1, an ER membrane protein that is a component of the retro-translocon (*9, 10*), binds to PDI and facilitates CTA1 retro-translocation (*11*). However, the precise mechanism by which PDI engages Derlin-1 is not clear.

In this study, we used both loss- and gain-of-function approaches to probe the role of Ero1α in facilitating retro-translocation of CTA1. We found that down-regulation of Ero1α attenuates retro-translocation of CTA1 by increasing levels of reduced PDI and blocking toxin release. Similarly, overexpression of Ero1α decreases CTA1 retro-translocation by increasing oxidation of PDI, thus preventing it from engaging the toxin efficiently. Intriguingly, we discovered that Ero1α down-regulation stabilizes the interaction between PDI and Derlin-1. These findings demonstrate that Ero1α has two crucial roles in mediating CTA1 retro-translocation. First, Ero1α controls the temporal binding-release cycle of CTA1 from PDI during retro-translocation, and second, regulates the spatial association of PDI with components of the retro-translocon.

2-2. Materials and Methods

Materials

Primary antibodies used were as follows: polyclonal PDI, polyclonal Hsp90 (Santa Cruz Biotechnology, Santa Cruz, CA), monoclonal PDI, polyclonal CTB (Abcam, Cambridge, MA), polyclonal Ero1α (Cell Signaling Technology, Beverly, MA), monoclonal BiP (BD Biosciences, San Jose, CA), monoclonal FLAG (Sigma-Aldrich, St. Louis, MO), and monoclonal p97 (RDI Division of Fitzgerald Industries International, Concord, MA). Monoclonal antibodies against Myc and HA were gifts from K. Verhey (University of Michigan, Ann Arbor, MI). The polyclonal antibody against Derlin-1 was a gift from T. Rapoport (Harvard Medical School, Boston, MA). The polyclonal antibody against ERp57 was a gift from S. High (University of Manchester, Manchester, England). The polyclonal CTA antibody was produced against denatured CTA purchased from EMD Biosciences (Sand Diego, CA). Purified CT was purchased from EMD Biosciences. HA-tagged CD3δ and T-cell receptor alpha (TCRα) expression plasmids were gifts from C. Wojcik (Indiana University, Indianapolis, IN).

Mutagenesis of Ero1α

Mutagenesis of Ero1α was achieved using the Stratagene QuikChange II Site-directed Mutagenesis Kit (La Jolla, CA) and pcDNA3.1(+)-Ero1α plasmid construct (a gift from Roberto Sitia at Universita Vita-Salute-San Raffaele Scientific Institute) as a template for generation of the Cys94 to Ala94 mutant. The resulting pcDNA3.1(+)-C94A Ero1α construct was used in turn as a

template for the generation of the pcDNA3.1(+)-C94/99A Ero1α construct. The mutated Ero1α constructs were confirmed by sequencing.

Tissue culture, transfection, and protein down-regulation

HEK293T cells were cultured in DMEM with 10% fetal bovine serum (FBS) and penicillin/streptomycin. All expression constructs used were transfected into 30% confluent cells on 10- or 6-cm dishes using the Effectene system (Qiagen, Chatsworth, CA). Small interfering RNA (siRNA) against Ero1α (5'-UUUCUAACCAGGUCUCUUGUU-3') was synthesized by Invitrogen (Carlsbad, CA). Duplexed siRNA at 200 nM was transfected into 15-30% confluent 293T cells using Oligofectamine (Invitrogen) according to the manufacturer's protocol.

XBP1 splicing

Splicing was described previously in Uemura *et. al*. (*12*).

Retro-translocation assay

293T cells were intoxicated with 10 nM CT in HBSS for 45 minutes at 37°C. Cells ($2x10^6$) were permeabilized in 100 µL of 0.01% digitonin in HCN buffer (50 mM HEPES, pH 7.5, 150 mM NaCl, 2 mM $CaCl_2$, 10 mM N-ethylmaleimide [NEM], and protease inhibitors), incubated on ice for 10 minutes, and centrifuged at 16,000 x g for 10 minutes at 4°C. The supernatant was removed, and the pellet was resuspended in 100 µL of sample buffer. Fractions were analyzed by non-reducing SDS-PAGE and immunoblot.

cAMP assay

CT-induced cAMP levels were analyzed as previously described (*7*).

Pulse-chase analysis of TCRα

Analysis of TCRα-hemagglutinin (HA) degradation followed a previously published protocol (*13*).

Mal-PEG modification

In vivo analysis of PDI and ERp57 reduction/oxidation states were done using the double NEM-alkylation variant of mal-PEG (maleimide polyethylene glycol 5000) modification that was previously described (*14*). In lieu of metabolic labeling, samples were analyzed by non-reducing SDS-PAGE and immunoblot.

Immunoprecipitation and chemical cross-linking

293T cells were incubated with or without 100 nM CT for 90 minutes as indicated. Where indicated, NEM (5 mM) was added to the cells for 30 minutes after the cells were initially exposed to CT for 60 minutes. Cells were then harvested, lysed in a buffer containing Trsi-HCl (30 mM), pH 7.5, $MgCl_2$ (4 mM), KOAc (150 mM), and NEM (10 mM) with either 1% deoxy BigChap (DBP)or 1% Triton X-100, and centrifuged for 10 minutes at 16,000 x g. The supernatant was collected used for immunoprecipitation (IP). The specified antibodies were added to the supernatant and incubated overnight at 4°C. Immune complexes were captured by addition of protein A agarose beads (Invitrogen), washed, and subjected to non-reducing SDS-PAGE and immunoblot analysis. Where designated, cells were subjected to *in vivo* cross-linking by incubation with 2 mM dithiobis

succinimidyl propionate (DSP; Thermo Fisher Scientific, Waltham, MA) in PBS for 30 minutes before lysis. Before analysis, all cross-linked samples were reduced by boiling for 5 minutes in sample buffer containing 5% β-mercaptoethanol (βME).

2-3. Results

Ero1α Down-regulation decreases retro-translocation of CTA1

We down-regulated Ero1α in 293T cells to assess its function in retro-translocation of CTA1. Cells were treated with either a control (scrambled) or an Ero1α-specific siRNA and whole cell lysates (WCL) were subjected to non-reducing SDS-PAGE and immunoblotted with the indicated antibodies. Cells treated with the Ero1α-specific siRNA (Ero1α^{-} cells) had significantly reduced levels of Ero1α protein in comparison to control cells (Figure 2-1A, top panel, cf. lane 2 with lane 1). Under this condition, the unfolded protein response (UPR) markers BiP, PDI, and Derlin-1 (*15*) were not significantly up-regulated (Figure 2-1A, second through fifth panels, cf. lane 2 with lane 1). Expression of Ero1β, the other Ero1 isoform, was also not affected (Figure 2-1A, fifth panel, cf. lane 2 with lane 1). In contrast to incubating cells with the known ER stress inducers dithiothreitol (DTT) and tunicamycin, transfection of neither scrambled nor Ero1α-specific siRNA triggered the splicing of the XBP1 transcription factor mRNA (Figure 2-1A, cf. lanes 3 and 4 with lanes 5 and 6). These findings indicate that down-regulation of Ero1α does not induce the UPR.

To measure toxin retro-translocation efficiency, control and Ero1α⁻ cells were subjected to a previously established ER-to-cytosol retro-translocation assay (*7, 11*). Cells were intoxicated with 10 nM CT for 45 min, harvested, and treated with a low digitonin concentration (0.01%) to permeabilize the plasma membrane while leaving intracellular membranes intact. Cells were then subjected to fractionation by centrifugation to separate cytosolic (supernatant) and membrane-bound (pellet) fractions. Hsp90 protein acts as a marker for the cytosol (Figure 2-1B, fourth panel). The majority of PDI, an ER lumenal protein, was present in the pellet fraction (Figure 2-1B, cf. seventh and third panels), demonstrating that digitonin treatment did not significantly disrupt the ER membrane. Thus, any CTA1 that appears in the supernatant is due to retro-translocation and not non-specific leakage. Several control experiments validated this assay. First, we found previously that treatment with brefeldin A (an agent that blocks COPI-dependent retrograde transport to the ER) or incubation at 4°C prevents ER arrival of CT, reduction to CTA1, and appearance of CTA1 in the supernatant (*7, 11*). Second, a mutant CT that is presumed to not undergo ER-to-cytosol transport does not appear in the supernatant (*7*). Finally, conditions that blocked CT-induced cAMP synthesis also caused a decrease in CTA1 levels in the supernatant (*7, 11*).

Using this assay, we observed that the supernatant levels of CTA1 were decreased in Ero1α⁻ cells (Figure 2-1B, top panel, cf. lane 2 with lane 1; quantified in Figure 2-1C). Likewise, CT-induced cAMP level decreased in the

Ero1α⁻ cells when compared with control cells (Figure 2-1D). Together, these findings indicate that Ero1α plays an important role in regulating CTA1 retro-translocation. We then asked if down-regulation of Ero1α affects the degradation of other retro-translocation substrates. Metabolic pulse-chase experiments showed that the rate of TCRα (*16*) degradation was not significantly disrupted in Ero1α⁻ cells when compared with control cells (Figure 2-1E, top two panels; quantified below). Similarly, the steady-state level of transfected HA-tagged CD3δ (*17*) was unaltered (Figure 2-1F, top panel, cf. lanes 1 and 2). These data demonstrate substrate specificity for Ero1α-mediated retro-translocation.

Ero1α overexpression attenuates retro-translocation of CTA1

To supplement our loss-of-function approach, we used a gain-of-function strategy to further analyze the role of Ero1α in mediating toxin retro-translocation. Wild-type (WT) and enzymatically inactive Ero1α (*18*), Ero1α(C94A:C99A), were overexpressed to the same levels in 293T cells (Figure 2-2A, top panel, cf. lane 2 with lane 1 and lane 4 with lane 3). As with the knockdown, we found that overexpression of WT Ero1α affects neither the levels of PDI, BiP, and Derlin-1 (Figure 2-2A, second, third, and fourth panels, cf. lane 2 with lane 1) nor splicing of XBP1 (Figure 2-2A, cf. lanes 5 and 6 with lanes 7 and 8). These findings indicate that overexpressing Ero1α does not profoundly trigger ER stress.

To establish a functional correlation to toxin retro-translocation, cells transfected with vector, WT Ero1α and Ero1α(C94A:C99A) were subjected to the retro-translocation assay described in Figure 2-1. We found that cells

overexpressing WT Ero1α, but not Ero1α(C94A:C99A), displayed increased levels of CTA1 in the supernatant when compared with vector-transfected cells (Figure 2-2B, top panel, cf. lane 2 with lanes 1 and 3; quantified in Figure 2-2E). Consistent with our previous finding (*11*), CTA1 retro-translocation also decreased in cells overexpressing dominant-negative Derlin-1 (i.e., Derlin-1-YFP; quantified in Figure 2-2E). These data indicate that increasing the level of enzymatically active Ero1α disrupts retro-translocation of CTA1.

Because both knockdown (Figure 2-1) and overexpression of Ero1α (Figure 2-2) resulted in decreased CTA1 retro-translocation, we reasoned that the *in vivo* steady-state ratio of Ero1α to PDI may be important for timing toxin retro-translocation. To test this possibility we over-expressed PDI simultaneously with WT Ero1α to restore the appropriate Ero1α:PDI ratio (Figure 2-2C, lane 3). As anticipated, this co-overexpression permitted functional rescue of toxin retro-translocation. These findings not only underscore a functional role for Ero1α, but further suggest that a balanced Ero1α-PDI ratio is critical for toxin retro-translocation. Interestingly, overexpression of Ero1β did not appear to affect toxin retro-translocation (Figure 2-2E).

Altering the Ero1α level in cells affects the redox state of PDI

The ability of catalytically active Ero1α to regulate CTA1 retro-translocation in a PDI-specific manner/fashion suggests that Ero1α controls the PDI–CTA1 interaction in a redox-dependent manner. PDI contains six cysteines, four of which are in redox-active thioredoxin domains and cycle between oxidized

and reduced states. To test if down-regulation or overexpression of WT Ero1α alters PDI redox state, we applied a technique that measures the redox state of PDI (*14*). Briefly, cells were incubated with the alkylating agent NEM to modify free (reduced) cysteines on PDI and lysed. PDI was then immunoprecipitated from the resulting lysate and disulfide-bonded cysteines were subsequently reduced by the strong reducing agent tris(2-carboxyethyl) phosphine (TCEP). The newly formed free cysteines were then modified by the 5-kDa thiol-modifying reagent maleimide PEG 5000 (MPEG), and the immunoprecipitated sample was subjected to SDS-PAGE followed by immunoblotting with a PDI-specific antibody. It is important to emphasize that this protocol only results in MPEG modification of cysteines that were originally oxidized. Consequently, higher molecular weight species represent predominantly oxidized PDI.

In the presence of MPEG, the various redox forms of steady state PDI could be detected (Figure 2-3A, cf. lane 2 with lane 1); the designation of specific redox forms of PDI is based on previous analysis (*14*). Importantly, the pool of high molecular weight PDI species in the Ero1α^{-} cells was depleted in comparison to control cells (Figure 2-3B, cf. lane 2 with lane 1), indicating less modification of PDI in the Ero1α^{-} cells. In contrast, we found that the redox state of ERp57 was not affected in the Ero1α^{-} cells (Figure 2-3C, cf. lane 2 with lane 1). This result is consistent with a previous finding that showed that Ero1α does not control the redox state of ERp57 (*19*). These findings demonstrate that PDI, but not ERp57, is oxidized less efficiently in Ero1α^{-} cells, thereby confirming that

Ero1α functions as a PDI oxidase. Therefore, the inhibition of CTA1 retro-translocation observed in the Ero1α^{-} cells (Figure 2-1) can be attributed to a decrease in the pool of oxidized PDI.

Conversely, we found that the pool of high molecular weight PDI species increased when Ero1α was overexpressed (Figure 2-3D, cf. lane 2 with lane 1), thereby indicating that PDI is more oxidized. Hence, the decrease in toxin retro-translocation observed in Ero1α-overexpressing cells (Figure 2-2) is likely due to an increase in the pool of oxidized PDI.

The level of Ero1α controls PDI-CTA1 interaction

According to the redox-dependent model, reduced PDI binds and unfolds CTA1 (*1*); subsequent oxidation of PDI by Ero1α releases the toxin (*6*). As such, this model suggests that a lack of Ero1α precludes PDI oxidation, effectively trapping the toxin on PDI. We have shown thus far that a knockdown of Ero1α decreases both PDI oxidation and CTA1 retro-translocation. Mechanistically, the simplest explanation of these results is that CTA1 is inefficiently released from PDI in Ero1α^{-} cells. To test this prediction, we assessed the PDI–CTA1 interaction in control and Ero1α^{-} cells. 293T cells were transfected with FLAG-tagged WT PDI (WT PDI FLAG), intoxicated with CT, incubated with or without the thiol-cleavable and membrane-permeable cross-linker DSP, and lysed with either 1% Triton X-100 or 1% deoxy BigChap (DBC). CTA immunoprecipitates from the WCLs were subjected to reducing SDS-PAGE (non reducing SDS-

PAGE used for DBC lysates) and subsequently immunoblotted with the indicated antibodies.

Using DSP and 1% Triton X-100, we found that a low level of WT PDI FLAG co-precipitated with CTA1 from the intoxicated cells (Figure 2-4A, top panel, cf. lane 2 with lane 1). Importantly, the level of WT PDI FLAG that co-precipitated with CTA1 increased in the Ero1α^{-} cells (Figure 2-4A, top panel, cf. lane 3 with lane 2). Increased PDI–toxin interaction was similarly observed under the Ero1α^{-} condition when cells were lysed with 1% DBC (without DSP; Figure 2-4B, top panel, cf. lane 3 with lane 2). These results, which suggest that CTA1 is trapped on reduced PDI in the Ero1α^{-} cells, are consistent with the redox-dependent model and provide a mechanistic basis by which down-regulation of Ero1α attenuates retro-translocation of CTA1.

To further demonstrate that reduced PDI has higher affinity for CTA1 *in vivo*, cells were treated with NEM to alkylate free cysteine residues on PDI, thereby "locking" it in the reduced state. We found that PDI from cells treated with NEM binds with a much higher efficiency to CTA1 than PDI from untreated cells (Figure 2-4C, top panel, cf. lane 2 with lane 1), suggesting that alkylated PDI displays a higher affinity for the toxin than non-alkylated PDI. This result parallels previous *in vitro* data showing that alkylated PDI binds to CTA1 with high affinity (*1*) and further supports our assertion that binding of PDI to CTA1 operates in a redox-driven manner.

The redox-dependent model also predicts that overexpression of Ero1α would block CTA1 retro-translocation by oxidizing PDI and preventing it from engaging CTA1 effectively. To test this possibility, we examined the PDI–CTA1 interaction in control and Ero1α-overexpressing cells; the amount of PDI bound to toxin was in fact decreased in the Ero1α-overexpressing cells (Figure 2-4D, top panel, cf. lane 3 with lane 2). Consequently, the decrease in CTA1 retro-translocation observed in the Ero1α-overexpressing cells (Figure 2-2) is likely due to the inability of oxidized PDI to engage the toxin efficiently.

Down-regulating Ero1α increases PDI-Derlin-1 interaction

Our findings demonstrate that, in cells, Ero1α regulates the binding and releasing of CTA1 through the redox state of PDI, a process essential to initiation of toxin retro-translocation. However, whether the redox state of PDI affects other aspects of the retro-translocation process is unknown. We previously found that PDI associates with Derlin-1 (*11*), an ER membrane protein implicated as a component of the retro-translocon (*9, 10*). This interaction permits coupling of the unfolding reaction with events on the ER membrane. Here, we test if Ero1α regulation of the redox state of PDI controls the PDI–Derlin-1 interaction.

Cells were transfected with WT PDI FLAG and lysed with 1% DBC; the lysates were immunoprecipitated with a control Myc or Derlin-1-specific antibody. Immunoprecipitated samples were subjected to non-reducing SDS-PAGE and immunoblotted with the indicated antibodies. In control cells, a small amount of WT PDI FLAG was specifically found in the Derlin-1 immunoprecipitate (Figure 2-

5A, top panel, cf. lane 2 with lane 1), reaffirming that Derlin-1 binds to PDI (*11*). Interestingly, an increased amount of PDI was found to interact with Derlin-1 in the Ero1α^{-} cells (Figure 2-5A, top panel, cf. lane 3 with lane 2). This finding suggests that reduced PDI exhibits a higher affinity for both CTA1 and Derlin-1. I272W PDI, which was previously shown not to interact with substrates (*20*), also exhibits an increased interaction with Derlin-1 in Ero1α^{-} cells (Figure 2-5B, top panel, cf. lane 3 with lane 2). This result indicates that Derlin-1 is an unlikely substrate of PDI; instead, it is a stable binding partner whose association with PDI is redox-regulated. Similar to the observed increased interaction between alkylated PDI and CTA1 (Figure 2-4C), PDI from cells treated with NEM also interacts with Derlin-1 more efficiently than PDI from untreated cells (Figure 2-5E, top panel, cf. lane 2 with lane 1). Overexpression of Ero1α in cells overexpressing PDI FLAG did not alter the PDI–Derlin-1 interaction (Figure 2-5F, top panel, cf. lane 3 with lane 2), consistent with the functional data presented in Figure 2-2E. Together, the results from the Ero1α knockdown, overexpression and the NEM studies demonstrate that Ero1α functions to regulate the redox-dependent interaction between PDI and Derlin-1.

We recently observed that PDI binds to Hrd1 (*21*), an integral ER membrane-bound E3 ubiquitin ligase and component of the retro-translocon (*22-24*). Down-regulating Ero1α did not affect this interaction (Figure 2-5C, top panel, cf. lane 3 with lane 2). In addition, the established interaction between Derlin-1 and the cytosolic chaperone p97 (*10*) was not affected by Ero1α down-regulation

(Figure 2-5D, top panel, cf. lane 3 with lane 2). These findings demonstrate that Ero1α specifically impacts the PDI-Derlin-1 interaction.

2-4. Discussion

A pivotal, yet poorly understood, step in the intoxication of CT is the transfer of the catalytic CTA1 subunit from the ER lumen into the cytosol. Using an *in vitro* approach, we previously determined that the ER lumenal proteins PDI and Ero1α likely regulate this process in a redox-dependent manner. Specifically, we found that the reduced form of PDI binds and unfolds CTA1 (*1*); subsequent oxidation of PDI by Ero1α releases the toxin from PDI (*6*). We postulated that these events coordinate unfolding and retro-translocation of CTA1 in cells. Using a siRNA-mediated approach, we observed that PDI is essential for CTA1 retro-translocation *in vivo* (*7*). However, whether or not the role of Ero1α translated to cells remained unverified.

Using loss- and gain-of-function approaches, we have demonstrated in this study that Ero1α plays a critical role in facilitating retro-translocation of CTA1. We found that down-regulation of Ero1α decreases toxin retro-translocation without inducing ER stress. Moreover, down-regulation of Ero1α does not affect the retro-translocation and degradation of the established ERAD substrates TCRα and CD3δ. Instead, we showed that down-regulation of Ero1α specifically leads to a decrease in PDI oxidation, precludes efficient toxin release from PDI, and blocks toxin transport.

Likewise, overexpression of catalytically active Ero1α blocks CTA1 retro-translocation. In this case, Ero1α overexpression increases oxidation of PDI and prevents the PDI from engaging CTA1 effectively. These two findings confirm that the PDI-Ero1α redox cycle observed *in vitro* is critical for CTA1 retro-translocation *in vivo* (Figure 2-6). Furthermore, our analyses demonstrate that reduced PDI displays an increased affinity for its binding partner Derlin-1, a key component of the retro-translocon. Overall, reduced PDI engages both CTA1 and Derlin-1; oxidation of PDI by Ero1α releases the unfolded toxin from PDI as well as PDI from Derlin-1. This cycle allows for efficient temporal and spatial coupling of toxin unfolding and retro-translocation (Figure 2-6).

Our findings implicate that, under normal conditions, a cell maintains a fine balance of Ero1α and PDI levels. This balance enables sufficient amounts of reduced PDI to bind and unfold the toxin while simultaneously maintaining enough oxidation equivalents to subsequently oxidize PDI and induce toxin release. The observation that simultaneous overexpression of PDI and Ero1α rescues toxin transport validates this idea. Although the cellular concentration of PDI is much higher than that of Ero1α, only a small fraction of PDI is likely dedicated to substrate retro-translocation. Consistent with this idea, we previously observed that only a small fraction of PDI binds to Derlin-1 (*11*). According to our current finding, this pool of PDI is functionally linked to retro-translocation.

The Ero1α-PDI redox cycle described in this study is not designed primarily for pathogen entry. Instead, this system is likely tuned to drive the retro-translocation of misfolded substrates during ERAD (*25*). For example, PDI displays redox-dependent binding to ERAD substrates such as BACE (*26*) and the non-glycosylated pro-α factor (*27*), implying that Ero1α may act in the retro-translocation of these substrates. Although the specific ER factors have not yet been identified, cellular redox state also appears to control the degradation of several ER proteins (*28-30*), signifying that the Ero1α-PDI complex may be involved. It is important to note that in addition to the redox-mediated chaperone activity described here, PDI is classically recognized as an enzyme that catalyzes the formation, breakage, and rearrangement of disulfide bonds during the protein folding process (*31*).

We acknowledge that down-regulation of Ero1α does not completely block toxin retro-translocation. This may be due to the incomplete knockdown of Ero1α or to the complementary activity of other undiscovered PDI oxidases. However, our previous *in vitro* analysis suggested that the Ero1β isoform (*32*) does not promote release of CTA1 by oxidizing PDI (*6*). Recent *in vivo* data demonstrates that overexpression of Ero1β does not affect toxin retro-translocation (data not shown). Furthermore, Ero1β is found to be expressed at low levels in 293T cells (*32*), implying that it does not contribute significantly to the toxin transport process.

Structurally, the observation that PDI engages a substrate and a binding partner in a redox-dependent manner suggests that the PDI redox state may regulate the conformation of multiple binding sites. In this context, we previously demonstrated that reduced and oxidized PDI exist in different conformations (*1*). Discerning the specific sites on PDI that interact with CTA1 (*33*) and Derlin-1 will be vital to determining how PDI conformation and chaperone activity correlate its redox state.

The fact that reduced PDI binds to Derlin-1 with increased affinity has major implications for the mechanism by which the unfolding process is coupled to the ER membrane. Preferential targeting of reduced PDI to the retro-translocation machinery permits efficient temporal and spatial interactions with CTA1. Subsequent oxidation of PDI by Ero1α, which is tethered to the ER membrane by a poorly described mechanism (*34*), would thereby allow direct presentation of unfolded toxin to the retro-translocon. Oxidized PDI, which is incapable of binding and unfolding toxin, is then released from the membrane and replaced by reduced PDI. This binding–release cycle is perpetuated by regeneration of reduced PDI by unknown reductase activity. Examining how Ero1α is coupled physically to the retro-translocation machinery, as well as how reduced PDI is regenerated, will elucidate the precise mechanism by which CTA1 is primed for retro-translocation across the ER membrane.

2-5. Figures

Figure 2-1. Ero1α down-regulation decreases retro-translocation of CTA1

(A) 293T cells were transfected with a scrambled siRNA (lane 1) or an Ero1α-specific siRNA (lane 2). Cells were harvested and lysed, and the lysates were subjected to immunoblot analysis with the indicated antibodies. Lanes 3–6, RT-PCR analysis of the unspliced (u) and spliced (s) forms of the XBP1 mRNA from cells treated with DTT or tunicamycin or from cells transfected with a scrambled or Ero1α-specific siRNA. (B) Cells transfected with a scrambled or an Ero1α-specific siRNA were treated with 10 nM CT and subjected to the retro-translocation assay. Supernatant and pellet fractions were analyzed by nonreducing SDS-PAGE, followed by immunoblotting with the indicated antibodies. CTA is 28 kDa and CTA1 is 22 kDa. (C) The intensity of the CTA1 band generated in B was quantified with ImageJ (NIH; http://rsb.info.nih.gov/ij/). Mean ± SD of at least three independent experiments is shown. A two-tailed *t* test was used. (D) Cells transfected with a scrambled or Ero1α-specific siRNA were treated with 10 nM CT, and the cAMP level was measured with a cAMP Biotrak Enzyme Immunoassay System (GE Healthcare). Data were normalized against the forskolin-induced cAMP level, as demonstrated previously (*7*). Mean ± SD of at least three independent experiments is shown. A two-tailed *t* test was used. (E) 293T cells transiently expressing TCRα were transfected with a scrambled or an Ero1α-specific siRNA, labeled with [^{35}S]methionine, and harvested at the indicated chase times, and the resulting cell lysate was used for TCRα immunoprecipitation. Signals were detected by autoradiography. Bottom panel, quantification of the intensity of the TCRα band from three independent experiments; values are expressed as a total percentage of the TCRα band at chase time = 0. Error bars, ±SD.

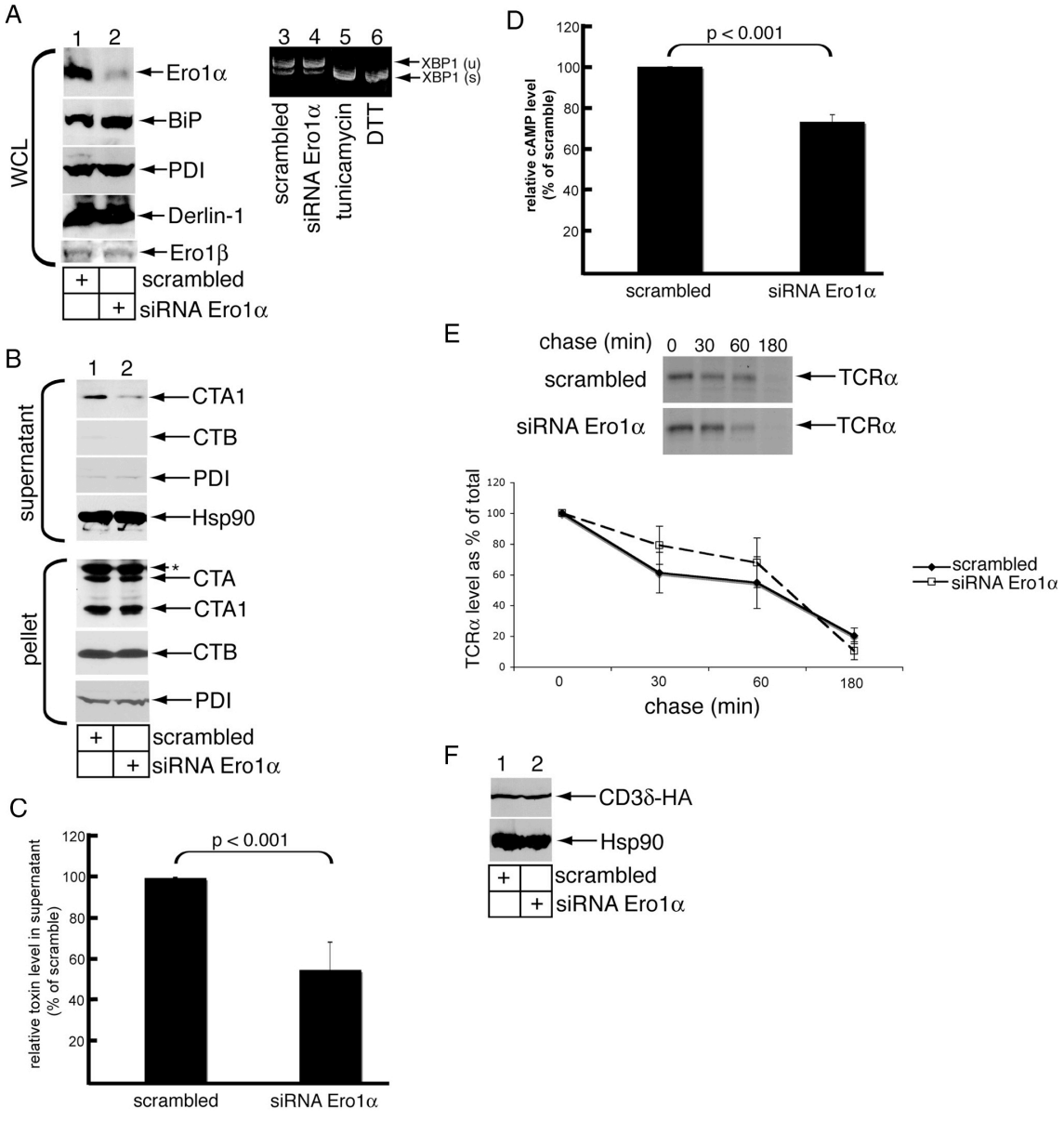
A
1 2
Ero1α
BiP
PDI
Derlin-1
Ero1β
WCL
+
scrambled
siRNA Ero1α
3 4 5 6
XBP1 (u)
XBP1 (s)
scrambled
siRNA Ero1α
tunicamycin
DTT
B
1 2
CTA1
CTB
PDI
Hsp90
supernatant
*
CTA
CTA1
CTB
PDI
pellet
scrambled
siRNA Ero1α
C
p < 0.001
relative toxin level in supernatant (% of scramble)
120
100
80
60
40
20
scrambled
siRNA Ero1α
D
p < 0.001
relative cAMP level (% of scramble)
120
100
80
60
40
20
scrambled
siRNA Ero1α
E
chase (min) 0 30 60 180
scrambled
TCRα
siRNA Ero1α
TCRα
TCRα level as % of total
120
100
80
60
40
20
0
0
30
60
180
chase (min)
scrambled
siRNA Ero1α
F
1 2
CD3δ-HA
Hsp90
scrambled
siRNA Ero1α

Figure 2-2. Ero1α overexpression attenuates retro-translocation of CTA1.

(A) Lanes 1–4, lysates from 293T cells transfected with vector, WT Ero1α, or Ero1α(C94A:C99A) were analyzed for expression of Ero1α, BiP, PDI, Derlin-1, and Hsp90. Lanes 5–8, RT-PCR analysis of the unspliced (u) and spliced (s) forms of the XBP1 mRNA from cells treated with DTT or tunicamycin or from cells transfected with vector or a WT Ero1α construct. (B) Cells in A were subjected to the retro-translocation assay as described in Figure 1. (C) Lysates from 293T cells transfected with vector, WT Ero1α, or WT Ero1α and PDI were analyzed for expression of Ero1α, PDI, and Hsp90. (D) Cells in C were subjected to the retro-translocation assay as in Figure 1. (E) Quantification of the CTA1 band intensity in B and D. Mean ± SD of at least three independent experiments is shown. A two-tailed *t* test was used. Results from overexpression of Ero1β and Derlin-1-YFP on CTA1 retro-translocation are also included.

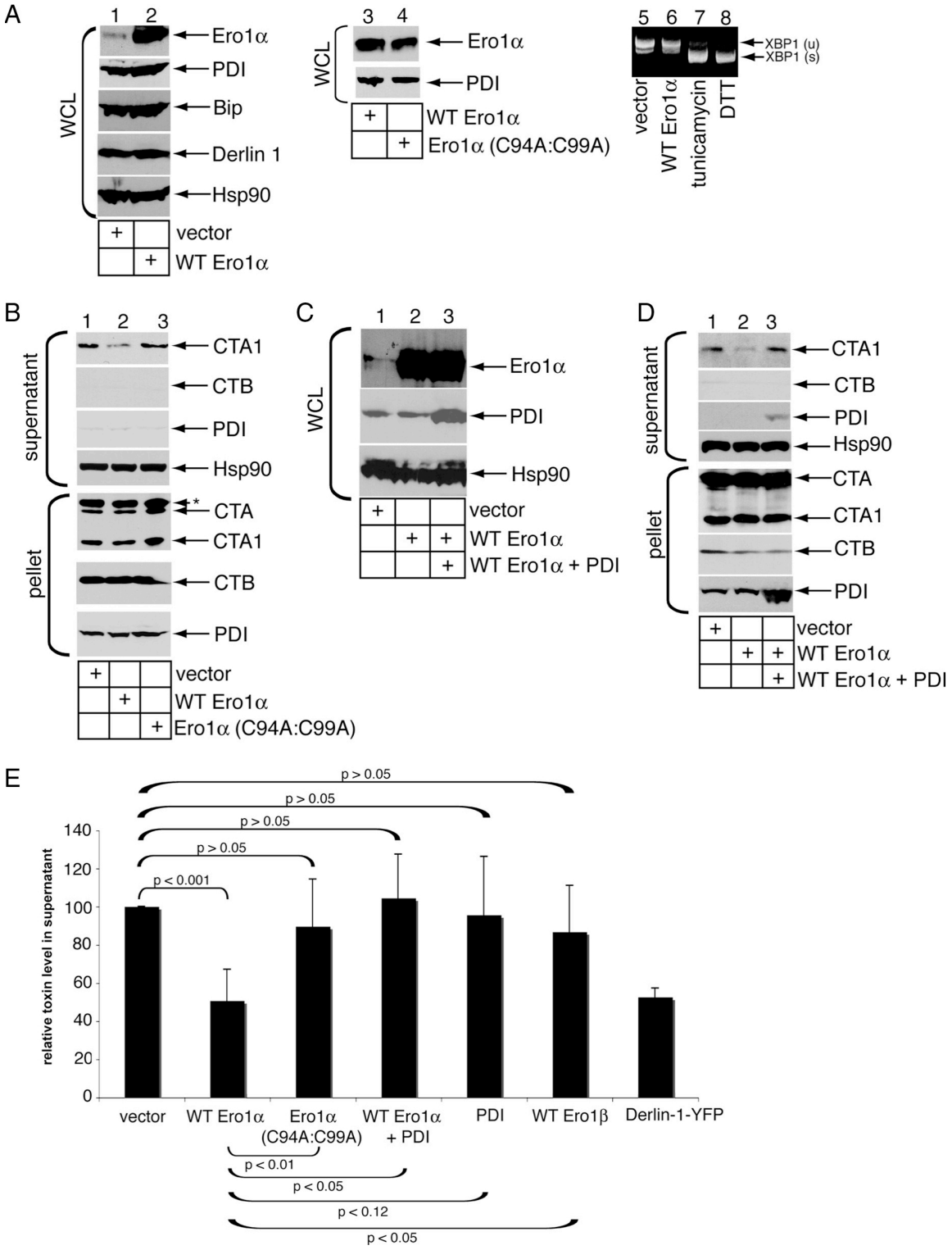
A
1 2
Ero1α
PDI
Bip
Derlin 1
Hsp90
WCL
vector
WT Ero1α
3 4
Ero1α
PDI
WCL
WT Ero1α
Ero1α (C94A:C99A)
5 6 7 8
XBP1 (u)
XBP1 (s)
vector
WT Ero1α
tunicamycin
DTT
B
1 2 3
CTA1
CTB
PDI
Hsp90
supernatant
CTA
CTA1
CTB
PDI
pellet
vector
WT Ero1α
Ero1α (C94A:C99A)
C
1 2 3
Ero1α
PDI
Hsp90
WCL
vector
WT Ero1α
WT Ero1α + PDI
D
1 2 3
CTA1
CTB
PDI
Hsp90
supernatant
CTA
CTA1
CTB
PDI
pellet
vector
WT Ero1α
WT Ero1α + PDI
E
relative toxin level in supernatant
0
20
40
60
80
100
120
140
p > 0.05
p > 0.05
p > 0.05
p > 0.05
p < 0.001
vector
WT Ero1α
Ero1α (C94A:C99A)
WT Ero1α + PDI
PDI
WT Ero1β
Derlin-1-YFP
p < 0.01
p < 0.05
p < 0.12
p < 0.05

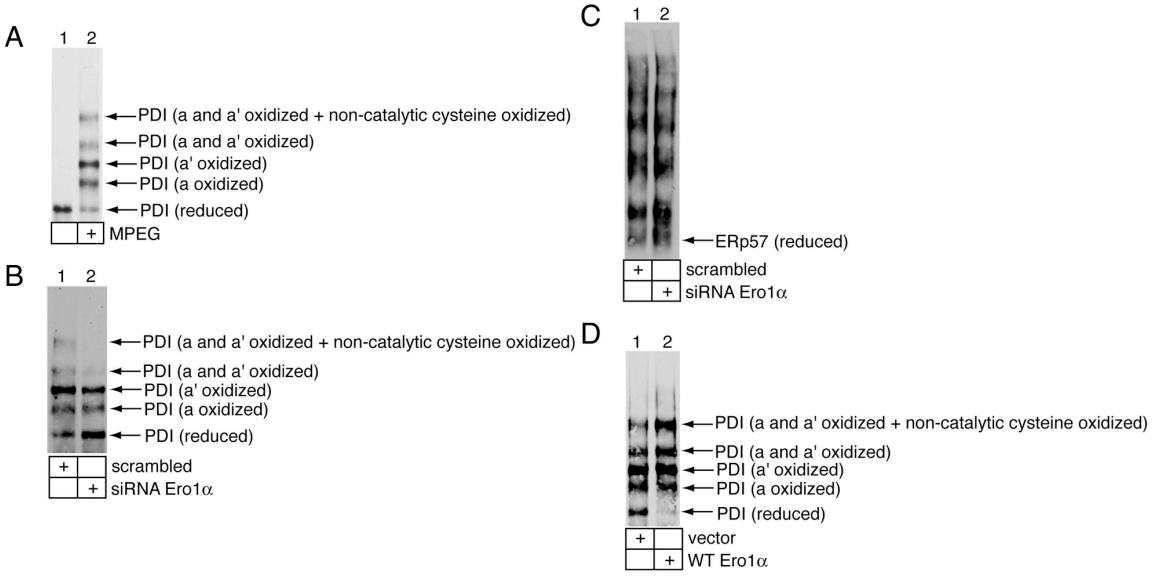

Figure 2-3. Altering Ero1α levels in cells affects the redox state of PDI

Altering Ero1α level in cells affects the redox state of PDI. (A) 293T cells were treated with NEM and lysed, and the endogenous PDI was immunoprecipitated from the lysate. The immunoprecipitate was incubated with TCEP, washed, and treated with or without MPEG. Samples were analyzed by SDS-PAGE and immunoblotted with an antibody against PDI. (B) 293T cells transfected with a scrambled or an Ero1α-specific siRNA were analyzed as in A, with the exception that both samples were treated with MPEG. (C) As in B, except ERp57 was immunoprecipitated and immunoblotted instead of PDI. (D) 293T cells transfected with vector or WT Ero1α were analyzed as in B.

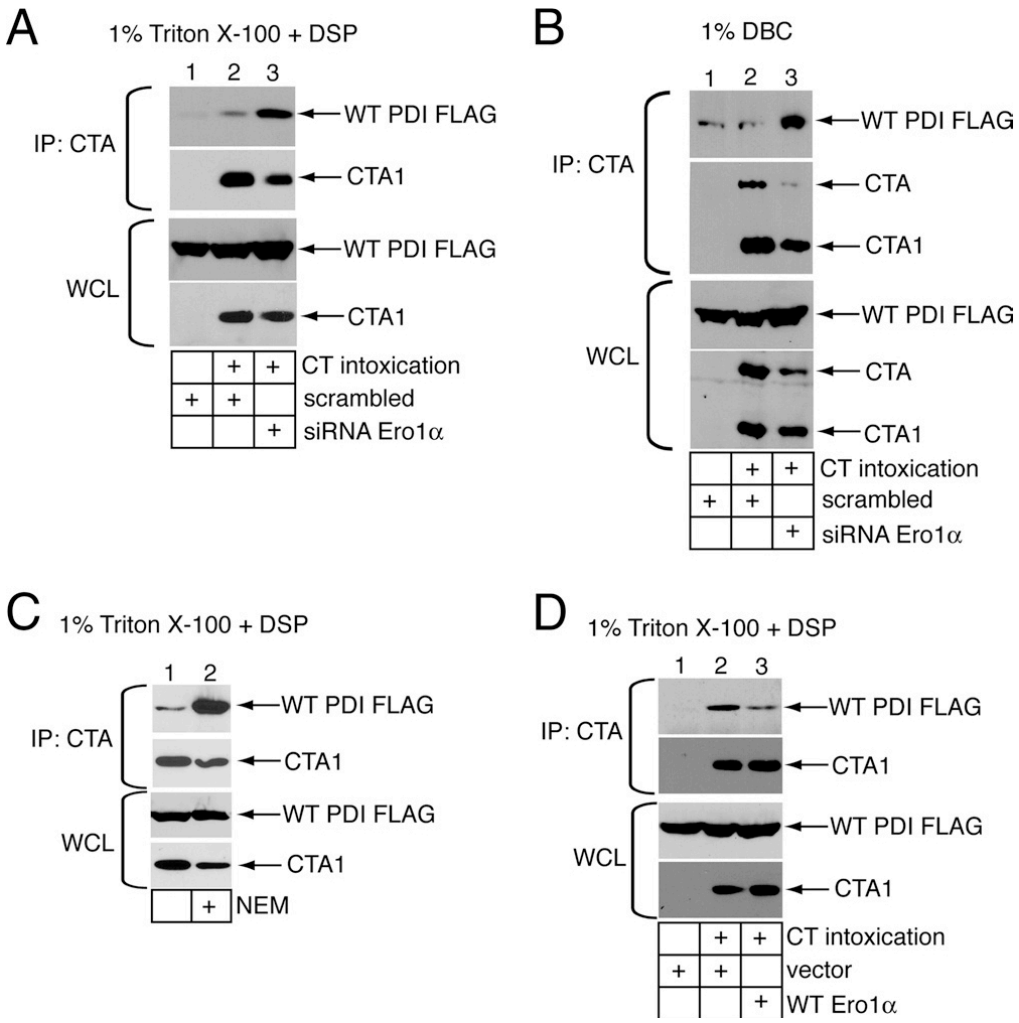

Figure 2-4. The level of Ero1α controls PDI-CTA1 interaction

The level of Ero1α controls PDI–CTA1 interaction. (A) 293T cells were transfected with WT PDI FLAG and either a scrambled or an Ero1α-specific siRNA, followed by incubation of the cells with or without CT. DSP cross-linker was added to the cells, followed by lysis with 1% Triton X-100. A CTA-specific antibody was incubated with the resulting lysate, and the precipitated sample was subjected to reducing SDS-PAGE followed by immunoblotting with the indicated antibodies. (B) As in A, except no DSP was added, and DBC was used instead of Triton X-100. Samples were subjected to nonreducing SDS-PAGE. (C) Cells overexpressing WT PDI FLAG were treated with or without NEM 60 min after CT intoxication, and the PDI–CTA1 interaction was analyzed as in A. (D) As in A, except cells were transfected with either vector or WT Ero1α.

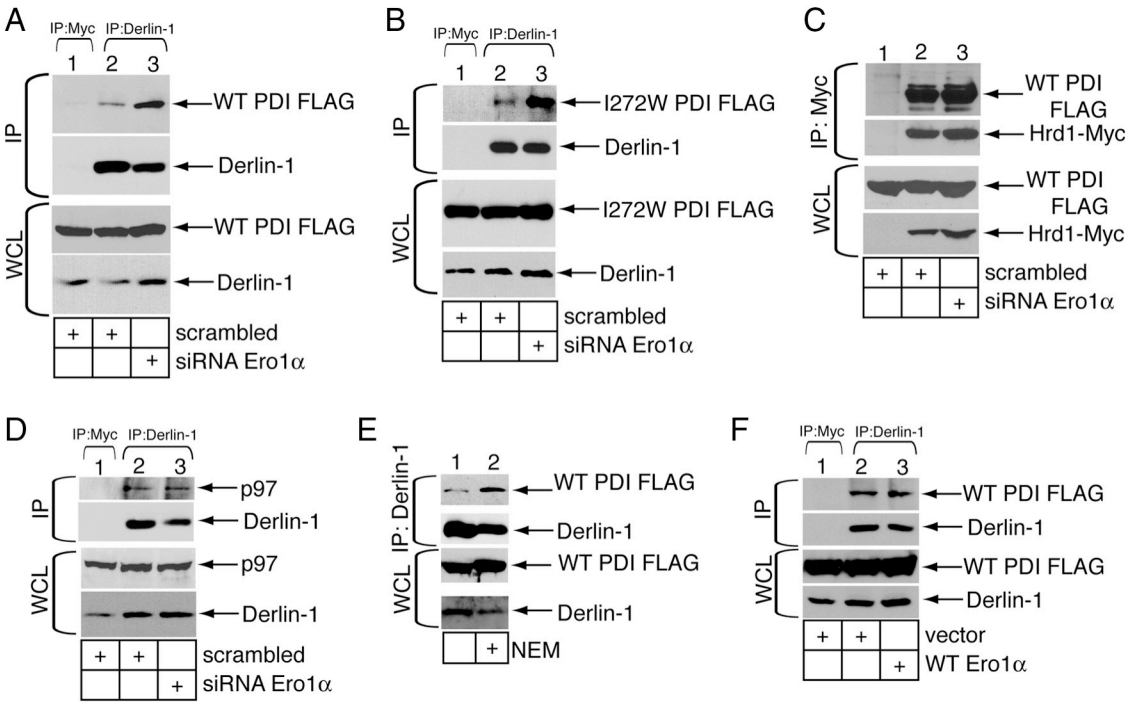

Figure 2-5. Down-regulation of Ero1α increases PDI-Derlin-1 interaction

Down-regulation of Ero1α increases PDI–Derlin-1 interaction. (A) 293T cells were transfected with WT PDI FLAG and either a scrambled or an Ero1α-specific siRNA. The cells were lysed with 1% DBC, and the lysate was incubated with either a control Myc or a Derlin-1–specific antibody. The immunoprecipitated sample was subjected to reducing SDS-PAGE and immunoblotted with the indicated antibodies. (B) As in A, except I272W PDI FLAG was transfected instead of WT PDI FLAG. (C) As in A, except Hrd1-Myc was transfected where indicated. (D) As in A, except no WT PDI FLAG was transfected, and endogenous p97 was immunoblotted. (E) Cells overexpressing WT PDI FLAG were treated with or without NEM 30 min before harvesting, and the PDI–Derlin-1 interaction analyzed as in A. (F) Cells were transfected with WT PDI FLAG and either vector or WT Ero1α, and the PDI–Derlin-1 interaction analyzed as in A.

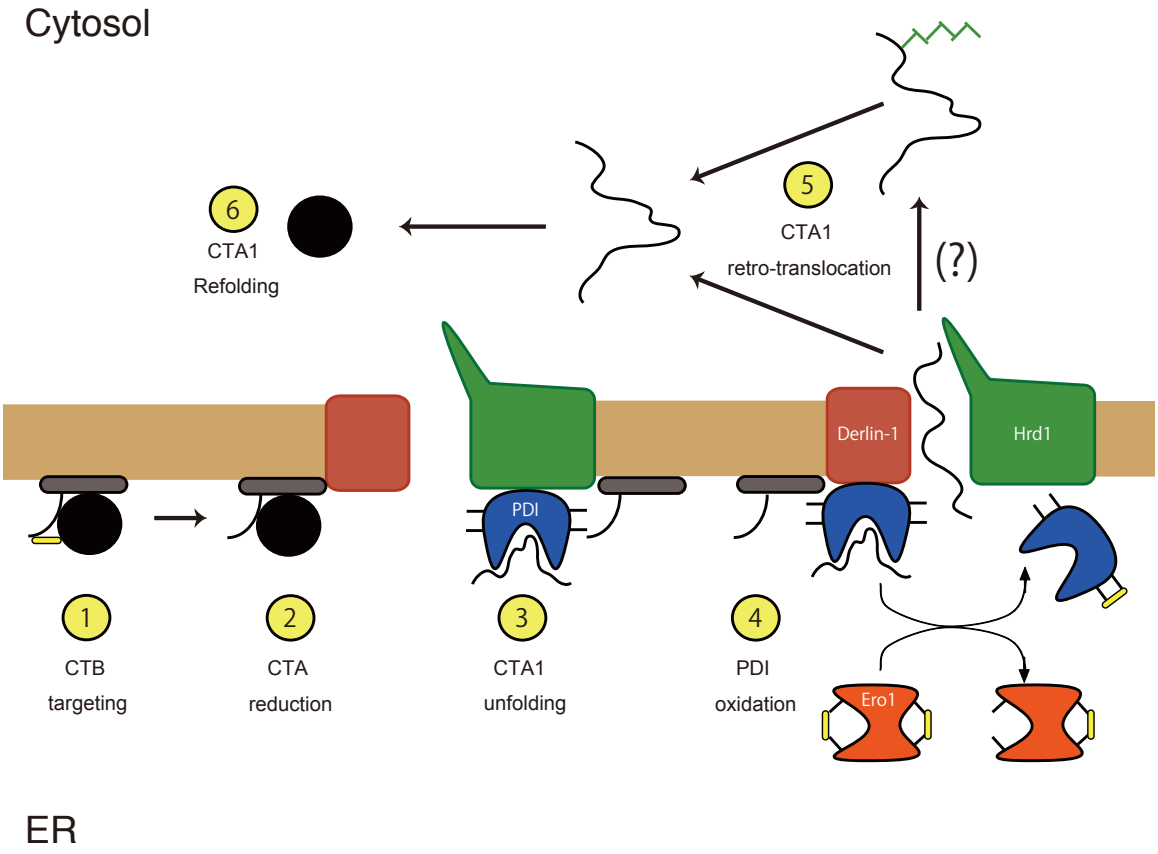

Figure 2-6. Ero1α regulates temporal and spatial release of CTA1 from PDI

In the ER, CT is first targeted to the Derlin-1/Hrd1 membrane complex (step 1). The toxin is then reduced by an unknown reductase (step 2), generating CTA1. PDI bound to Derlin-1/Hrd1 then unfolds CTA1 (step 3). Oxidation of PDI by Ero1α releases unfolded CTA1 (step 4) for retro-translocation while inducing release of PDI from Derlin-1. Whether the toxin undergoes E3-mediated ubiquitination is unclear. A ubiquitin-dependent reaction, potentially involving cytosolic chaperones, pulls the toxin into the cytosol (step 5) where it automatically refolds (step 6). See text for further discussion.

2-6. References

1. B. Tsai, C. Rodighiero, W. I. Lencer, T. A. Rapoport, Protein disulfide isomerase acts as a redox-dependent chaperone to unfold cholera toxin. *Cell* **104**, 937 (Mar 23, 2001).
2. A. R. Frand, C. A. Kaiser, The ERO1 gene of yeast is required for oxidation of protein dithiols in the endoplasmic reticulum. *Molecular cell* **1**, 161 (Jan, 1998).
3. M. G. Pollard, K. J. Travers, J. S. Weissman, Ero1p: a novel and ubiquitous protein with an essential role in oxidative protein folding in the endoplasmic reticulum. *Molecular cell* **1**, 171 (Jan, 1998).
4. A. Cabibbo *et al.*, ERO1-L, a human protein that favors disulfide bond formation in the endoplasmic reticulum. *The Journal of biological chemistry* **275**, 4827 (Feb 18, 2000).
5. C. S. Sevier, C. A. Kaiser, Ero1 and redox homeostasis in the endoplasmic reticulum. *Biochimica et biophysica acta* **1783**, 549 (Apr, 2008).
6. B. Tsai, T. A. Rapoport, Unfolded cholera toxin is transferred to the ER membrane and released from protein disulfide isomerase upon oxidation by Ero1. *The Journal of cell biology* **159**, 207 (Oct 28, 2002).
7. M. L. Forster *et al.*, Protein disulfide isomerase-like proteins play opposing roles during retrotranslocation. *The Journal of cell biology* **173**, 853 (Jun 19, 2006).
8. C. Rodighiero, B. Tsai, T. A. Rapoport, W. I. Lencer, Role of ubiquitination in retro-translocation of cholera toxin and escape of cytosolic degradation. *EMBO reports* **3**, 1222 (Dec, 2002).
9. B. N. Lilley, H. L. Ploegh, A membrane protein required for dislocation of misfolded proteins from the ER. *Nature* **429**, 834 (Jun 24, 2004).
10. Y. Ye, Y. Shibata, C. Yun, D. Ron, T. A. Rapoport, A membrane protein complex mediates retro-translocation from the ER lumen into the cytosol. *Nature* **429**, 841 (Jun 24, 2004).
11. K. M. Bernardi, M. L. Forster, W. I. Lencer, B. Tsai, Derlin-1 facilitates the retro-translocation of cholera toxin. *Molecular biology of the cell* **19**, 877 (Mar, 2008).
12. A. Uemura, M. Oku, K. Mori, H. Yoshida, Unconventional splicing of XBP1 mRNA occurs in the cytoplasm during the mammalian unfolded protein response. *Journal of cell science* **122**, 2877 (Aug 15, 2009).
13. H. Zhang *et al.*, Cysteine string protein interacts with and modulates the maturation of the cystic fibrosis transmembrane conductance regulator. *The Journal of biological chemistry* **277**, 28948 (Aug 9, 2002).
14. C. Appenzeller-Herzog, L. Ellgaard, In vivo reduction-oxidation state of protein disulfide isomerase: the two active sites independently occur in the

reduced and oxidized forms. *Antioxidants & redox signaling* **10**, 55 (Jan, 2008).
15. Y. Oda *et al.*, Derlin-2 and Derlin-3 are regulated by the mammalian unfolded protein response and are required for ER-associated degradation. *The Journal of cell biology* **172**, 383 (Jan 30, 2006).
16. H. Yu, G. Kaung, S. Kobayashi, R. R. Kopito, Cytosolic degradation of T-cell receptor alpha chains by the proteasome. *The Journal of biological chemistry* **272**, 20800 (Aug 15, 1997).
17. S. Tiwari, A. M. Weissman, Endoplasmic reticulum (ER)-associated degradation of T cell receptor subunits. Involvement of ER-associated ubiquitin-conjugating enzymes (E2s). *The Journal of biological chemistry* **276**, 16193 (May 11, 2001).
18. G. Bertoli *et al.*, Two conserved cysteine triads in human Ero1alpha cooperate for efficient disulfide bond formation in the endoplasmic reticulum. *The Journal of biological chemistry* **279**, 30047 (Jul 16, 2004).
19. A. Mezghrani *et al.*, Manipulation of oxidative protein folding and PDI redox state in mammalian cells. *The EMBO journal* **20**, 6288 (Nov 15, 2001).
20. A. Pirneskoski *et al.*, Molecular characterization of the principal substrate binding site of the ubiquitous folding catalyst protein disulfide isomerase. *The Journal of biological chemistry* **279**, 10374 (Mar 12, 2004).
21. K. M. Bernardi *et al.*, The E3 ubiquitin ligases Hrd1 and gp78 bind to and promote cholera toxin retro-translocation. *Molecular biology of the cell* **21**, 140 (Jan 1, 2010).
22. Y. Ye *et al.*, Recruitment of the p97 ATPase and ubiquitin ligases to the site of retrotranslocation at the endoplasmic reticulum membrane. *Proceedings of the National Academy of Sciences of the United States of America* **102**, 14132 (Oct 4, 2005).
23. B. N. Lilley, H. L. Ploegh, Multiprotein complexes that link dislocation, ubiquitination, and extraction of misfolded proteins from the endoplasmic reticulum membrane. *Proceedings of the National Academy of Sciences of the United States of America* **102**, 14296 (Oct 4, 2005).
24. A. Schulze *et al.*, The ubiquitin-domain protein HERP forms a complex with components of the endoplasmic reticulum associated degradation pathway. *Journal of molecular biology* **354**, 1021 (Dec 16, 2005).
25. S. S. Vembar, J. L. Brodsky, One step at a time: endoplasmic reticulum-associated degradation. *Nature reviews. Molecular cell biology* **9**, 944 (Dec, 2008).
26. M. Molinari, C. Galli, V. Piccaluga, M. Pieren, P. Paganetti, Sequential assistance of molecular chaperones and transient formation of covalent complexes during protein degradation from the ER. *The Journal of cell biology* **158**, 247 (Jul 22, 2002).

27. J. Wahlman *et al.*, Real-time fluorescence detection of ERAD substrate retrotranslocation in a mammalian in vitro system. *Cell* **129**, 943 (Jun 1, 2007).
28. J. Young, L. P. Kane, M. Exley, T. Wileman, Regulation of selective protein degradation in the endoplasmic reticulum by redox potential. *The Journal of biological chemistry* **268**, 19810 (Sep 15, 1993).
29. L. J. Wainwright, M. C. Field, Quality control of glycosylphosphatidylinositol anchor attachment in mammalian cells: a biochemical study. *The Biochemical journal* **321 (Pt 3)**, 655 (Feb 1, 1997).
30. J. Courageot, E. Fenouillet, P. Bastiani, R. Miquelis, Intracellular degradation of the HIV-1 envelope glycoprotein. Evidence for, and some characteristics of, an endoplasmic reticulum degradation pathway. *European journal of biochemistry / FEBS* **260**, 482 (Mar, 1999).
31. L. Ellgaard, L. W. Ruddock, The human protein disulphide isomerase family: substrate interactions and functional properties. *EMBO reports* **6**, 28 (Jan, 2005).
32. M. Pagani *et al.*, Endoplasmic reticulum oxidoreductin 1-lbeta (ERO1-Lbeta), a human gene induced in the course of the unfolded protein response. *The Journal of biological chemistry* **275**, 23685 (Aug 4, 2000).
33. M. L. Forster, J. J. Mahn, B. Tsai, Generating an unfoldase from thioredoxin-like domains. *The Journal of biological chemistry* **284**, 13045 (May 8, 2009).
34. M. Otsu *et al.*, Dynamic retention of Ero1alpha and Ero1beta in the endoplasmic reticulum by interactions with PDI and ERp44. *Antioxidants & redox signaling* **8**, 274 (Mar-Apr, 2006).

CHAPTER 3

A Novel Cytosolic Factor Releases Cholera Toxin from the ER Membrane

3-1. Introduction

Over the last decade our understanding of the lumenal components that drive cholera toxin retro-translocation has greatly improved; information on how the toxin is processed on the cytosolic side of the ER membrane, however, is scarce. As mentioned previously (see Chapter 1), the canonical ERAD pathway relies on sequential ubiquitination of substrates by E3 ligases, ubiquitin-dependent extraction by the p97-Ufd1-Npl4 complex, and degradation by the 26S proteasome. Cholera toxin, on the other hand, is neither detectably ubiquitinated nor degraded by the proteasome. It is speculated that a paucity of lysines and the ability of the toxin to spontaneously refold prevent ubiquitination and detection by the proteasome (*1*). However, this hypothesis fails to explain how the toxin can be dislocated from the ER membrane in a ubiquitin-independent manner. Furthermore, the sparse evidence at hand suggests that the toxin does not rely on p97 to reach the cytosol (*2, 3*). As such, it is believed that the toxin is released from the ER membrane and refolds in the cytosol by exploiting a pathway that diverges from canonical ERAD. There is some data suggesting that the toxin can be dislocated using Hsp90 or the 19S proteasome cap (*4, 5*); however, there remains no direct evidence that these components are truly involved *in vivo*.

Currently, there are two common methods used to study retro-translocation of cholera toxin: analysis of cAMP production and direct measurement of CTA1 levels in the cytosol. Because cAMP production is an indirect readout for toxin retro-translocation it is not our preferred method. Instead, our laboratory has developed a technique to directly monitor CTA1 retro-translocation (see Chapter 2). Briefly, in this assay, the plasma membrane of CT-intoxicated cells is permeabilized with a gentle detergent and the supernatant fraction separated from the pellet fraction by centrifugation. The CTA1 level in the supernatant fraction reflects retro-translocated toxin. By manipulating the activity of specific ER-resident factors and correlating their effects on toxin retro-translocation efficiency (*6-8*), we have been markedly successful in detailing the sequence of events that drive toxin unfolding and retro-translocation in the ER lumen. This approach, however, encounters significant caveats when applied to candidate proteins in the cytosol. Because a defined cytosolic protein often executes numerous cellular functions (*9-18*), such as control of cytosolic events during retro-translocation, vesicular trafficking, or general quality control, manipulating the cytosolic protein activity can confound data interpretation. To circumvent these complications, we modified our protocol into an *in vitro* retro-translocation assay using intact organelles and cytosolic extract (CE). Essentially, the cytosolic fraction from non-intoxicated cells is applied to the pellet fraction of intoxicated cells; addition of CE results in secondary, *in vitro* release of CTA1 into a new supernatant fraction. Ideally, direct manipulation of the CE

would permit examination of cytosolic retro-translocation machinery without inducing indirect effects.

The goal of this study is not only to validate this new approach to elucidate toxin retro-translocation but also to characterize the cytosolic machinery that dislocates CTA1 from the ER membrane. We confirm here that the cytosol contains an activity that specifically promotes release of CTA1 from a membrane fraction. CTA1 that appears in the secondary supernatant must be generated from toxin that traffics to the ER and is presented for retro-translocation normally. Furthermore, the *in vitro* released toxin is freely soluble and is refolded to the same extent as *in vivo* retro-translocated toxin. T-cell receptor α (TCRα), a well-characterized single-pass transmembrane ERAD substrate, also undergoes CE-mediated released from the ER membrane. Unlike CTA1, TCRα release requires proteasome inhibition and catalytically active p97 in order to be released both *in vivo* and *in vitro*. However, depletion of p97 from cytosolic extract does not affect release of CTA1 nor TCRα. Thus, p97 appears to regulate only the initial presentation of TCRα but not CTA1 on the cytosolic surface of the ER membrane. For both the toxin and TCRα, subsequent release into the cytosol requires an unknown additional cytosolic factor. Fractionation of the CE reveals that several prominent candidates for the cytosolic activity, including Hsp90 and the 19S proteasome cap, are not involved in release of CTA1 or TCRα. While the identities of the observed activities remain unknown, both CTA1 and TCRα are released in an energy-dependent manner. Intriguingly, CTA1 release displays a

dependency on GTP hydrolysis whereas TCRα may simply be dependent on nucleotide triphosphate (NTP) binding. These results demonstrate that the established *in vitro* retro-translocation assay is a useful tool to identify and characterize proteins that mediate retro-translocation not only of cholera toxin but also of endogenous ERAD substrates.

3-2. Materials and Methods

Materials

Primary antibodies used were as follows: polyclonal BAT3/Bag6, polyclonal His-probe, polyclonal Hsp90, polyclonal PDI (Santa Cruz Biotechnology, Santa Cruz, CA), monoclonal Hsc/p70, monoclonal p97/VCP, monoclonal PDI, polyclonal CTB (Abcam, Cambridge, MA), polyclonal S8/PA700 (Affinity Bioreagents, a subsidiary of Thermo Fisher Scientific, Waltham, MA), and polyclonal ERGIC53/p58 (Sigma-Aldrich, St. Louis, MO). Monoclonal antibody against HA was a gift from K. Verhey (University of Michigan, Ann Arbor, MI). Polyclonal CTA antibody was produced against denatured CTA purchased from EMD Biosciences (Sand Diego, CA). Purified CT was purchased from EMD Biosciences. Purified CTA was purchased from Enzo Life Sciences (Farmingdale, NY). R192G CT was a gift from W. Lencer (Boston Children's Hosptial, Boston, MA). HA-tagged T-cell receptor alpha (TCRα-HA) expression plasmid was a gift from C. Wojcik (Indiana University, Indianapolis, IN). His-tagged p97 constructs (p97-His and p97-QQ-His) were gifts from Y. Ye (National Institutes of Health, Bethesda, MD).

Tissue culture, transfection, and drug treatment

HEK293T cells were cultured in DMEM with 10% fetal bovine serum (FBS) and penicillin/streptomycin. All expression constructs used were transfected into 30% confluent cells on 10- or 6-cm dishes using the Effectene system (Qiagen, Chatsworth, CA). Where indicated, Brefeldin A (BFA; Sigma-Aldrich) was added to cells in complete media at 2 µg/mL one hour prior to intoxication and maintained in all subsequent media and buffers. Epoxomicin (Calbiochem, a subsidiary of EMD Millipore, Billerica, MA) was added in complete media at 0.5 µg/mL for two hours at 37°C and removed before harvesting cells. Peptide-N-glycosidase F (PNGase F) and Endoglycosidase H (Endo H) were used as according to the manufacturer (New England Biolabs, Ipswich, MA).

***In vivo* and *in vitro* retro-translocation assays**

293T cells were intoxicated with 10 nM CT in HBSS for 45 minutes at 37°C. Cells ($2x10^6$) were permeabilized in 100 µL of 0.01% digitonin in HCN buffer (50 mM HEPES, pH 7.5, 150 mM NaCl, 2 mM $CaCl_2$, and protease inhibitors), incubated on ice for 10 minutes, and centrifuged at 16,000 x g for 10 minutes at 4°C to generate supernatant (S1) and pellet (P1) fractions. The S1 fraction was spun in an ultracentrifuge at 100,000 x g for 30 minutes at 4°C to generate new supernatant (S1') and pellet fractions. The S1' fraction contains *in vivo* retro-translocated toxin. Non-intoxicated cells were permeabilized and fractionated as above. The final supernatant was collected as the cytosolic extract (CE). P1 fractions were resuspended in whole or modified CE, incubated at room

temperature for 30 minutes, and centrifuged at 16,000 x g for 10 minutes at 4°C to generate secondary supernatant (S2) and pellet (P2) fractions. The S2 fraction was spun in an ultracentrifuge at 100,000 x g for 30 minutes at 4°C to generate new secondary supernatant (S2') and pellet (P2') fractions. The S2' fraction contains *in vitro* retro-translocated toxin. All fractions were analyzed by non-reducing SDS-PAGE and immunoblot.

Trypsin sensitivity assays

S1', S2, S2' and CE fractions were prepared as above. CE fractions were supplemented with 2 nM purified CT or CTA1 that had been generated using 3 mM L-Glutathione (GSH; Sigma-Aldrich) or 20 mM DL-Dithiothreitol (DTT; Sigma-Aldrich) as indicated. Purified trypsin (Sigma-Aldrich) was added to fractions at a final concentration ranging from 0.02 – 0.3 mg/mL. Trypsin digestion followed on ice for one hour before termination with 4 mM TLCK (Sigma-Aldrich). Samples were analyzed by non-reducing SDS-PAGE and immunoblot.

Cytosolic extract modification

Immunodepletion of p97 was accomplished by addition of a monoclonal antibody against p97 to CE and incubation at 4°C for three hours. Immune complexes were captured by addition of protein A agarose beads (Invitrogen, Carlsbad, CA) and the resulting supernatant collected and applied to the *in vitro* retro-translocation assay. CE energy state was altered by addition of 1U/50 µL grade VII apyrase (Sigma-Aldrich) or ATPγS, GTPγS (Roche, Indianapolis, IN), AMP-PNP, or GMP-PNP (Sigma Aldrich) to a 10 mM final concentration. Modified

extracts were incubated at room temperature for 30 minutes, returned to ice, and then applied to the *in vitro* retro-translocation assay.

Size exclusion chromatography

1 mL of 293T CE was generated as above and passed through a Bio-Sil SEC 250 (Bio-Rad, Hercules, CA) size exclusion column using HCN buffer for the mobile phase. Individual fractions were collected in 250 µL increments and analyzed for protein content by UV absorption, coomassie brilliant blue staining, and immunoblot. Fractions were then applied to the *in vitro* retro-translocation assay to determine activity.

3-3. Results

Cytosolic extract releases CTA1 from the ER membrane

In order to study cytosolic factors involved in cholera toxin retro-translocation, we developed an assay that permits *in vitro* release of CTA1 from ER membranes (Figure 3-1A). Intoxicated cells were permeabilized with a mild detergent and centrifuged to generate pellet (P1) and supernatant (S1) fractions (Figure 3-1A, step 1; Figure 3-1B) that represent intact organelles and cytosol, respectively. As anticipated, the P1 fraction contains the ER lumenal marker PDI in addition to CTB, CTA and CTA1. The presence of CTA1 in the pellet indicates that toxin has successfully arrived at the ER and been reduced prior to retro-translocation (Figure 3-1B, lanes 1 and 2). The S1 fraction, on the other hand, should only contain cytosolic proteins such as Hsp90 and CTA1 (lane 5). While

the absence of PDI in the S1 fraction indicates that there is not significant leakage of proteins from the ER, the presence of CTA implies that some toxin is erroneously reaching the cytosol. Furthermore, the presence of ERGIC53, a marker for the ER-Golgi intermediate compartment, in the S1 suggests that vesicles are not being removed in the initial fractionation. Ultracentrifugation of the S1 fraction remedied these inconsistencies as the new supernatant fraction (S1') contained only *in vivo* retro-translocated CTA1 (Figure 3-1A, step 2; Figure 3-1B, lanes 3 and 4).

If CTA1 relies on a cytosolic factor to complete retro-translocation, then a cytosolic extract should promote release of toxin exposed on the cytosolic side of the ER membrane, poised to be released into the cytosol. To test this possibility, we resuspended the P1 fraction in buffer, cytosolic extract, or heat-inactivated cytosolic extract. After incubation at room temperature and subsequent centrifugation we analyzed the secondary pellet (P2) and supernatant (S2) fractions (Figure 3-1A, step 3; Figure 3-1C, lanes 1-8). The presence of CTB, CTA, and CTA1 in the S2 fraction regardless of exposure to the cytosolic extract demonstrate that the holotoxin is being released from the pellet, possibly due to vesicle budding (Figure 3-1C, lanes 5-8). To remove potential membrane vesicles from the S2 fraction, the S2 fraction was subjected to ultracentrifugation to generate another set of pellet (P2') and supernatant (S2') fractions (Figure 3-1A, step 4; Figure 3-1C, lanes 9-16). The membrane vesicle marker ERGIC53 was present only in P2' and not S2' fraction (Figure 3-1C, compare lanes 9-12 to

13-16), indicating that ultracentrifugation removed membrane vesicles. Importantly, only CTA1 but not CTA or CTB is found in the S2' fraction derived from samples treated with the cytosolic extract (Figure 3-1C, lanes lanes 9-12 with 13-16). Thus, CTA1 in the S2' fraction likely represents *in vitro* retro-translocated toxin. That heat inactivation of the cytosolic extract prevents arrival of CTA1 in the S2' fraction demonstrates that a proteinaceous cytosolic component drives the release process (cf. lane 14 with 15 and 16).

Prior to retro-translocation, CTA must be proteolytically cleaved, trafficked to the ER, and reduced to CTA1 (see Chapter 1-2). Failure to follow this pathway prevents toxin presentation to the cytosol. As such, the appearance of CTA1 in the S2' fraction should depend on proper processing of the toxin. CT-R192G, a form of cholera toxin that is resistant to CTA proteolytic cleavage, traffics to the ER but is retro-translocation deficient (*6*). Accordingly, CTA-R192G can be found in the P1 but not in the S2' fraction (Figure 3-1D, cf. lane 1 with 2 and 3 with 4). To inhibit delivery of CT to the ER, cells were pre-treated with Brefeldin A (BFA). As expected, CTA in BFA treated cells does not undergo sufficient reduction and is not efficiently released into the S2' fraction (Figure 3-1E, cf. lane 1 with 2 and 3 with 4). These data verify that CTA1 must be generated in the ER to be released in the *in vitro* retro-translocation assay. However, it remains possible that CTA1 is not truly retro-translocated into the S2' fraction.

We next envision that the released toxin in this *in vitro* assay should be freely soluble, and not surrounded by vesicles. To test this hypothesis, we asked

whether the released toxin is sensitive to trypsin digestion. When pure CT is incubated with a high trypsin concentration (0.3 mg/ml), both CTA and CTA1 are degraded efficiently (Figure 3-2A, compare lane 2 to 1 and lane 4 to 3), consistent with our previous report (*6*). However, in the S2 fraction, only CTA1 but not CTA is trypsin-sensitive (Figure 3-2A, compare land 6 to 5), suggesting that CTA1 is free and exposed while CTA is protected by membranes. Importantly, in the S2' fraction, CTA1 is largely sensitive to proteolysis (Figure 3-2A, compare lane 8 to 7), indicating that the toxin exists in a free and soluble form. To further support this conclusion, we found that CTA1 was efficiently immunodepleted from the S2' fraction using two different CTA antibodies (Figure 3-2B, cf. lane 1 with 2 and 3 with 4). Together, these data suggest that CTA1 is generated in the ER and released into the cytosol as a freely soluble peptide.

CTA1 is postulated to spontaneously refold once released from the retro-translocation machinery into the cytosol, a reaction thought to prevent the toxin from engaging the proteasome (*1*). We therefore hypothesize that *in vivo* and *in vitro* retro-translocated toxin ought to refold to a similar extent upon reaching the cytosol. To assess the folding state of retro-translocated CTA1, we compared the sensitivity of CTA1 to increasing trypsin concentration in the S1' and S2' fractions to that of native CTA1, as native CTA1 represents folded toxin. Pure CT is incubated with DTT at 37°C initially to generate CTA1. Subsequent addition of increasing trypsin concentration at 4°C (ranging from 0.02 to 0.16 mg/ml) demonstrates that native CTA1 becomes increasingly sensitive to proteolysis,

with most obvious degradation occurring at 0.16 mg/ml (Figure 3-2C, top panel, compare lanes 1-5). Strikingly, CTA1 in both the S1' and S2' fractions also displayed a similar sensitivity profile, with most clear proteolysis evident at 0.16 mg/ml trypsin (Figure 3-2C, second and third panels, compare lanes 1-5). Hsc70 in the cytosolic extract also exhibits clear trypsin-mediated degradation at this highest concentration (Figure 3-2C, fourth panel, compare lanes 1-5). In all cases, when the samples were incubated at 65°C to induce partial protein unfolding followed by trypsin addition at 4°C, CTA1 and Hsc70 were vulnerable to degradation at lower trypsin concentrations, as expected (Figure 3-2C, compare lanes 6-10 to 1-5). We conclude that both *in vivo* and *in vitro* retro-translocated toxin refold to a similar extent as native toxin upon release into the cytosol. It remains undetermined whether CTA1 is refolded to a catalytically active conformation.

Cytosolic extract stimulates release of deglycosylated TCRα

The data from the previous section demonstrate that our *in vitro* assay accurately simulates *in vivo* retro-translocation of cholera toxin. However, for the assay to be a generally useful tool it must be applicable to retro-translocation of both pathogens and canonical ERAD substrates. As stated above, one of the most well documented ERAD substrates is TCRα. Unlike cholera toxin, TCRα is a single-pass transmembrane protein that is glycosylated upon insertion into the ER membrane and ubiquitinated prior to targeting to the proteasome for degradation. Furthermore, in contrast to the toxin, ERAD of TCRα is dependent

on the p97-Ufd1-Npl4 complex for membrane extraction and presentation to the 26S proteasome (*19-23*). Despite these obvious differences, we asked whether our established in vitro retro-translocation assay could be utilized to clarify cytosolic events guiding release of TCRα from the ER membrane.

Ectopically expressed TCRα is normally observed as a high molecular weight, fully glycosylated species in the ER membrane (+CHO; Figure 3-3A, cf. lane 1 with 2). Because it is rapidly extracted from the membrane and degraded, deglycosylated TCRα (-CHO) is ordinarily not observed in the P1 or S1' fractions (Figure 3-3A, cf. lanes 1 and 2 with 4 and 5). Proteasomal inhibition with epoxomicin, however, permits accumulation of deglycosylated TCRα species in both the P1 and S1' fractions (Figure 3-3A, cf. lanes 2 with 3 and 5 with 6); species in the S1' fraction have been fully extracted and released from the ER membrane. As with CTA1, *in vitro* release of TCRα into the S2' fraction requires cytosolic extract. However, only TCRα from epoxomicin-treated pellets is accessible for release (Figure 3-3A, cf. lanes 7-11). Intriguingly, once released into the cytosol TCRα stability is no longer dependent on proteasome inhibition (cf. lanes 12 and 13), indicating that proteasomal targeting and degradation of TCRα only occur on the ER membrane.

To confirm that epoxomicin specifically affects TCRα stability and release, we analyzed cholera toxin retro-translocation with or without drug treatment. As anticipated, toxin arrival at the ER and subsequent reduction to CTA1 were unaffected by proteasome inhibition (Figure 3-3B, cf. lanes 1-3). Toxin levels in

the S1' fraction were also unaffected by the presence of epoxomicin, verifying that *in vivo* retro-translocated CTA1 is not targeted to the proteasome (Figure 3-3B, cf. lanes 4-6). Most importantly, toxin that is released into the S2' was not sensitive to proteasomal degradation (Figure 3-3B, cf. lanes 7-11). These results confirm not only that epoxomicin treatment specifically affects proteasome substrates but also that *in vitro* released CTA1 behaves normally.

Using heat-inactivated cytosolic extracts, we demonstrated earlier that CTA1 release is mediated by a proteinaceous cytosolic factor (Figure 3-1C). Similarly, a heat-inactivated cytosolic extract cannot induce TCRα release from epoxomicin-treated pellets (Figure 3-3D, cf. lane 2 with 3 and 4), suggesting that a protein-dependent activity is responsible for promoting this reaction. Because TCRα can undergo processing in the ER and the Golgi, it is possible that the cytosolic activity releases species from either organelle. To verify that TCRα is released from the ER membrane specifically, S2' fractions were treated with peptide-N-glycosidase F (PNGase F) or Endoglycosidase H (Endo H). PNGase F cleaves N-linked glycans en bloc, thereby fully deglycosylating target proteins. TCRα from fractions treated with PNGase F collapsed into a discrete band, confirming that the observed species result from various degrees of deglycosylation, not proteolysis (Figure 3-3C, cf. lane 2 with 5 and 6). Endo H, on the other hand, can only cleave N-linked glycans that have not been modified in the Golgi. Treatment of S2' fractions with Endo H also resulted in the collapse of TCRα into a single band (cf. lane 2 with 3 and 4). These results confirm that

deglycosylated TCRα is released directly from the ER membrane in the *in vitro* retro-translocation assay.

As a transmembrane protein, TCRα should be incapable of refolding in the cytosol. We analyzed the conformation of retro-translocated TCRα by using the trypsin sensitivity assay. Compared to CTA1 (Figure 3-2D), TCRα in both the S1' and S2' fractions was significantly more sensitive to degradation (Figure 3-3E). Moreover, both *in vivo* and *in vitro* retro-translocated TCRα displayed the same degree of trypsin sensitivity (cf. lanes 1-4 with 5-8). These observations indicate that TCRα is neither refolded nor protected against degradation by associated factors.

The above data indicate that our *in vitro* assay recreates cytosolic release of TCRα. Retro-translocated TCRα is normally extracted and degraded at the ER membrane, but in the absence of active proteasome it becomes available for release by a proteinaceous cytosolic factor. Whether cholera toxin and TCRα share the same mechanism of release remains to be evaluated.

Substrate release from the ER membrane occurs independently of p97

The AAA-ATPase p97, when in complex with Ufd1 and Npl4, is a fundamental regulator of ERAD. The p97 complex forms dual hexameric rings that are targeted to the retro-translocation machinery through interactions with transmembrane chaperones including VIMP and Derlin-1 and E3 ligases such as Hrd1 (*24-28*). As ERAD substrates emerge from the retro-translocon, the p97 complex binds to poly-ubiquitin chains and sequentially hydrolyses ATP to

ratchet proteins out of the ER membrane (*19-23*). These proteins are thereby susceptible to degradation by the 26S proteasome. The role of p97 in extraction of TCRα has been thoroughly investigated (*19-21, 23*); it is commonly believed that p97 is the sole factor responsible for release of TCRα from the ER membrane. The link between cholera toxin and p97, on the other hand, is tenuous at best (*2, 3*). The development of the *in vitro* retro-translocation assay thus affords an excellent opportunity to clarify the role of p97 in controlling CTA1 and TCRα retro-translocation.

To assess the requirement of p97 in TCRα retro-translocation, either wild type (WT p97) or hydrolysis deficient p97 (QQ p97) was co-transfected with TCRα. These cells were treated with epoxomicin and fractionated as per usual. The pellets were resuspended in unmodified CE and subjected to the *in vitro* retro-translocation assay. While overexpression of WT p97 did not produce any phenotypic abnormalities (Figure 3-4A, cf. lanes 1 with 4 and 2 with 5), QQ p97 decreased the appearance of deglycosylated TCRα in both the P1 and S1' fractions (cf. lanes 2 and 5 with 3 and 6). Likewise, QQ p97, but not WT p97, precluded CE-induced release of TCRα into the S2' (cf. lanes 7-9). While our *in vitro* assay clearly reveals that p97 executes a critical step in release of TCRα from the ER membrane to the cytosol, it remains possible that additional cytosolic factors are recruited to drive this reaction.

The function of p97 in CTA1 retro-translocation was tested in the same manner (minus epoxomicin). Overexpression of neither WT nor QQ p97

influenced trafficking and reduction of CTA in the ER (Figure 3-4B, cf. lanes 1-3). Likewise, neither protein altered the efficiency of CTA1 retro-translocation *in vivo* (cf. lanes 4-6). Lastly, CE-induced release of CTA1 *in vitro* was unaffected (cf. lanes 7-9). According to this data, retro-translocation of cholera toxin must proceed independently of the catalytic activity of p97.

To further assess the role of p97 in cytosolic release, cytosolic extracts were mock depleted or depleted of p97; immunodepletion of p97 was nearly 100% efficient (Figure 3-4C, cf. lane 1 with 2 and 3 with 4). Intriguingly, p97 depleted extracts were as effective as the control extracts at releasing TCRα (Figure 3-4D, cf. lane 1 with 2 and 3 with 4) and CTA1 (Figure 3-4E, cf. lanes 1 with 2 and 3 with 4) from ER membranes. These results indicate that p97 is not the cytosolic factor responsible for completing retro-translocation of TCRα. Residual p97 on the pellet is not sufficient to drive this reaction because the assay relies on an intact, proteinaceous component in the cytosol (Figure 3-3D). Instead, p97 likely ratchets TCRα out of the membrane and presents it for release. This discrepancy infers that retro-translocation requires multiple, sequential interactions on the cytosolic face of the ER. Because CTA1 is not reliant on the catalytic activity of p97 it is unclear how it is presented for release.

Novel factors complete retro-translocation of ERAD substrates

Other than p97, only Hsp90 has been directly implicated in retro-translocation of cholera toxin (*4*). However, the evidence supporting the involvement of this protein is indirect and possibly non-specific. The primary goal

of this study was to create a physiologically relevant assay for directly examining the cytosolic mechanism of retro-translocation. So far, we have established that *in vitro* release of both cholera toxin and TCRα recapitulate the final step of *in vivo* retro-translocation. Here, we employ unbiased tactics to characterize the cytosolic activity.

First, cytosolic extract was prepared and subjected to size exclusion chromatography. Fractions were collected and analyzed for protein content using UV-absorption and Coomassie brilliant blue staining (data not shown). Consecutive even fractions were used for *in vitro* retro-translocation of cholera toxin. Fractions 36-40 contained the highest level of cytosolic activity as determined by CTA1 release (Figure 3-5A, top panel). Peak activity did not correlate with total protein concentration (data not shown). Preliminary analysis of the protein content revealed that neither p97 nor Hsp90 co-fractionated with the peak activity (cf. top with middle and bottom panels).

A separate pool of extract was fractionated as above and consecutive odd fractions were used in the *in vitro* assay. Fractions 35-39 represented the peak activity for both TCRα (Figure 3-5B, top panel) and CTA1 release (data not shown). Fractions were then immunoblotted for a variety of putative retro-translocation factors. Candidate selection was based on previous connections with cholera toxin (p97, Hsp90, 19S proteasome subunit S8) or on cytosolic chaperone activity (Hsc70, Bag6). With the exception of Hsc70, none of the tested proteins co-fractionated with the peak cytosolic activity (cf. top panel with

panels 2-6). Poor resolution of Hsc70 may be due to high protein levels or to formation of various complexes with co-chaperones. While these results do not identify the cytosolic activity, they reveal that several prominent candidates are involved in release of neither cholera toxin nor TCRα from the ER membrane.

To further characterize the cytosolic activity we subjected extracts to energy depletion. Depletion was accomplished either by introduction of non-hydrolyzable nucleotide triphosphate (NTP) analogs or by apyrase-catalyzed NTP hydrolysis. Combination of apyrase-treated extracts with intoxicated pellets revealed that CTA1 release is energy dependent (Figure 3-5C, cf. lanes 1, 2 and 5). Additionally, toxin release was more sensitive to treatment with GTPγS than ATPγS (cf. lanes 1-4). The observed guanine nucleotide preference was verified by repeating the experiment using GMP-PNP and AMP-PNP (Figure 3-5D). Intriguingly, release of TCRα was inhibited by neither ATPγS nor GTPγS (Figure 3-5C, cf. lanes 1-4); however, apyrase treatment revealed that TCRα release does require free NTPs (cf. lanes 1, 2 and 5). These data collectively suggest that cholera toxin is dependent on GTP hydrolysis for release into the cytosol. While the nucleotide dependency of TCRα cannot be inferred from this information, it is apparent that its mechanism of release diverges from that of cholera toxin.

3-4. Discussion

Before achieving cytotoxicity, the cholera toxin CTA1 subunit must cross the ER membrane in a process known as retro-translocation. By hijacking ERAD

machinery the toxin is unfolded in the ER lumen and becomes competent for crossing the membrane. However, once the toxin has been exposed to the cytosol it is unclear how it is released from the membrane and avoids proteasomal degradation. Targeted identification of cytosolic machinery is ultimately restricted by our limited knowledge of ERAD and the various roles that cytosolic factors play in cellular homeostasis. To overcome these caveats we created an *in vitro* assay that enables direct manipulation of cytosolic factors without inducing pleiotropic effects. Furthermore, this method is physiologically relevant because it relies on cholera toxin that has been processed *in vivo*.

To validate the assay we demonstrated that release of CTA1 from intoxicated pellets is induced by addition of cytosolic extract. By subjecting cytosolic fractions to ultracentrifugation, trypsin digestion and immunodepletion we determined that *in vitro* released CTA1 is freely soluble and refolded to the same extent as *in vivo* retro-translocated toxin. Furthermore, the assay specifically relies on toxin that has trafficked to and been processed in the ER. Most importantly, CTA1 release depends on an intact proteinaceous factor in the cytosol. These data verify that the *in vitro* assay successfully replicates the final steps of *in vivo* retro-translocation of cholera toxin.

In order to broaden the scope of our assay we analyzed retro-translocation of T-cell receptor α, an endogenous ERAD substrate. Unsurprisingly, release of TCRα from the ER membrane was also dependent on an active cytosolic factor. Because misfolded TCRα is quickly degraded, inhibition of the 26S proteasome

was required to visualize retro-translocation of the substrate. Interestingly, proteasome inhibition was only required in the pellet fraction. Consistent with its rapid destruction, TCRα is likely targeted to proteasome tethered to the ER membrane. However, if TCRα avoids degradation and is completely released from the membrane it is not targeted to active proteasome contributed by the cytosolic extract. This phenomenon may result from uncoupling of deubiquitination and degradation or dissociation of factors that assist in targeting of TCRα to the proteasome.

Inclusion of TCRα in our assay permitted the investigation of canonical ERAD components in the retro-translocation of cholera toxin. The most well established cytosolic factor involved in retro-translocation is p97. While its relationship with cholera toxin is ambiguous (*2, 3*), p97 is considered the primary driving force for extraction and release of TCRα from the ER membrane (*19-21, 23*). As anticipated, disruption of p97 activity at the ER membrane hindered retro-translocation of TCRα, but not CTA1, in both the *in vivo* and *in vitro* assays. Because knockdown of p97 leads to severe non-specific effects we were unable to investigate retro-translocation under that condition. Therefore, it is still possible that cholera toxin requires p97 as a scaffold for recruiting the cytosolic release factor.

The most salient data is that immunodepletion of p97 from a cytosolic extract did not affect CTA1 and TCRα release. In the context of TCRα, this observation indicates that p97 is not solely responsible for catalyzing the entire

dislocation reaction propelling TCRα from the ER membrane to the cytosol. Rather, p97 is necessary for initial extraction and presentation of substrate for final release. This data, however, does not indicate how CTA1 is presented for release from the membrane. As mentioned previously, cholera toxin can spontaneously refold upon release from PDI (*1*). Refolding would not only assist the toxin in avoiding degradation but would also prevent backsliding of the toxin into the ER (Figure 3-6). Furthermore, this change in conformation might improve interactions with cytosolic factors. For example, binding of CTA1 to Arf family members is contingent on refolding of the toxin (*29*). We are currently employing several techniques to infer the folding state of CTA1 on the cytosolic face of the ER membrane.

Further modification of the cytosolic extract revealed that numerous candidate factors are neither required for *in vitro* release of cholera toxin nor of TCRα. It should be noted that these factors may still play crucial roles in processing of ERAD and UPS substrates, but they do not appear to take part in dislocation from the ER membrane. Using size exclusion or ion exchange (data not shown) chromatography we were unable to resolve Hsc/Hsp70 from the cytosolic activity. Analysis of this ATPase is complicated by its abundance in the cytosol and the diverse range of complexes it forms with co-chaperones. However, our data indicate that release of CTA1 is dependent on hydrolysis of GTP (Figure 3-6), thereby decreasing the likelihood that Hsc70 is involved. Interestingly, the small GTPase Ran and its co-factor importin β were recently

implicated in the degradation of another established ERAD substrate, mutant α1-antitrypsin (*30*). Whether or not this correlation extends to cholera toxin and TCRα remains to be determined.

Our energy dependency results also exposed a divergence in the mechanism of release for CTA1 and TCRα. However, our current approach does not discriminate between energy expenditure at the ER membrane and in the cytosol. As such, the data do not rule out the possibility that these two substrates rely on a common factor. Further analysis of the energy requirement for membrane release will be necessary to discern the nature of the cytosolic activity. Moreover, the differences observed between cholera toxin and TCRα emphasize the need to apply the *in vitro* retro-translocation assay to other ERAD substrates. For example, α1-antitrypsin and pro-α-factor are structurally unique in comparison to toxin and TCRα. Their inclusion would highlight the specific interactions that drive substrate presentation and release from the membrane. Ultimately, the further we characterize the cytosolic factor the closer we are to revealing its identity.

Figures

Figure 3-1. Establishment of an *in vitro* retro-translocation assay

(A) Flow diagram of the *in vitro* retro-translocation assay. Steps 1-4 indicate generation of unique fractions. (B) 293T cells were intoxicated with or without 10 nM CT for 45 minutes, permeabilized with digitonin, and centrifuged to generate pellet (P1) and supernatant fractions (S1). S1 fractions were spun in an ultracentrifuge to generate S1' fractions. Fractions were analyzed by immunoblot with the indicated antibodies. (C) Intoxicated P1 fractions were resuspended in buffer, cytosolic extract, or heat-inactivated cytosolic extract. After incubation for 30 minutes at room temperature, samples were centrifuged to generate P2 and S2 fractions. S2 fractions were subsequently spun in an ultracentrifuge to generate P2' and S2' fraction. Fractions were analyzed by immunoblot with the indicated antibodies. (D) Cells were intoxicated with WT or R192G CT and subjected to the *in vitro* retro-translocation assay. P1 and S2' fractions were analyzed by immunoblot with the indicated antibodies. (E) Cells were treated with vehicle or BFA prior to and during intoxication. Intoxicated cells were then subjected to the *in vitro* retro-translocation assay and P1 and S2' fractions analyzed by immunoblot with the indicated antibodies.

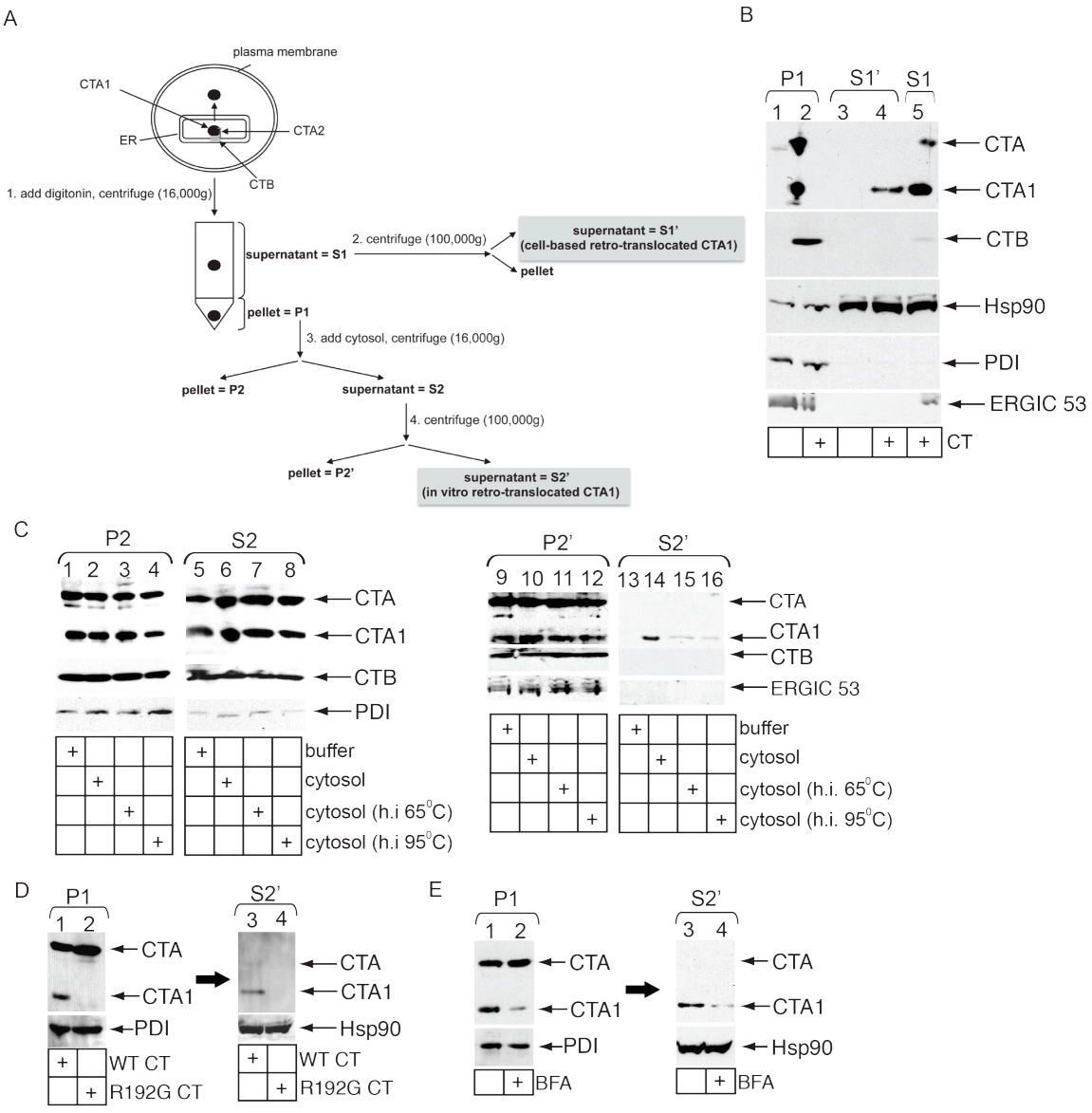
A
plasma membrane
CTA1
CTA2
ER
CTB
1. add digitonin, centrifuge (16,000g)
supernatant = S1
2. centrifuge (100,000g)
supernatant = S1'
(cell-based retro-translocated CTA1)
pellet
pellet = P1
3. add cytosol, centrifuge (16,000g)
pellet = P2
supernatant = S2
4. centrifuge (100,000g)
pellet = P2'
supernatant = S2'
(in vitro retro-translocated CTA1)
B
P1
S1'
S1
1 2 3 4 5
CTA
CTA1
CTB
Hsp90
PDI
ERGIC 53
CT
C
P2
S2
1 2 3 4 5 6 7 8
CTA
CTA1
CTB
PDI
buffer
cytosol
cytosol (h.i 65°C)
cytosol (h.i 95°C)
P2'
S2'
9 10 11 12 13 14 15 16
CTA
CTA1
CTB
ERGIC 53
buffer
cytosol
cytosol (h.i. 65°C)
cytosol (h.i. 95°C)
D
P1
S2'
1 2
3 4
CTA
CTA1
PDI
Hsp90
WT CT
R192G CT
E
P1
S2'
1 2
3 4
CTA
CTA1
PDI
Hsp90
BFA

Figure 3-2. *In vitro* retro-translocated CTA1 is freely soluble and refolded

(A) Purified CT in 3mg/mL BSA were treated with buffer or 3 mM GSH (First and second panels, respectively). S2 and S2' fractions were generated from intoxicated cells as previously described (Third and fourth panels, respectively). Fractions were incubated with buffer or 0.3 mg/mL trypsin on ice for one hour before reactions were stopped with TLCK and sample buffer. Samples were analyzed by immunoblot with an antibody against CTA (B) S2' fractions were generated as previously described and incubated with control antibody or one of two different antibodies against CTA. Immune complexes were precipitated using protein A agarose beads and supernatants were analyzed by immunoblot with an antibody against CTA. (C) Purified CT was added to CE and reduced with 20 mM DTT. S1' and S2' fractions were generated as previously described. Samples were pre-treated at 37°C (left panels) or 65°C and then incubated with the indicated concentration of trypsin for one hour on ice. Reactions were stopped with TLCK and sample buffer and samples were analyzed by immunoblot with the indicated antibodies.

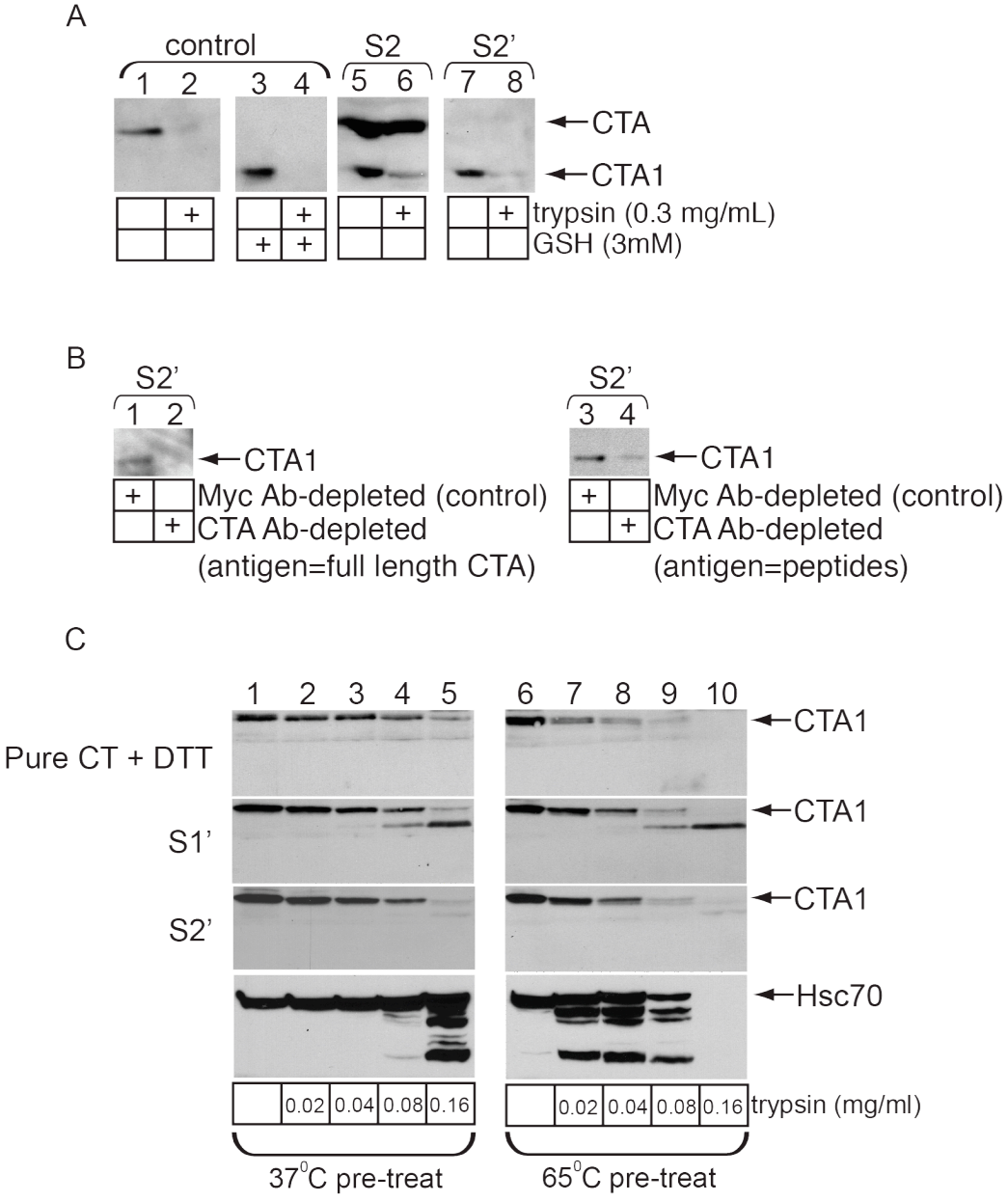
A
control
S2
S2'
1 2 3 4 5 6 7 8
CTA
CTA1
trypsin (0.3 mg/mL)
GSH (3mM)
B
S2'
1 2
CTA1
Myc Ab-depleted (control)
CTA Ab-depleted
(antigen=full length CTA)
S2'
3 4
CTA1
Myc Ab-depleted (control)
CTA Ab-depleted
(antigen=peptides)
C
1 2 3 4 5 6 7 8 9 10
Pure CT + DTT
S1'
S2'
CTA1
CTA1
CTA1
Hsc70
0.02 0.04 0.08 0.16 0.02 0.04 0.08 0.16 trypsin (mg/ml)
37°C pre-treat
65°C pre-treat

Figure 3-3. Proteasome inhibition permits *in vitro* release of TCRα

(A) 293T cells were transfected with vector or TCRα-HA. Transfected cells were pre-treated with or without epoxomicin for two hours before permeabilization. S2' fractions were generated by incubating P1 fractions with buffer, CE from untreated cells, or CE from epoxomicin treated cells. Fractions were analyzed by immunoblot with the indicated antibodies. Observed TCRα-HA species were either fully glycosylated (+CHO) or deglycosylated to various degrees (-CHO). (B) Intoxicated cells were pre-treated with or without epoxomicin for two hours before being subjected to the *in vitro* retro-translocation assay. P1, S1' and S2' fractions were analyzed by immunoblot with the indicated antibodies. (C) Cells transfected with TCRα-HA were subjected to the *in vitro* retro-translocation assay. S2' fractions were generated by the addition of buffer, CE, or heat-inactivated CE and then analyzed by immunoblot. (D) Cells transfected with TCRα-HA were subjected to the *in vitro* retro-translocation assay. S2' fractions were generated by the addition of buffer or CE. Where indicated, samples were treated with either Endo H or PNGase F at two different concentrations and then analyzed by immunoblot. (E) S1' and S2' fractions were generated from cells expressing TCRα-HA. Samples were incubated with the indicated concentration of trypsin for one hour on ice. Reactions were stopped with TLCK and sample buffer and samples were analyzed by immunoblot with the indicated antibodies.

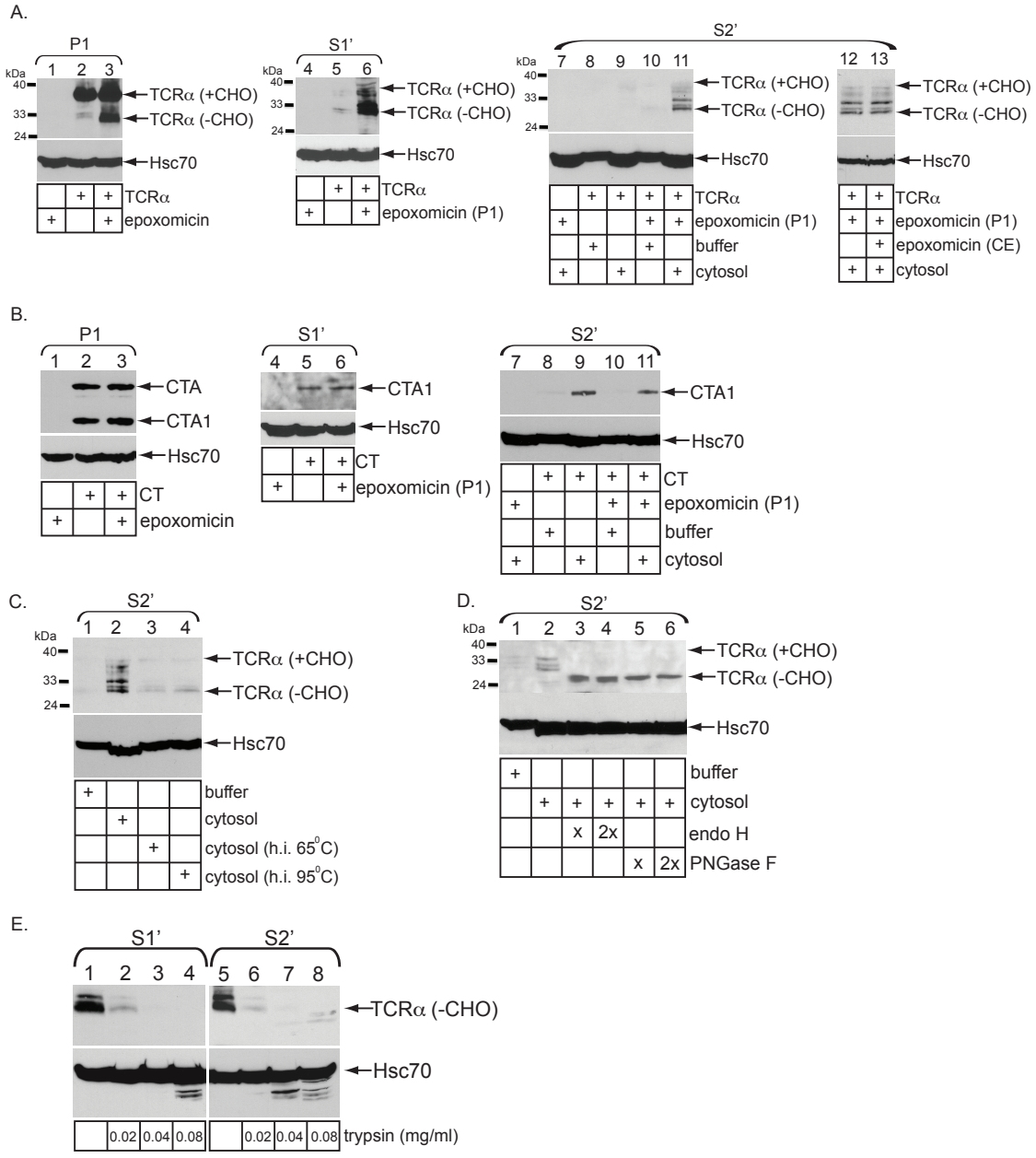
A.
P1
S1'
S2'
kDa
TCRα (+CHO)
TCRα (-CHO)
Hsc70
TCRα
epoxomicin
epoxomicin (P1)
buffer
cytosol
epoxomicin (CE)
B.
CTA
CTA1
CT
C.
cytosol (h.i. 65°C)
cytosol (h.i. 95°C)
D.
endo H
PNGase F
E.
trypsin (mg/ml)

Figure 3-4. Substrate release follows extraction from the ER membrane

(A) 293T cells expressing TCRα-HA were co-transfected with vector, p97-His (WT p97) or p97-QQ-His (QQ p97). Cells were treated with epoxomicin and subjected to the *in vitro* retro-translocation assay. P1, S1' and S2' fractions were analyzed by immunoblot with the indicated antibodies. (B) Intoxicated cells were transfected with vector, WT p97 or QQ p97. Cells were subjected to the *in vitro* retro-translocation assay and the P1, S1' and S2' fractions were analyzed by immunoblot with the indicated antibodies. (C) CE was incubated with control antibody or antibody against p97. Immune complexes were precipitated using protein A agarose beads and the resulting supernatants were analyzed by immunoblot (two unique experiments shown). (D) Immunodepleted extracts from (C) were combined with P1 fractions from epoxomicin-treated cells expressing TCRα-HA. The resulting S2' fractions were analyzed by immunoblot (two unique experiments shown). (E) Same as in (D) except P1 from intoxicated cells were used.

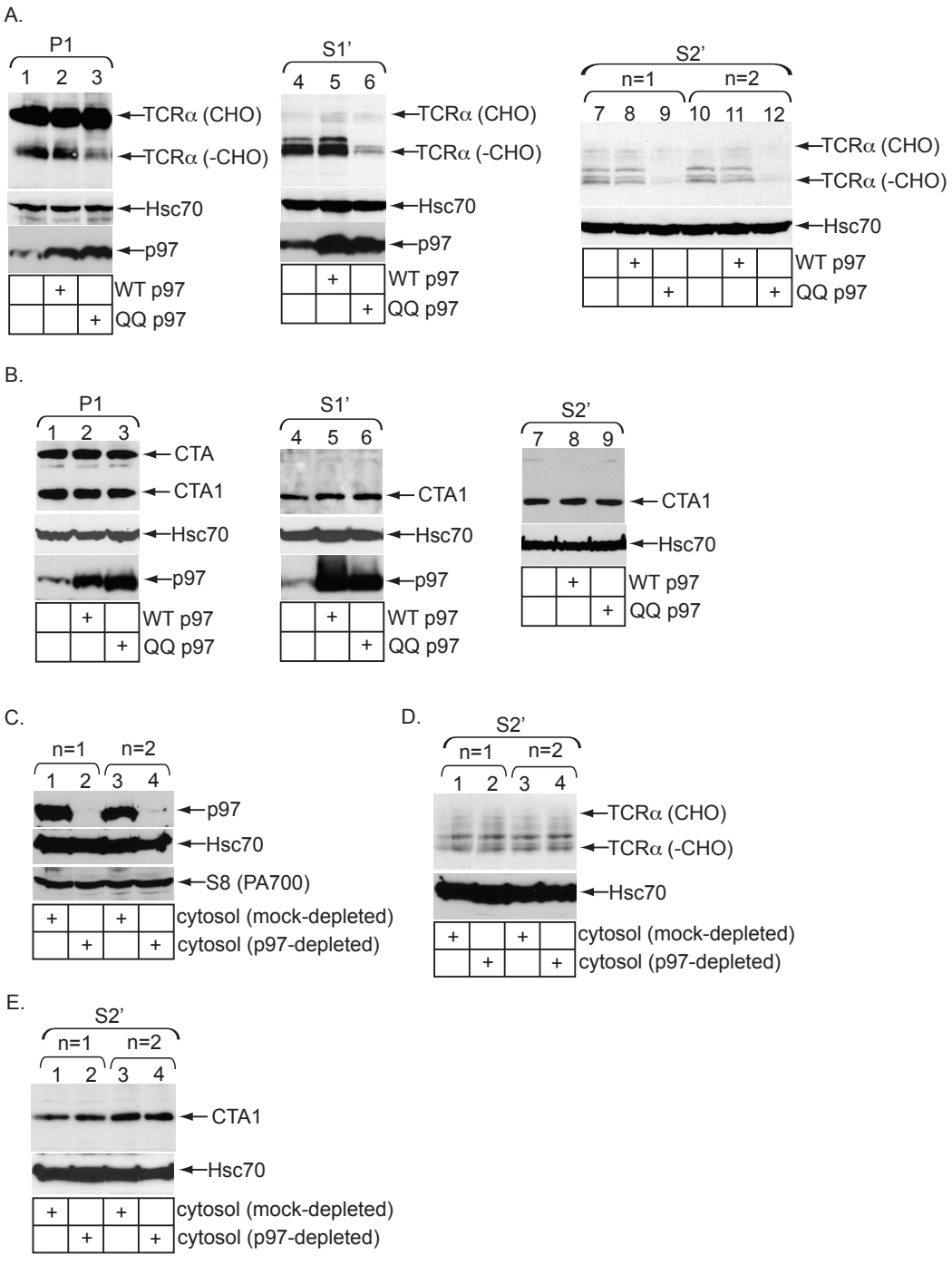
A.
P1
1 2 3
TCRα (CHO)
TCRα (-CHO)
Hsc70
p97
WT p97
QQ p97
S1'
4 5 6
S2'
n=1
n=2
7 8 9 10 11 12
B.
CTA
CTA1
C.
n=1 n=2
1 2 3 4
S8 (PA700)
cytosol (mock-depleted)
cytosol (p97-depleted)
D.
E.

Figure 3-5. A novel cytosolic factor releases CTA1 from the ER membrane

(A) CE was subjected to size exclusion chromatography by passage through a Bio-Sil SEC 250 column. Even fractions were collected and used for *in vitro* retro-translocation of CTA1 from intoxicated cells. CTA1 release in the resulting S2' fractions was analyzed by immunoblot (top panel). Even fractions were directly analyzed for protein content by immunoblot with the indicated antibodies (bottom panels). (B) Same as in (A) except odd fractions were collected and used for *in vitro* retro-translocation of TCRα-HA from epoxomicin-treated cells. TCRα-HA release in the resulting S2' fractions was analyzed by immunoblot (top panel). Even fractions were directly analyzed for protein content by immunoblot with the indicated antibodies (bottom panels). (C) P1 fractions from intoxicated cells were combined with buffer or cytosolic extracts pre-treated with ATPγS, GTPγS or apyrase. The resulting S2' fractions were analyzed by immunoblot. (D) Same as in (C) except extracts were pre-treated with buffer, AMP-PNP or GMP-PNP. (E) Same as in (C) except P1 fractions were generated from epoxomicin-treated cells expressing TCRα-HA.

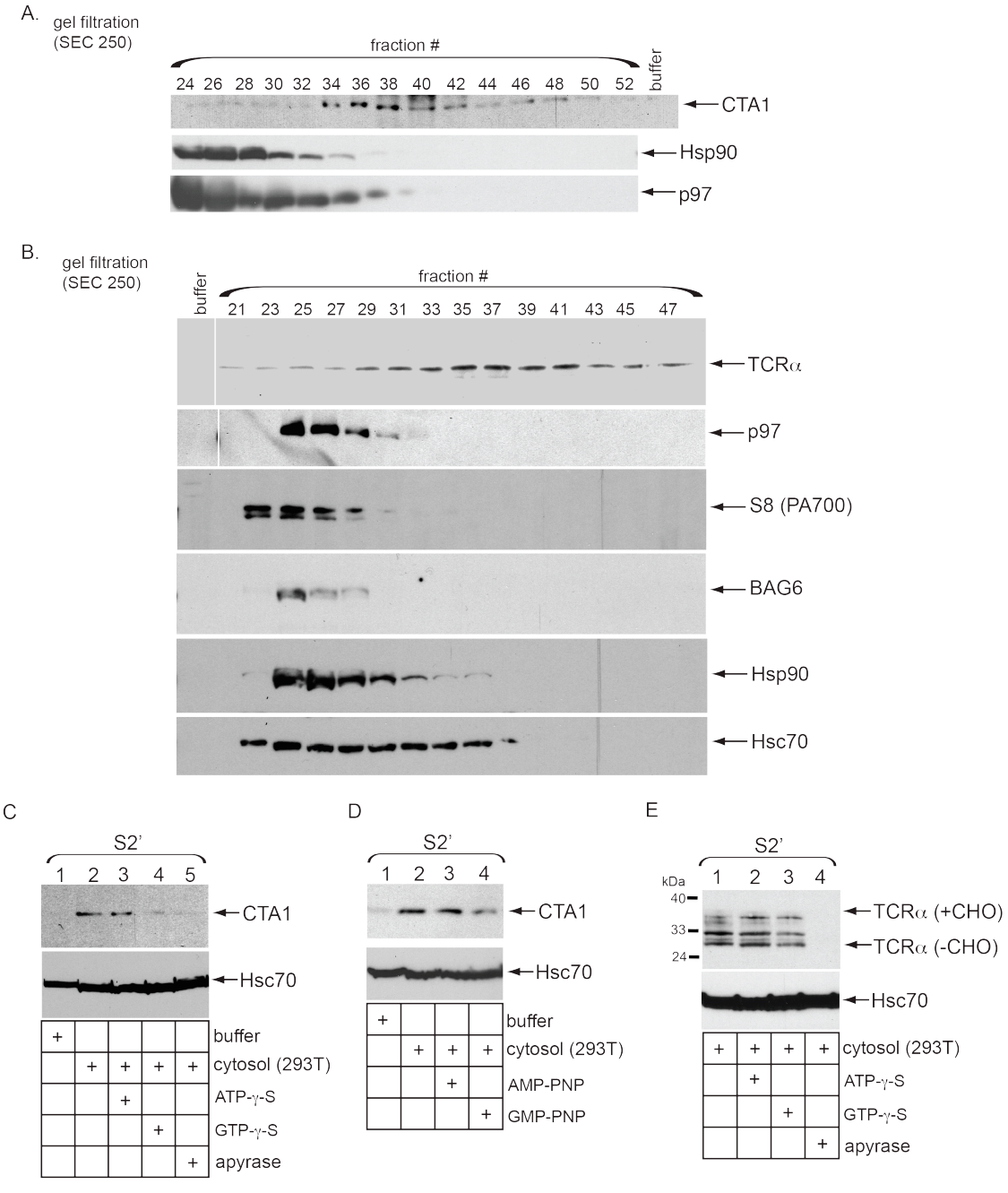
A.
gel filtration
(SEC 250)
fraction #
24 26 28 30 32 34 36 38 40 42 44 46 48 50 52
buffer
CTA1
Hsp90
p97
B.
gel filtration
(SEC 250)
buffer
fraction #
21 23 25 27 29 31 33 35 37 39 41 43 45 47
TCRα
p97
S8 (PA700)
BAG6
Hsp90
Hsc70
C
S2'
1 2 3 4 5
CTA1
Hsc70
buffer
cytosol (293T)
ATP-γ-S
GTP-γ-S
apyrase
D
S2'
1 2 3 4
CTA1
Hsc70
buffer
cytosol (293T)
AMP-PNP
GMP-PNP
E
S2'
1 2 3 4
kDa
40
33
24
TCRα (+CHO)
TCRα (-CHO)
Hsc70
cytosol (293T)
ATP-γ-S
GTP-γ-S
apyrase

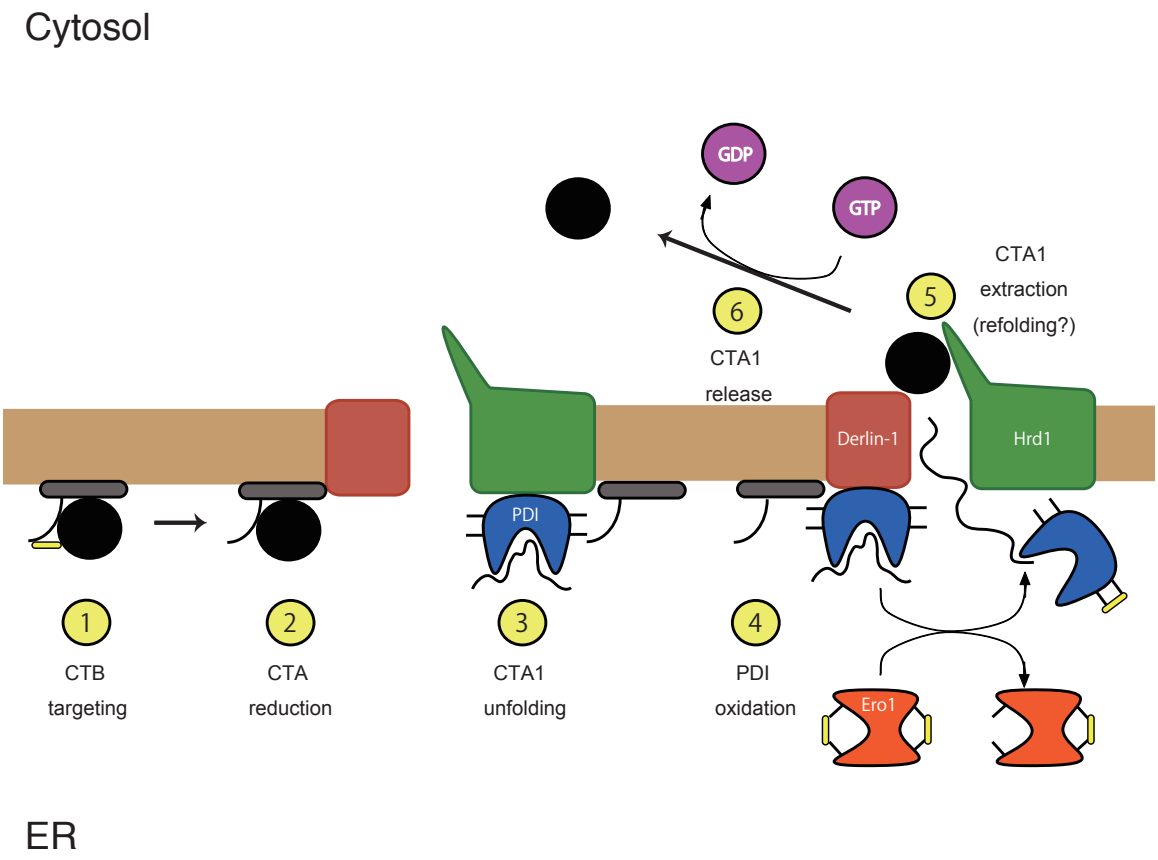

Figure 3-6. A cytosolic protein releases CTA1 from the ER membrane

In the ER, CT is first targeted to the Derlin-1/Hrd1 membrane complex (step 1). The toxin is then reduced by an unknown reductase (step 2), generating CTA1. PDI bound to Derlin-1/Hrd1 then unfolds CTA1 (step 3). Oxidation of PDI by Ero1α releases unfolded CTA1 (step 4) for retro-translocation while inducing release of PDI from Derlin-1. Upon exposure to the cytosol, CTA1 is extracted from the membrane (step 5). Extraction may be driven by spontaneous refolding of the toxin. This may also allow toxin to bypass the proteasome. Finally, a proteinaceous cytosolic factor, coupled with GTP hydrolysis, releases CTA1 into the cytosol to complete retro-translocation (step 6). See text for further discussion.

3-5. References

1. C. Rodighiero, B. Tsai, T. A. Rapoport, W. I. Lencer, Role of ubiquitination in retro-translocation of cholera toxin and escape of cytosolic degradation. *EMBO reports* **3**, 1222 (Dec, 2002).
2. M. Kothe *et al.*, Role of p97 AAA-ATPase in the retrotranslocation of the cholera toxin A1 chain, a non-ubiquitinated substrate. *The Journal of biological chemistry* **280**, 28127 (Jul 29, 2005).
3. R. J. Abujarour, S. Dalal, P. I. Hanson, R. K. Draper, p97 Is in a complex with cholera toxin and influences the transport of cholera toxin and related toxins to the cytoplasm. *The Journal of biological chemistry* **280**, 15865 (Apr 22, 2005).
4. M. Taylor *et al.*, Hsp90 is required for transfer of the cholera toxin A1 subunit from the endoplasmic reticulum to the cytosol. *The Journal of biological chemistry* **285**, 31261 (Oct 8, 2010).
5. R. J. Lee *et al.*, Uncoupling retro-translocation and degradation in the ER-associated degradation of a soluble protein. *The EMBO journal* **23**, 2206 (Jun 2, 2004).
6. M. L. Forster *et al.*, Protein disulfide isomerase-like proteins play opposing roles during retrotranslocation. *The Journal of cell biology* **173**, 853 (Jun 19, 2006).
7. K. M. Bernardi, M. L. Forster, W. I. Lencer, B. Tsai, Derlin-1 facilitates the retro-translocation of cholera toxin. *Molecular biology of the cell* **19**, 877 (Mar, 2008).
8. P. Moore, K. M. Bernardi, B. Tsai, The Ero1alpha-PDI redox cycle regulates retro-translocation of cholera toxin. *Molecular biology of the cell* **21**, 1305 (Apr 1, 2010).
9. T. Okiyoneda, P. M. Apaja, G. L. Lukacs, Protein quality control at the plasma membrane. *Current opinion in cell biology* **23**, 483 (Aug, 2011).
10. T. Okiyoneda *et al.*, Peripheral protein quality control removes unfolded CFTR from the plasma membrane. *Science* **329**, 805 (Aug 13, 2010).
11. M. Chatenay-Lapointe, G. S. Shadel, Stressed-out mitochondria get MAD. *Cell metabolism* **12**, 559 (Dec 1, 2010).
12. E. B. Taylor, J. Rutter, Mitochondrial quality control by the ubiquitin-proteasome system. *Biochemical Society transactions* **39**, 1509 (Oct, 2011).
13. J. M. Heo *et al.*, A stress-responsive system for mitochondrial protein degradation. *Molecular cell* **40**, 465 (Nov 12, 2010).
14. S. Xu, G. Peng, Y. Wang, S. Fang, M. Karbowski, The AAA-ATPase p97 is essential for outer mitochondrial membrane protein turnover. *Molecular biology of the cell* **22**, 291 (Feb 1, 2011).

15. H. Meyer, M. Bug, S. Bremer, Emerging functions of the VCP/p97 AAA-ATPase in the ubiquitin system. *Nature cell biology* **14**, 117 (Feb, 2012).
16. S. Patury, Y. Miyata, J. E. Gestwicki, Pharmacological targeting of the Hsp70 chaperone. *Current topics in medicinal chemistry* **9**, 1337 (2009).
17. A. G. Tamayo, A. Bharti, C. Trujillo, R. Harrison, J. R. Murphy, COPI coatomer complex proteins facilitate the translocation of anthrax lethal factor across vesicular membranes in vitro. *Proceedings of the National Academy of Sciences of the United States of America* **105**, 5254 (Apr 1, 2008).
18. R. Ratts *et al.*, The cytosolic entry of diphtheria toxin catalytic domain requires a host cell cytosolic translocation factor complex. *The Journal of cell biology* **160**, 1139 (Mar 31, 2003).
19. Y. Ye, H. H. Meyer, T. A. Rapoport, The AAA ATPase Cdc48/p97 and its partners transport proteins from the ER into the cytosol. *Nature* **414**, 652 (Dec 6, 2001).
20. E. Jarosch *et al.*, Protein dislocation from the ER requires polyubiquitination and the AAA-ATPase Cdc48. *Nature cell biology* **4**, 134 (Feb, 2002).
21. E. Rabinovich, A. Kerem, K. U. Frohlich, N. Diamant, S. Bar-Nun, AAA-ATPase p97/Cdc48p, a cytosolic chaperone required for endoplasmic reticulum-associated protein degradation. *Molecular and cellular biology* **22**, 626 (Jan, 2002).
22. Y. Ye, Y. Shibata, C. Yun, D. Ron, T. A. Rapoport, A membrane protein complex mediates retro-translocation from the ER lumen into the cytosol. *Nature* **429**, 841 (Jun 24, 2004).
23. N. W. Bays, S. K. Wilhovsky, A. Goradia, K. Hodgkiss-Harlow, R. Y. Hampton, HRD4/NPL4 is required for the proteasomal processing of ubiquitinated ER proteins. *Molecular biology of the cell* **12**, 4114 (Dec, 2001).
24. K. Bagola, M. Mehnert, E. Jarosch, T. Sommer, Protein dislocation from the ER. *Biochimica et biophysica acta* **1808**, 925 (Mar, 2011).
25. B. N. Lilley, H. L. Ploegh, A membrane protein required for dislocation of misfolded proteins from the ER. *Nature* **429**, 834 (Jun 24, 2004).
26. Y. Ye *et al.*, Recruitment of the p97 ATPase and ubiquitin ligases to the site of retrotranslocation at the endoplasmic reticulum membrane. *Proceedings of the National Academy of Sciences of the United States of America* **102**, 14132 (Oct 4, 2005).
27. N. W. Bays, R. G. Gardner, L. P. Seelig, C. A. Joazeiro, R. Y. Hampton, Hrd1p/Der3p is a membrane-anchored ubiquitin ligase required for ER-associated degradation. *Nature cell biology* **3**, 24 (Jan, 2001).
28. X. Zhong *et al.*, AAA ATPase p97/valosin-containing protein interacts with gp78, a ubiquitin ligase for endoplasmic reticulum-associated degradation. *The Journal of biological chemistry* **279**, 45676 (Oct 29, 2004).

29. C. J. O'Neal, M. G. Jobling, R. K. Holmes, W. G. Hol, Structural basis for the activation of cholera toxin by human ARF6-GTP. *Science* **309**, 1093 (Aug 12, 2005).
30. Y. Zhong *et al.*, Importin beta interacts with the endoplasmic reticulum-associated degradation machinery and promotes ubiquitination and degradation of mutant alpha1-antitrypsin. *The Journal of biological chemistry* **286**, 33921 (Sep 30, 2011).

CHAPTER 4

Conclusions

4-1. Discussion

Protein folding, ERAD, and cholera toxin

Newly translated proteins must integrate a variety of intra- and intermolecular forces to achieve a functional, folded state. Changes in internal and external cellular environments introduce stressors that reduce the efficiency of protein folding. In many cases, mutations in key structural domains prevent proteins from achieving a properly folded conformation. Regardless of the cause, misfolding eventually leads to loss-of-function or gain-of-function aggregates that impair important cellular and organismal functions. Cells must respond quickly to maintain homeostasis and to avoid crippling stress and possibly death. To this end, a number of protein quality control pathways have evolved to ensure proteins are properly folded or, when necessary, targeted for degradation. The most well studied pathway is ER-associated degradation.

As its name suggests, ERAD is tailored to the processing of terminally misfolded proteins in the ER. In general, ERAD pathways follow the basic pattern of substrate recognition, retro-translocation, ubiquitination and degradation. This is accomplished by a concerted effort between chaperones, pore-forming transmembrane proteins, ubiquitin ligases, and the 26S proteasome. Chronic

misfolding of ER proteins or disrupted communication between components of the ERAD machinery can lead to a disease state on the organismal level. As the number of known ERAD-related diseases increases so does the need to dissect the mechanism by which the pathway operates. Ironically, investigating how ERAD goes wrong has been the most productive way to detail how it correctly operates.

Interestingly, many pathogens have developed the ability to co-opt cellular machinery to cross biological membranes and promote toxicity. Cholera toxin, for example, traffics to the ER where it masquerades as a misfolded protein, hijacks ERAD chaperones, and undergoes retro-translocation to the cytosol. Due to a number of biochemical advantages, cholera toxin is an excellent tool for resolving how ERAD machinery recognizes and processes distinct substrates. This thesis is a tale of the two sides of cholera toxin retro-translocation.

Cholera toxin in the ER lumen

When cholera toxin arrives in the ER the CTA subunit exists as two peptides joined by a disulfide bond. Reduction of this disulfide bond enables the catalytic CTA1 peptide to be isolated from the holotoxin, partially unfold, and be marked as a substrate for ERAD (*1*). Collective *in vitro* and *in vivo* data suggested that the toxin is unfolded by PDI and presented for retro-translocation through a pore putatively composed of Derlin-1 and Hrd1 (*2-4*). Due to the propensity of the toxin to spontaneously refold (*5*), it was hypothesized that release of the toxin from PDI must be physically coupled to the retro-translocon.

Previous *in vitro* data indicated that Ero1α regulates release of CTA1 from PDI in a redox-dependent manner (*6*). As such, I set out to clarify the role of the PDI-Ero1α redox cycle in cells.

Using both gain- and loss-of-function techniques I determined that Ero1α is important for *in vivo* retro-translocation of cholera toxin. Specifically, Ero1α directly oxidizes PDI to induce release of the unfolded toxin. Consequently, the ratio of Ero1α to PDI must be balanced in order to allow sequential binding, unfolding and release of the toxin. It was also revealed that manipulation of Ero1α altered the binding affinity of PDI for the membrane chaperone Derlin-1. Further analysis established that reduced PDI is targeted to the ER membrane through interaction with Derlin-1. This not only brings PDI into proximity with the holotoxin but also couples unfolding of CTA1 to the retro-translocon. Subsequent oxidation of PDI by Ero1α thereby permits direct release of CTA1 through the ER membrane. In short, the PDI-Ero1α redox cycle regulates both temporal and spatial processing of cholera toxin in the ER lumen.

Recent evidence shows that cholera toxin retro-translocation depends on coordination between BiP, ERdj5 and Sel1L (*7*). This pathway may act in conjunction with or parallel to PDI and Ero1α. When CTA is reduced in the ER, thermal instability in the C-terminus of CTA1 leads to conformational shifts across the entire peptide that promote recognition by PDI (*1*). It is unclear whether PDI recognizes several subdomains of misfolded CTA1, and if so, whether multiple PDI proteins work in tandem to unfold CTA1. Due to the non-specific nature of

hydrophobic interactions, it is likely that BiP would also recognize misfolding of the same subdomains of CTA1, suggesting that the two aforementioned chaperone complexes play redundant roles. However, if BiP and PDI do target distinct sites of CTA1 it opens the possibility that they play cooperative roles in toxin retro-translocation. PDI and BiP may simultaneously target and unfold a single CTA1 peptide or they may work on the toxin processively.

Inevitably, studying other ERAD substrates will help elucidate the specificity of chaperone-substrate interactions in the ER lumen. For example, α1-antitrpysin (A1AT) and its mutant variants are soluble lumenal proteins that are strongly linked to ERAD and human disease. Moreover, their retro-translocation and degradation have been linked both to PDI (*8, 9*) as well as to complexes containing BiP (*10, 11*). Because the type of A1AT mutation influences how the protein is recognized by ERAD machinery it would be interesting to evaluate which, if any, variants follow the pathways co-opted by cholera toxin. Specifically, do any variants rely on PDI-Ero1α, BiP-ERdj5-Sel1L, or both? By answering such questions we will deepen our understanding of how cholera toxin and endogenous ERAD substrates are recognized and presented for retro-translocation.

Release of cholera toxin in the cytosol

Upon arrival at the cytosolic side of the ER membrane, canonical ERAD substrates are poly-ubiquitinated and targeted for degradation by the proteasome. While it has been established that the p97-Ufd1-Npl4 complex is

important for the recognition and extraction of ubiquitinated proteins from the ER membrane, little else is known about how the cytosolic phase of ERAD is orchestrated. Because cholera toxin is neither ubiquitinated nor degraded by the proteasome it is even less clear how it is released into the cytosol. Due to overlapping cellular quality control and trafficking pathways, identification and characterization of cytosolic retro-translocation factors have been ineffective. My goal was to develop an unbiased assay that permitted direct manipulation of cytosolic factors without incurring negative side effects.

Addition of wild-type cytosolic extracts to intoxicated membrane induced release of CTA1 from ER membranes. Using a variety of biochemical assays it was confirmed that *in vitro* released toxin is processed normally and is structurally similar to *in vivo* retro-translocated toxin. *In vitro* release of TCRα was also successful, indicating that the assay can be broadly applied to endogenous ERAD substrates. By exploiting the differences between toxin and TCRα it was fortuitously discovered that membrane extraction and release are two distinct steps of retro-translocation; extraction presents substrates to the cytosol and makes them accessible to cytosolic release factors. This challenges the conventional model that p97 is solely responsible for extracting and releasing ERAD substrates from the ER membrane to the cytosol (*12-15*). Instead, p97 may double as a scaffold for cytosolic chaperones that maintain substrate solubility and directly target them for proteasomal destruction. Because lumenal and transmembrane substrates might be differentially targeted to proteasome in

the cytosol or at the ER membrane, separation of extraction and release would provide another degree of specificity for substrate retro-translocation.

Because the assay was designed for direct manipulation of cytosolic activity, extracts were subjected to fractionation and energy depletion. Fractionation revealed that a host of cytosolic factors are neither required for dislocation of CTA1 nor of TCRα into the cytosol. However, the data do not rule out the possibility that these proteins play a different role in substrate retro-translocation. In fact, it is evident that the cytosolic facet of ERAD is far more complicated than simple membrane extraction and release. For example, the deubiquitinases Yod1 and Ataxin-3 appear to regulate cholera toxin retro-translocation despite the fact that the toxin is not directly ubiquitinated (*16*). However, in the *in vitro* assay they influence neither presentation nor dislocation of CTA1 from the ER membrane (data not shown).

Energy depletion of cytosolic extracts indicated that release of cholera toxin depends on hydrolysis of GTP. Whether the cytosolic factor performs hydrolysis itself or simply activates a membrane associated GTPase is uncertain. Regardless, this is only the second finding indicating involvement of a small GTPase in retro-translocation; another recent study links Ran and importin β to ERAD of A1AT (*17*). TCRα also requires energy expenditure for release but does not appear to rely on NTP hydrolysis; the cytosolic activity for TCRα release may simply require binding of NTPs. While it remains possible that cholera toxin and

TCRα share the same release factor, the data nonetheless highlight how their pathways continue to diverge.

In order to detail the mechanism of cytosolic extraction and release, we must expand the cytosolic assay to include a larger variety of ERAD substrates. A1AT and CFTR would be excellent candidates for the *in vitro* assay not only because of their prominence in the ERAD field but also due to their strong link to human disease. As A1AT and its mutant variants are soluble substrates they would be effective tools to analyze the cytosolic machinery used in the retro-translocation of CTA1. As in the ER lumen, it would be interesting to see how their pathways converge or diverge upon reaching the cytosol. This is especially true considering that A1AT is processed as a canonical ERAD substrate and is degraded by the proteasome whereas CTA1 escapes proteasomal degradation altogether. In that regard, it is possible that A1AT has more in common with TCRα.

CFTR and its mutants, like TCRα, are transmembrane ERAD substrates. However, because CFTR is composed of several hydrophobic transmembrane domains, cytosolic solubilization of the protein is energetically unfavorable. As such, it is believed that CFTR is not completely dislocated from the ER membrane; instead, CFTR is partially solubilized by cytosolic chaperones and quickly targeted to the proteasome (*18-20*). For this reason, it is important to discern whether CFTR, like TCRα, can be released from the ER membrane under proteasomal inhibition. Furthermore, depending on how it misfolds CFTR is

targeted to different ERAD pathways. Divergence of these pathways is likely reflected in CFTR retro-translocation. If CFTR can indeed be released from the membrane in the *in vitro* assay, it would be vital to resolve how diverse folding lesions influence interactions on the cytosolic face of the ER membrane, especially in comparison to TCRα.

Ultimately, the most important step to exposing the cytosolic mechanism of retro-translocation is identification of the cytosolic factor. Straightforward biochemical fractionation of cytosolic extracts has thus far proved ineffective due to successive loss of specific activity. To open a new avenue for identification of the factor, it is my goal to exploit the energy dependence of cytosolic release. Currently, energy depletion is accomplished by addition of non-hydrolyzable energy analogs or apyrase to cytosolic extracts. These elements are not removed prior to incubation with pellet fractions and therefore any observed effects may not be specific to the cytosol. To circumvent this problem I have adapted a system to biotinylate apyrase so that it can be added to extracts and subsequently removed ahead of incubation with the P1 fraction. This will resolve whether the cytosolic activity or a membrane-associated factor is energy dependent. Supplementation of energy depleted extracts with ATP or GTP will confirm nucleotide specificity. If the cytosolic factor for CTA1 release proves to be a small GTPase, extracts will be fractionated, energy depleted and candidate proteins isolated using GTP-agarose beads. Any factors identified by this

approach will be verified *in vivo* and further examined for activity towards endogenous substrates such as TCRα, A1AT and CFTR.

Closing Remarks

The work presented here provides insights into the machinery that cholera toxin co-opts on both sides of the ER membrane. Using this information I have enhanced the current model of cholera toxin retro-translocation (Figure 3-6); however, this model is still a gross oversimplification of the complex crosstalk between substrates, chaperones and the ubiquitin-proteasome system. In the future, research on cholera toxin must go beyond *what* is required for retro-translocation and focus on *how* the structure of the toxin determines its interactions with the ERAD machinery in both the lumen and the cytosol. At the same time, the scope must be widened to include a larger variety of substrates so we can correlate how toxin mimics a misfolded protein to how the cell normally orchestrates protein folding. Only then can cholera toxin be effectively used to improve our understanding of how ERAD works and why, at times, it goes wrong.

4-2. References

1. T. Banerjee *et al.*, Contribution of subdomain structure to the thermal stability of the cholera toxin A1 subunit. *Biochemistry* **49**, 8839 (Oct 19, 2010).
2. B. Tsai, C. Rodighiero, W. I. Lencer, T. A. Rapoport, Protein disulfide isomerase acts as a redox-dependent chaperone to unfold cholera toxin. *Cell* **104**, 937 (Mar 23, 2001).
3. K. M. Bernardi, M. L. Forster, W. I. Lencer, B. Tsai, Derlin-1 facilitates the retro-translocation of cholera toxin. *Molecular biology of the cell* **19**, 877 (Mar, 2008).
4. K. M. Bernardi *et al.*, The E3 ubiquitin ligases Hrd1 and gp78 bind to and promote cholera toxin retro-translocation. *Molecular biology of the cell* **21**, 140 (Jan 1, 2010).
5. C. Rodighiero, B. Tsai, T. A. Rapoport, W. I. Lencer, Role of ubiquitination in retro-translocation of cholera toxin and escape of cytosolic degradation. *EMBO reports* **3**, 1222 (Dec, 2002).
6. B. Tsai, T. A. Rapoport, Unfolded cholera toxin is transferred to the ER membrane and released from protein disulfide isomerase upon oxidation by Ero1. *The Journal of cell biology* **159**, 207 (Oct 28, 2002).
7. J. Williams, T. Inoue, L. Banks, B. Tsai, The ERdj5-Sel1L complex facilitates cholera toxin retro-translocation *(Unpublished Data)*, (2012).
8. E. Papp, P. Szaraz, T. Korcsmaros, P. Csermely, Changes of endoplasmic reticulum chaperone complexes, redox state, and impaired protein disulfide reductase activity in misfolding alpha1-antitrypsin transgenic mice. *FASEB journal : official publication of the Federation of American Societies for Experimental Biology* **20**, 1018 (May, 2006).
9. T. Horibe *et al.*, Different contributions of the three CXXC motifs of human protein-disulfide isomerase-related protein to isomerase activity and oxidative refolding. *The Journal of biological chemistry* **279**, 4604 (Feb 6, 2004).
10. N. Hosokawa *et al.*, Human XTP3-B forms an endoplasmic reticulum quality control scaffold with the HRD1-SEL1L ubiquitin ligase complex and BiP. *The Journal of biological chemistry* **283**, 20914 (Jul 25, 2008).
11. C. M. Cabral, Y. Liu, K. W. Moremen, R. N. Sifers, Organizational diversity among distinct glycoprotein endoplasmic reticulum-associated degradation programs. *Molecular biology of the cell* **13**, 2639 (Aug, 2002).
12. Y. Ye, H. H. Meyer, T. A. Rapoport, The AAA ATPase Cdc48/p97 and its partners transport proteins from the ER into the cytosol. *Nature* **414**, 652 (Dec 6, 2001).
13. E. Jarosch *et al.*, Protein dislocation from the ER requires polyubiquitination and the AAA-ATPase Cdc48. *Nature cell biology* **4**, 134 (Feb, 2002).
14. E. Rabinovich, A. Kerem, K. U. Frohlich, N. Diamant, S. Bar-Nun, AAA-ATPase p97/Cdc48p, a cytosolic chaperone required for endoplasmic

reticulum-associated protein degradation. *Molecular and cellular biology* **22**, 626 (Jan, 2002).
15. N. W. Bays, S. K. Wilhovsky, A. Goradia, K. Hodgkiss-Harlow, R. Y. Hampton, HRD4/NPL4 is required for the proteasomal processing of ubiquitinated ER proteins. *Molecular biology of the cell* **12**, 4114 (Dec, 2001).
16. K. M. Bernardi, B. Tsai, *(Unpublished Data)*.
17. Y. Zhong *et al.*, Importin beta interacts with the endoplasmic reticulum-associated degradation machinery and promotes ubiquitination and degradation of mutant alpha1-antitrypsin. *The Journal of biological chemistry* **286**, 33921 (Sep 30, 2011).
18. A. Ahner, K. Nakatsukasa, H. Zhang, R. A. Frizzell, J. L. Brodsky, Small heat-shock proteins select deltaF508-CFTR for endoplasmic reticulum-associated degradation. *Molecular biology of the cell* **18**, 806 (Mar, 2007).
19. Y. Zhang *et al.*, Hsp70 molecular chaperone facilitates endoplasmic reticulum-associated protein degradation of cystic fibrosis transmembrane conductance regulator in yeast. *Molecular biology of the cell* **12**, 1303 (May, 2001).
20. R. T. Youker, P. Walsh, T. Beilharz, T. Lithgow, J. L. Brodsky, Distinct roles for the Hsp40 and Hsp90 molecular chaperones during cystic fibrosis transmembrane conductance regulator degradation in yeast. *Molecular biology of the cell* **15**, 4787 (Nov, 2004).